SENSING AND RELAYING THE AUTOPHAGIC SIGNAL BY THE ULK1 KINASE COMPLEX

by

Cindy Puente

A Dissertation

Presented to the Faculty of the Louis V. Gerstner, Jr.

Graduate School of Biomedical Sciences,

Memorial Sloan-Kettering Cancer Center

in Partial Fulfillment of the Requirement for the Degree of

Doctor of Philosophy

New York, NY

May, 2016

_____ _____

Xuejun Jiang, PhD
Dissertation Mentor

Date

To my husband, son, family and friends for their indefinite love and support

ABSTRACT

Autophagy is a conserved catabolic process that utilizes a defined series of membrane trafficking events to generate a double-membrane vesicle termed the autophagosome, which matures by fusing to the lysosome. Subsequently, the lysosome facilitates the degradation and recycling of the cytoplasmic cargo. Autophagy plays a vital role in maintaining cellular homeostasis, especially under stressful conditions, such as nutrient starvation. As such, it is implicated in a plethora of human diseases, particularly age-related conditions such as neurodegenerative disorders. The long-term goals of this proposal were to understand the upstream molecular mechanisms that regulate the induction of mammalian autophagy and understand how this signal is transduced to the downstream, core machinery of the pathway.

In yeast, the upstream signals that modulate the induction of starvation-induced autophagy are clearly defined. The nutrient-sensing kinase Tor inhibits the activation of autophagy by regulating the formation of the Atg1-Atg13-Atg17 complex, through hyper-phosphorylation of Atg13. However, in mammals, the homologous complex ULK1-ATG13-FIP200 is constitutively formed. As such, the molecular mechanism by which mTOR regulates mammalian autophagy is unknown. Here we report the identification and characterization of novel nutrient-regulated phosphorylation sites on ATG13: Ser-224 and Ser-258. mTOR directly phosphorylates ATG13 on Ser-258 while Ser-224 is modulated by the AMPK pathway. In *ATG13* knockout cells reconstituted with an unphosphorylatable mutant of ATG13, ULK1 kinase activity is more potent, and amino acid starvation

induced more rapid ATG13 and ULK1 translocation. These events culminated in a more potent starvation-induced autophagy response. Therefore, ATG13 phosphorylation plays a crucial role in autophagy regulation.

Although the ULK1/Atg1 kinase is required for the induction of starvation-induced autophagy, few substrates have been elucidated. As such, it is unclear how the ULK1 complex transmits the autophagy induction signal downstream to the core machinery. We undertook to identify novel substrates of ULK1 using a quantitative phospho-proteomics approach. Our data was validated by the identification of a known ULK1 binding partner, FIP200, as a putative substrate. We were able to confirm two novel *in vitro* substrates of the ULK1 kinase, ARHGEF2 and GLIPR2. Upon further analyzes, I discerned that *ARHGEF2* -/- MEF cells have an increased autophagy flux, and so ARHGEF2 is a negative regulator of starvation-induced autophagy. Overall, my study has elucidated how starvation-induced autophagy is regulated molecularly and has identified novel modulators of the pathway.

VITAE

Cindy was born in New York City where she remained for her graduate studies

ACKNOWLEDGEMENTS

I would like to extend my greatest gratitude to my advisor Dr. Xuejun Jiang. I thank you for the privilege to join your laboratory and always extending your scientific insight, passion, encouragement and mentorship.

I would also like to thank former and current laboratory members for their help, support and friendship: Dr. Ian Ganley, Dr. Du Lam, Dr. Taya Feldman, Dr. Noor Gammoh, Dr. Pui-Mun Wong, Dr. Yuji Shi, Dr. Junru Wang, Dr. Minghui Gao, Dr. Rui Zhang, Dr. Yan Feng, Tao Yun, Helen Kang and Prashant Monian.

I would also like to thank Dr. Ronald C. Hendrickson, Hediye Erdjument-Bromage, Dr. Rajesh Soni and John Philip, from the Proteomics and microchemistry core facility at Memorial Sloan Kettering (MSKCC), for their invaluable mass spectrometry analysis and insight. Their support and insight were true pillars in my research.

I would like to thank the members of my thesis committee, Dr. Michael Overholtzer and Dr. Xiaolan Zhao, for their guidance and fruitful discussion throughout the project. I also extend my thanks to Dr. Marilyn Resh for taking the time to Chair my thesis defense. I would also like to acknowledge Dr. Jill Bargonetti, who is serving as my external examiner. Dr. Bargonetti was my undergraduate research mentor and I'm indebted to her for her early support and unwavering guidance.

I owe a special appreciation to my family and close friends: Payson R.E. Armstrong, Carlos E. Puente, Mary Angulo, Ivonne M. Puente, Andres E. Puente, April J. Suhadi, Kevin Bohan, Carol Bohan, Ryan Bohan, Melissa Rosso,

Stephany Rosal, and all members of the Angulo family. Thank you for filling my days with love and joy, and extending your generous support.

Most importantly, I want to extend my greatest acknowledgement to my best friend and husband, Payton H. Armstrong, for his unwavering love, support, smiles, hugs, patience and commitment to walk down the road of life with me.

TABLE OF CONTENTS

LIST OF FIGURES

LIST OF TABLES

LIST OF ABBREVIATIONS

AMPK – 5'-AMP-activated protein kinase

ARHGEF2/GEF-H1 – Rho/Rac guanine nucleotide exchange factor 2

ARSG – Arylsulfatase G

ATG – Autophagy-related gene

AB –Autophagosome body

AV – Autophagosome vacuole

DARS2 – Aspartyl-tRNA Synthetase 2, mitochondrial

EM – Electron microscopy

FIP200 – Focal adhesion kinase (FAK) family interacting protein of 200 kDa

F/S-ATG13 – Tandem FLAG-S- tagged ATG13

ISYNA1 – Inositol-3-phosphate synthase

LC3 – Microtubule associated protein 1B light chain 3

mTOR – Mammalian target of rapamycin

mTORC1 – mTOR complex 1

mTORC2 – mTOR complex 2

p62/SQSTM1 – Ubiquitin-binding protein p61/Sequestosome 1

SNX13 – Sorting nexin 13

TRIM28 – Tripartite motif-containing 28

ULK1 – UNC-51-like kinase 1

ULK2 – UNC-51-like kinase 2

UVRAG – UV radiation-associated gene

VPS34 – Vacuolar protein sorting mutant 34

CHAPTER 1. INTRODUCTION

1.1 Autophagy: a lysosome-dependent degradation pathway

Cells must generate necessary proteins to mediate important intracellular processes. Until the 1980s, it was widely believed that most proteins are long-lived. This assumption was first questioned in 1935 when Rudolph Schoenheimer introduced the isotopic tracer technique in metabolic research. His experiments eventually revolutionized our understanding of metabolism and introduced a novel concept, that cells are in a dynamic state of continual regeneration (1,2). As such, just as cells manufacture components, they must also break them down. In order to maintain this balance, the cell employs two degradation machineries: the proteasome and the lysosome. The proteasome is responsible for the breakdown of most short-lived proteins. The lysosome is responsible for the degradation of the majority of long-lived proteins, protein aggregates and entire organelles. In order to deliver these components to the lysosome, the cell uses autophagy.

Autophagy is a conserved catabolic process that facilitates the degradation of cytoplasmic contents in a lysosome-dependent manner. It functions to promote cellular homeostasis by maintaining protein and organelle quality control, and sustaining cellular metabolism, under stress conditions such as starvation (3,4). Autophagy is conserved in all eukaryotic cells and is indispensable for normal development (5). There are three different types of autophagy: chaperone-mediated autophagy (CMA), microautophagy and macroautophagy. CMA utilizes

chaperone proteins to recruit proteins tagged with a pentapeptide motif to receptors on the lysosome for unfolding and degradation (6). In microautophagy cytoplasmic components are recruited to the lysosomal membrane and subsequently engulfed by the lysosome (7). In this dissertation, I focused on macroautophagy. Macroautophagy, hereafter referred to as autophagy, uses the autophagosome, a *de novo* double-membrane vesicle that forms in the cytoplasm, to sequester bulk cytoplasmic components. The autophagosome matures by fusing to the lysosome, leading to the degradation of the contents inside (8) (4).

The discovery of the lysosome

The discovery of autophagy first begins with the discovery of the lysosome by Christian de Duve in 1955, for which he shared the Nobel Prize in Physiology or Medicine in 1974. This serendipitous discovery stemmed from his work with glucose-6-phosphatase. He was optimizing the purification of this enzyme from rat liver cells, using centrifugal fractionation. He noted that when he lysed cells harshly using a blender, the enzyme precipitated into an insoluble fraction. He amended his protocol to use mild homogenization conditions, which was designed to maintain the integrity of subcellular organelles. Using this new protocol, he additionally monitored another enzyme as a control, acid phosphatase. Unfortunately, the activity of this control enzyme was significantly lower than expected. However, to his surprised, the activity increased after ‘ageing’ the samples in the refrigerator for five days. This result steered De

Duve's research onto a new path. On the basis of additional experiments, he was able to surmise that the latent acid phosphatase activity was the result of a sequestering membrane sac. On the basis of analytical biochemical procedures and centrifugal fractionation, he was able to purify a new organelle. The discovery of additional acid hydrolases suggested that this newly discovered organelle functioned in intracellular digestion of macromolecules (9,10). He termed this organelle the lysosome, derived from the Greek words *lysis*, meaning "to loosen," and soma, meaning "body."

The autophagic phenomenon

The field of autophagy began as a phenomenon. Using electron microscopy, researchers described membrane-bounded cytoplasmic particles, which they termed 'dense bodies.' The first reference of this structure was made in 1957 and described the presence of mitochondria inside these dense bodies (11). These observations were subsequently linked to the lysosome by a study in 1959 which demonstrated that these dense bodies are positive for acid phosphatase activity (12). This 'phenomenon' was further characterized by electron microscopy (EM) imaging the organs of rats treated with different agents (13). Treated animals demonstrated an increase in the number of acid phosphatase positive cytoplasmic inclusions. The authors surmised that these 'dense bodies' might function to sequester parts of the cytoplasm, upon focal injury, and mediate focal cytoplasmic degradation. The presence of these dense bodies in normal cells also suggested that the function of these particles extends beyond limiting injury

and might function more generally in reutilization of cellular materials. In addition, Hruban and colleagues where able to recognize that the formation of these dense bodies progressed in at least three continuous stages: (1) sequestration (2) formation of complex dense bodies (3) formation of lysosome-like bodies (13). These findings inspired Christian de Duve, in 1963 at the Ciba Foundation symposium, to coin the term “autophagy,” from the Greek words auto, meaning “self,” and phagein, meaning “to eat” to describe this new process and the term “autophagosome” to describe the sequestration particle. He suggested that the autophagic process is most likely present in most eukaryotic cells, and functions to facilitate nonspecific bulk digestion in a lysosome-dependent fashion. De Duve additionally conjectured that this process might even mediate the selective degradation of targeted cellular contents (14). These early studies provided the basis for the autophagy field to transition from a phenomenon to a novel recognized degradation process.

The morphological and biochemical-physiological era of autophagy

These early studies of autophagy were limited to EM imaging of rat hepatocytes. Nevertheless, they provide the basis for our current understanding of autophagy as an adaptive response, and a continuous process involving membrane rearrangements that culminates with fusion to the lysosome.

Characterizing the autophagic process. These early studies were critical in characterizing the autophagic process. Unlike transient transport vesicles that shuttle proteins between the cisternae of the Golgi apparatus, the autophagosome forms *de novo*. It was initially proposed that the growth of the nascent autophagosome was mediated by *de novo* synthesis of the limiting membranes (15). However, subsequent studies established that it was more likely that the limiting membranes of the nascent autophagosomes are provided by preformed cytoplasmic membranes, most likely from the ER or the Golgi apparatus (16-18). The early and intermediate stages of autophagosome formation were described using eletroinjected radioactive probes. This study identified and described the phagophore, the initial sequestered organelle that matures into an autophagosome (19). Autophagosomes are heterogeneous. Their walls vary in thickness and they can be multilayered or double-layered (20). Mammalian autophagosomes also very in size which span 0.5 μm to 1.5 μm (21). The contents of the autophagosome are also heterogeneous, and may contain intact and recognizable parts of the cell, including mitochondria, small vesicles and tubules, ribosomes and even cytoskeletal structures (22,23). Once formed, the average life of autophagosomes is approximately 9 minutes, as estimated by electron microscopic morphometry (24). This rapid turnover is underscored by the fact that autophagy may account for 70-80% of intercellular protein degradation (25).

Autophagy and cellular metabolism. The connection between cellular metabolism and autophagy started to emerge in the 1970s. Several studies elucidated that nutrient availability and hormones associated with food intake regulate autophagic activity in the rodent liver. Perfusion of rodent liver with glucagon stimulates autophagy whereas insulin is a potent inhibitor of the pathway (26,27). The addition of glucagon increases the volume occupied by autophagic vacuoles by as much as 50% (27). Amino acid deprivation can also stimulate autophagy; however, this function is limited to a few select amino acids, including Leu, Tyr, Phe, Gln, Pro, Met, Trp and His (28,29). These studies are the foundation of our understanding of autophagy as a catabolic, energy-producing mechanism.

Validation of the De Duve Fusion Model. 1962, Ashford and colleagues visualized an increase of “microbodies,” in rat hepatocytes following perfusion with glucagon (15). They mistakenly identified these microbodies as lysosomes, because they stained positive for acid phosphatase activity, and challenged the concept of the lysosome as a well-defined organelle. Instead, they theorized “lysosomes represent portions of the cytoplasm set aside for hydrolysis” (15). This study exemplifies the divide in the autophagic field between two opposing theories. One theory, proposed by Novikoff stipulates that autophagy is a mechanism that facilitates the generation of new lysosomes (30). The other theory advanced by De Duve considered preexisting lysosomes as the source of the hydrolytic enzymes found in autophagosomes, and that the transfer of

proteins in mediated by a fusion event between the two vesicles (14). Several studies attempted to resolve this dispute, however the discordant findings only added to the uncertainty (31-35). The answer came from a study using endosome and lysosome fractions, labeled with different sizes of colloidal gold. It became apparent that lysosome enzyme delivery to nascent autophagosomes occurs primarily by fusion with pre-existing mature lysosomes (36). This finding is in line with *in vitro* studies, which demonstrate that nascent autophagosomes show little proteolytic activity whereas mature autophagosomes are enriched in proteolysis (37).

Selective Autophagy. In the 1960s, Christian de Duve suggested that macroautophagy, in addition to bulk degradation, might also facilitate the selective degradation of intracellular components. This hypothesis was corroborated by multiple studies. In 1973, one study characterized the removal of phenobarbital-induced membranes from hepatocytes after cessation of treatment (38). Treatment with phenobarbital causes a proliferation of the endoplasmic reticulum (ER). Upon cessation of treatment and subsequent involution of the ER, there is an increase in the volume (800%) and number (96%) of autophagic vacuoles (AVs). Most importantly, he also observed a twofold increase in the number of AVs containing portions of the ER. These results suggested that autophagy was selectively induced and was preferentially facilitating the degradation of the ER (38). In 1977, another study suggested that autophagy could selectively remove mitochondria, during insect metamorphosis (39). During

the early phases of metamorphosis-related degeneration of the intersegmental muscles in *Antheraea polyphemus*, the number of autophagic vacuoles, containing mitochondria increases dramatically; after which the number of mitochondria in the cytoplasm is drastically reduced (39). In 1983, selective degradation of peroxisomes was described in the yeast *Hansenula polymorpha* (40). These methylotrophic yeast expand the peroxisome compartment, when grown in methanol-containing media, in order to facilitate the oxidative metabolism of methanol. When these yeast are transferred to media containing excess glucose, there is a rapid decrease in the peroxisome compartment that is selectively mediated by the autophagic process (40). These early studies were critical because they established a role for autophagy in cellular remodeling through the selective removal of superfluous organelles. In addition, these findings posed the immediate query as to whether autophagy also plays a role in selectively removing damaged organelles (41).

Pathophysiology. Although lacking in causation, many of these early studies implicated autophagy in pathophysiological relevant conditions. Several studies identified autophagy during physiological remodeling of cells. Autophagy was identified in embryonic cells undergoing differentiation (34,42). Autophagy was also identified in tissues undergoing involution, such as the mammary gland in the post-lactation period and the prostate gland after castration (43,44). These later studies are important to note because they alluded to a role in programmed cell death. A series of other studies identified autophagy in pathologically altered

cells. Authophagy could be induced by multiple conditions or agents including hypoxia (17), ischemia (37), metabolic inhibitors (35) and irradiation (45). These studies are of particular importance to the field because they established autophagy as an adaptive process that can be induced by a series of conditions.

The molecular era of autophagy

Genetic Screens. In order to understand the molecular mechanisms that govern the formation of autophagosomes, the field needed to surmount the limitations of transmission electron microscopy. The discovery of autophagy in yeast revolutionized the field and ushered the beginning of the molecular era. The pioneering work of Ohsumi identified autophagy in yeast (46). This revolutionary study demonstrated the accumulation of autophagic bodies (AB) inside the yeast vacuole, the mammalian equivalent to the lysosome. In yeast, autophagy can be induced by culturing cells in nitrogen or amino acid-deficient media, and forced to accumulate AB by inhibiting vacuolar serine protease activity. The Ohsumi group used the light microscope to assay for the absence of autophagic bodies in the vacuole. The identification of autophagy in yeast was critical for the development of the field because it provided a genetically tractable system from which individual mutants could be isolated and characterized. In 1993, Ohsumi reported the first genetic screen for autophagy in yeast, in which mutants defective in the accumulation of AB were isolated by light microscopy (47). This approach identified a single autophagy-defective mutant, *apg1*, which not only failed to accumulate AB upon starvation but also demonstrated a drastic decline

in viability, under nitrogen starvation conditions. By exploiting the loss of viability phenotype, Ohsumi isolated a total of 15 autophagy-defective mutants (47). This work was followed by additional screens that identified critical mediators of the autophagic process (48,49). However, not all screens for autophagy mutants used a genetics approach, many also utilized a biochemical approach. For example, one approach used the fatty acid synthase marker to identify autophagy-defective mutants (50). Fatty acid synthase is a cytosolic enzyme that is degraded in the vacuole, during starvation in a wild-type strain. Conversely, this enzyme accumulates in autophagy-defective mutants, and facilitates the identification of mutants by immunostaining. This approach isolated a total of nine mutants. Another approach developed and used the Pho8Δ60 alkaline phosphatase assay to screen for autophagy mutants (51). Pho8Δ60 is an N-terminal truncation of Pho8, a vacuolar alkaline phosphatase. This deletion ablates targeting to the vacuole and instead localizes Pho8Δ60 to the cytosol. As such, Pho8Δ60 is delivered to the vacuole only by an autophagic mechanism. Once Pho8Δ60 reaches the vacuole, it becomes activated by a C-terminal truncation and its activity can be measured enzymatically. Alternatively, this C-terminal truncation can by monitored by western blotting as it results in a novel band of 59 kDa (51).

The identification of autophagy-related genes in yeast facilitated the discovery of homologs in mammalian autophagy. It soon became apparent that many of these proteins are conserved in all eukaryotes. For example, *ATG12* was the first

mammalian autophagy gene identified through conservation to its yeast counterpart (52). ATG12 possesses 27% identity and 48% similarity with Apg12p. Beclin 1 shares 24% identify with Atg6. Furthermore, Beclin 1 is the functional homologue of Atg6 because expression of *Beclin1* in *Apg6*-deficient yeast restores autophagy (53). Additional screens performed in *C. elegans* and human cells identified mammalian specific components (54-56).

1.2 The Autophagic Machinery

This process was molecularly characterized largely with a series of yeast genetic screens that identified autophagy-related genes (ATG) (41,47,50). Thus far, more than 37 ATG proteins have been identified. However, canonical autophagy is only mediated by a core machinery of 15 ATG proteins while the remaining ATG proteins mediate selective autophagy. Selective autophagy utilizes adaptor proteins to target specific cellular components, such as bacteria, ribosomes, peroxisomes and mitochondria, for degradation (57,58). Canonical autophagy can be segmented into five discernable steps, each under the control of specific ATG proteins: (1) formation of the isolation membrane; (2) expansion; (3) maturation; (4) fusion with the lysosome; (5) degradation of the autophagosomal components in the lysosome (59,60).

Formation of the isolation membrane.

The autophagic process starts with the formation of the pre-autophagosome structure termed the isolation membrane or phagophore. The membrane

structure for the phagophore was originally theorized to be generated *de novo* from precursor molecules; however, now it is proposed to be derived from the ER (61) The ER-mitochondria interface plays an important role in the genesis of the autophagosome (62). Upon starvation, components of the autophagy-specific class III PI3K complex, including Vps34, Vps15, Beclin 1 and Atg14, accumulate at the mitochondria-associated ER membrane. Vps34 is the lipid kinase and its activity is enhanced by binding to Beclin 1 (63). The formation of the omegasome, an "Ω"-shaped membrane, functions as a platform for the formation of the phagophore (64). The recruited class II PI3K complex phosphorylates PtdIns (PI), producing PtdIns(3)P (PI3P). The accumulation of PI3P recruits proteins containing the FYVE motif, such as DFCP1 and WIPI1/2. However, the exact function of WIPI in autophagosome biogenesis is not fully understood. The PI3P accumulation recruits additional PI3P-effector proteins and ATG proteins that mediate the nucleation of the autophagosomal membrane.

Elongation.

Two distinct ubiquitin-like reactions promote the elongation of the phagophore membrane. In the ATG12 conjugation system, ATG12 becomes covalently conjugated to ATG5 by ATG7 and ATG10, which function as E1-like and E2-like enzymes, respectively (52). The ATG12-ATG5 complex is then non-covalently conjugated ATG16L1. This complex is essential for the elongation of the phagophore membrane, and dissociates from the fully formed autophagosome. As such, it serves as a marker of the early steps of autophagosome formation.

This complex then functions as an E3-like enzyme for the LC3-PE conjugation system (65). LC3, and the other mammalian Atg8 orthologues (LC3A/B/C, GABARAP and GABARAPL1/2/3), are conjugated to the lipid molecule phosphatidylethanolamine (PE) by ATG7 and ATG3, which function as E1-like and E2-like enzymes, respectively (66). Since PE-conjugated LC3 (i.e., LC3 II) is stably associated with the autophagosome, it functions as an autophagosomal marker for microscopic analysis of autophagy (67). Furthermore, LC3 II also displays an increase in electrophoretic mobility, as compared to LC3I, and so can be used to monitor autophagy by western blotting. Importantly, abrogating LC3-PE conjugation results in the accumulation of unclosed isolation membranes, suggesting that this conjugation system is essential for closure of the phagophore (68).

Maturation.

Once the lipid bilayers of the phagophore fuse, the double-membrane vesicle is termed the autophagosome. The autophagosome continues its maturation process by fusing with endosomal vesicles. UVRAG binds to the C-VPS/HOPS complex, a key component of the endosomal fusion machinery. This interaction stimulates the GTPase activity of Rab7 and promotes autophagosome fusion with late endosomes (69). The autophagosome maturation process can be hindered by the binding of Rubicon to UVRAG-HOPS complexes (70).

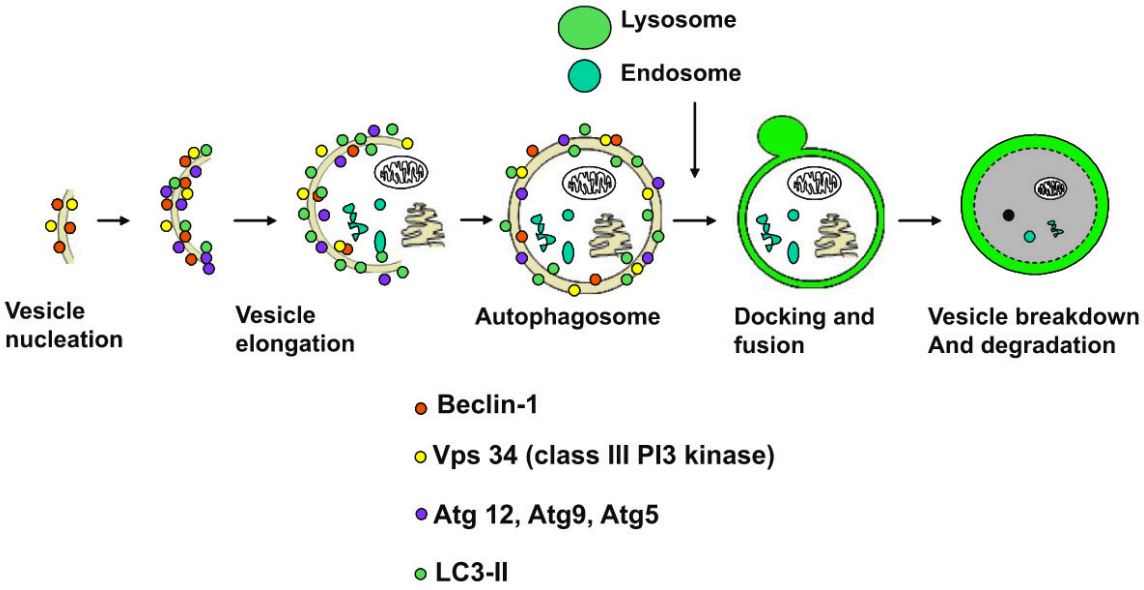

Figure 1.1 The autophagy pathway. The different steps in the autophagy pathway are depicted. The progression of the distinct stages is controlled by a set of autophagy-related proteins. Reprinted from Yang, C., Kaushal, V., Shah, S.V., Kaushal, G.P. (2008). Autophagy is associated with apoptosis in cisplatin injury to renal tubular epithelial cells. *Am. J. Physiol. Renal Physiol.* **294**, F777-87.

Fusion with the lysosome and degradation of contents.

Fusion of the autophagosome with the lysosome is mediated by the function of SNARE proteins, particularly VAMP8 and Vti1b (71,72). The Vit1b SNARE on the autophagosome mediates fusion with the VAMP8 SNARE located on the lysosome. Once the autophagosome fuses with the lysosome, this new vesicle is termed the autolysosome and its contents are degraded by the action of hydrolyzing enzymes.

1.3 The ULK1/Atg1 complex senses the autophagy induction signal

Upstream of the core machinery of autophagy is the ULK1/Atg1 kinase complex. The complex is composed of a kinase called ULK1/Atg1 and several binding partners, including ATG13. This complex is the focus of my dissertation. My work elucidates the molecular mechanism by which this complex senses the autophagy induction signal. This section will introduce the ULK1 complex in more detail and discuss the regulatory mechanisms that impinge on the complex.

The ULK1/Atg1 kinase

Atg1 was first discovered in a *Saccharomyces cerevisiae* genetic screen for autophagy-related genes (Atg) (47). It was identified as the sole Ser/Thr kinase, in autophagy, and placed at the most upstream step of autophagy induction (73). *Atg1* homologues were quickly identified in higher eukaryotes, and it became evident that Atg1 is an evolutionarily conserved kinase that is indispensable in autophagy. The *C. elegans Atg1* homologue, *Uncoordinated-51* (*Unc-51*), was

first identified in a screen for uncoordinated movement and implicated in axon guidance and neuronal vesicular movement (74). As in *C. elegans*, there is only one *Atg1* homologue in *Drosophila melanogaster* and it is also crucial in neuronal development (75,76).

The mammalian counterpart was identified as a homologue of *C. elegans Unc-51*, and designated *ULK1* (Unc-51-like kinase 1) (77,78). In mammals, there are five orthologues of *Atg1*, including *ULK1*, *ULK2*, *ULK3*, *ULK4* and *STK36* (79). Human ULK1 is a 140 kDa protein and has 41% overall similarity to the *C. elegans* UNC-51 homologue and 29% similarity to yeast Atg1 (77). Mouse ULK3, ULK4 and STK36 similarity to yeast Atg1 is limited to the N-terminal catalytic domain whereas ULK1 and ULK2 similarity also includes the central proline/serine-rich (PS) and C-terminal domains (78,80) (Figure 1.2). In fact, ULK1 and ULK2 share an overall 52% amino acid identity (80). Among the Atg1 mammalian homologs, only ULK1 and ULK2 regulate autophagy, in various cell types (81-83). However, an RNAi-based screen identified ULK1, as the only yeast Atg1 homologue, as an essential component of amino acid starvation-induced autophagy (84). Despite the fact that ULK1 is a key molecule in facilitating autophagy, *ULK1* knockout mice are viable (83). This is in sharp contrast to the neonatal lethality of core autophagy gene knockout mice (85,86). It became apparent that ULK2 can compensate for the loss of ULK1 and so loss of both is required for the characteristic perinatal-lethal phenotype (87).

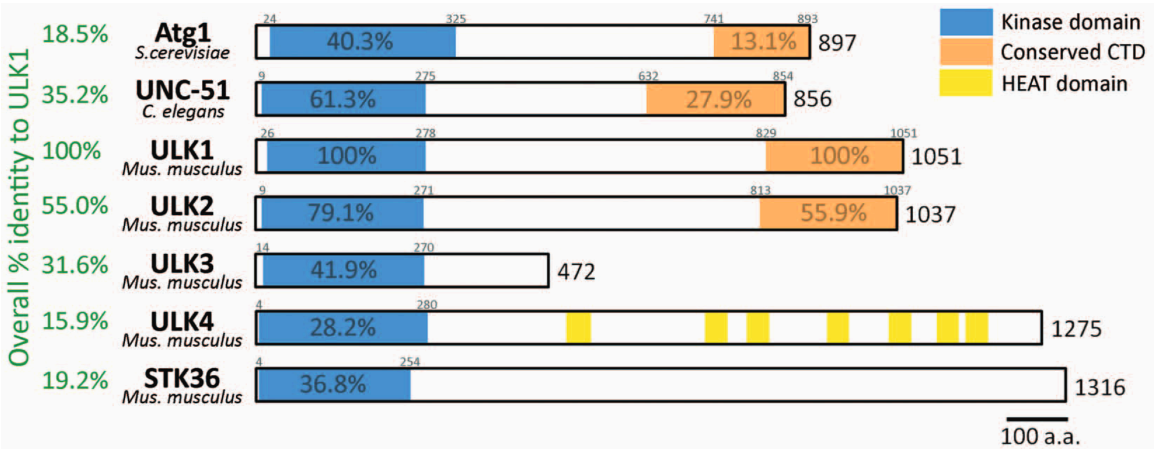

Figure 1.2 The domain structure of the Atg1/ULK1 kinase. The Atg1 kinase and its homologues share a high degree of identity in the kinase domains. However, the Atg1 C-terminal domain, which mediates many of the known protein-protein interactions is lost in the ULK3, ULK4 and the STK36 *Mus musculus* homologues. Reprinted from Wong, P. M., Puente, C., Ganley, I. G., and Jiang, X. (2013) The ULK1 complex: sensing nutrient signals for autophagy activation. *Autophagy* 9, 124-137.

ATG13: an ULK1 binding partner

Atg13 was originally identified by a yeast genetic screen for mutants defective in autophagy (47). Overexpression of *Atg1* in an *atg13Δ* mutant partially rescues the autophagy defect (88). This genetic interaction is reflective of the fact that Atg13 is an Atg1-associated protein that activates Atg1 kinase activity (89). *Atg13* is evolutionarily conserved. Highly divergent functional homologs were identified in *C. elegans* and *D. melanogaster* and mammals (81,90,91). However, there is only marginal sequence homology between human ATG13 and that of *S. cerevisiae* and *S. Pombe*, 11.7% and 19% identity, respectively. Although ULK1 was identified in 1999, it took more than 10 years to identify the respective mammalian homologue of Atg13 because it's very weakly conserved and could only be identified after an iterative PSI-BLAST (92).

In terms of structure function, Atg13 has a predicted unstructured region, at the center of the protein that mediates binding to Atg1 and Atg17 (93,94). The C-terminus of human ATG13 contains a highly conserved LC3-interacting region (LIR) motif that mediates binding to several mammalian homologues of Atg8 (95). The N-terminal domain of Atg13 is the only predicted ordered fold, which folds into a HORMA domain. Functionally, the HORMA domain is specifically involved in the recruitment of Atg14 and Atg9 vesicles, and is required for autophagy (96,97). HORMA domains can adopt two separate configurations O-Mad2 or C-Mad2, and the Atg13 HORMA domain corresponds to the C-Mad2 state. It is unknown whether Atg13 can also adopt an O-Mad2 conformation (96).

Interestingly, the Atg13 HORMA domain contains a pair of Arg residues (Arg118 and Arg205) that might function as putative phosphate sensors. The putative phosphate sensors are intriguing because they suggest that the Atg13 HORMA domain could undergo a phospho-regulated conformation switch or function as a conformation-dependent phosphate sensor (96). Although the HORMA domain is conserved in human ATG13, the phosphate binding site may not be conserved (98). The extreme N-terminus of ATG13 contains a basic region, which is highly conserved among higher eukaryotes, and mediates binding to phospholipids (99). Importantly, mutational analysis of this region suggests that it may function to facilitate the translocation of the entire ULK1 complex to punctate structures and autophagy progression (99).

The Atg1/ULK1 complex

The formation of the autophagosome is mediated by a series of ATG proteins, organized into separate functional units, which mediate each step of the autophagic process. The Atg1/ULK1 complex is the most upstream complex of autophagosome formation and is responsible for sensing the autophagic signal and relaying it to the downstream ATG core machinery (100,101).

In yeast, Atg1 forms a pentameric complex composed of Atg1, Atg13, Atg17, Atg29 and Atg31. Atg17-Atg29-Atg31 form a dimeric ternary complex, that is stably associated independent of nutrient conditions (102). This ternary complex then interacts with Atg1 via Atg13 in a starvation-dependent manner (93,103).

The Atg1-interacting proteins are important, in part, because they stabilize Atg1 and activate its kinase activity. The formation of the Atg1 complex is essential for the assembly of the phagophore structure, also known as the phagophore assembly site (PAS), and facilitating the recruitment and dissociation of core ATG proteins that nucleate and expand the autophagosome (104,105).

The mammalian counterpart of the Atg1 complex is comprised of an Atg1 homolog (ULK1 or ULK2), ATG13, FIP200 (also known as RB1CC1) and ATG101. Despite the low sequence homology, FIP200 is the proposed functional counterpart of Atg17 (100). ATG101 binds to and stabilizes ATG13 protein; this interaction is insensitive to nutrient availability. ATG101 is essential for autophagy and interacts with ULK1 via ATG13 (106). ATG101 is not conserved in yeast while Atg29 and Atg31 are not conserved in higher eukaryotes (100).

Regulation of the Atg1 complex in lower eukaryotes

As the most upstream ATG complex, the Atg1 complex functions as a hub to receive autophagy-initiating signals, which it then transmits downstream to the core machinery. The Atg1 complex coordinates nutritional signals from several pathways including TOR kinase complex 1 (TORC1) and cAMP-dependent protein kinase (PKA) pathway.

In *Saccharomyces cerevisiae*, the nutrient-sensing kinase TORC1 negatively regulates the induction of autophagy by inhibiting the formation of a multi-protein complex containing Atg1, Atg13 and Atg17-Atg29-Atg31, through the hyper-phosphorylation of Atg13 (89). The binding of Atg13 and Atg1 is essential to induce autophagy because Atg13 stabilizes Atg1 protein and enhances its kinase activity (89,93). Upon inactivation of TORC1 through starvation or pharmacological inhibition, Atg13 is rapidly dephosphorylated, allowing for the Atg1-Atg13-Atg17 complex to bind and promote the recruitment of downstream ATG proteins (Figure 1.3) (89,93,104,105,107). In fact, expression of an unphosphorylatable form of Atg13 is sufficient to enhance the interaction between Atg13 and Atg1, and induce autophagy in nutrient-replete conditions (108,109).

The PKA signaling pathway has also been implicated in the regulation of autophagy. Elevated levels of PKA activity can inhibit the induction of autophagy and conversely inhibiting the PKA pathway promotes the induction of autophagy (110,111). PKA phosphorylates Atg13 at multiple sites and expression of a combined alanine mutant for these sites is localized to the PAS, in both growing and nitrogen-starved cells (111). PKA regulates the PAS association of Atg13 by interfering with its interaction with Atg17 (111). Indeed, the identified PKA phosphorylation sites on Atg13 are located in a region that mediates binding to Atg17 (112). As compared to the TORC1 phosphorylations on Atg13, the PKA phosphorylations do not regulate the interaction between Atg13 and Atg1.

Interestingly, the control that PKA exerts on autophagy is independent of the TOR pathway (i.e., each pathway controls a distinct set of phosphorylation events on Atg13). As such, Atg13 is a vital regulatory component of autophagy that is responsive to environmental cues through a dynamic phosphorylation status (109).

Regulation of the ULK1 complex in mammals

In higher eukaryotes, several signaling pathways also regulate the induction of starvation-induced autophagy, mainly mTOR and AMPK. mTOR forms two distinct complexes: mTORC1 contains Raptor while mTORC2 contains Rictor. mTORC1 is responsible for sensing the cellular nutritional and energy status, and regulating autophagy (79,113). In higher eukaryotes, the mechanism by which mTOR negatively regulates autophagy is less understood. The mammalian counterpart of the initiator complex is the ULK1-ATG13-FIP200-ATG101 complex (81,82,114). FIP200 is the function counterpart of Atg17 while ATG101 has no functional equivalent in the yeast system (106,115). Under nutrient rich conditions, mTORC1 associates with the ULK1 complex via direct interaction between ULK1 and Raptor, and phosphorylates both ULK1 and ATG13 (81,82,116). Subsequently, upon mTORC1 inhibition, ULK1 and ATG13 are rapidly dephosphorylated; the ULK1 kinase activity increases and facilitates auto phosphorylation and that of its binding partners ATG13 and FIP200; and autophagy is induced.

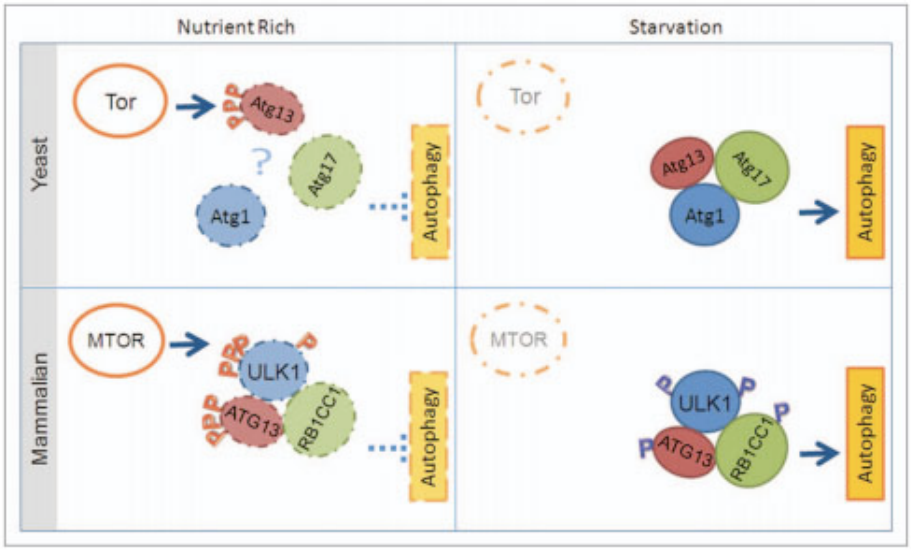

Figure 1.3 Tor/mTOR regulate the induction of autophagy by impinging on the Atg1/ULK1 complex. In yeast, Tor inhibits the induction of autophagy by hyper-phosphorylating Atg13 and preventing subsequent association of the Atg1 complex. Once Tor is inactivated, Atg13 is dephosphorylated, allowing for the formation of the Atg1 complex and downstream autophagy induction. In mammals, mTOR extends inhibitory phosphorylations on both ATG13 and ULK1; however, these phosphorylations don't modulate the formation of the ULK1 complex, which is constitutively formed. Once mTOR is inactivated, the inhibitory phosphorylations are dephosphorylated, ULK1 extends activating phosphorylations on itself and its' binding partners, and autophagy is activated. Reprinted from Wong, P. M., Puente, C., Ganley, I. G., and Jiang, X. (2013) The ULK1 complex: sensing nutrient signals for autophagy activation. *Autophagy* **9**, 124-137.

In contrast to the yeast Atg1 complex, the mammalian ULK1-ATG13-FIP200-ATG101 complex is stable, irrespective of nutrient conditions, and forms a ~3-MDa complex (Figure3 1.3) (81). As such, it is not clear if and how mTORC1-mediated phosphorylation of ATG13 controls the autophagy initiation function of the ULK1 kinase complex. Although TORC1-dependent phosphorylations have been mapped in yeast Atg13, no corresponding mTORC1-dependent phosphorylations have been identified in mammalian ATG13. mTORC1 phosphorylates ULK1 at Ser-757 and Ser-638 (117-119). These phosphorylations are through to be important in inhibiting the kinase activity of ULK1 and increasing the interaction between mTORC1 and ULK1.

mTORC1 is not the only kinase that regulates autophagy. In fact, AMP-activated protein kinase (AMPK), the energy-sensing kinase, phosphorylates ULK1 and possibly ATG13. As such, the ULK1 kinase complex needs to integrate multiple signals into a coherent autophagic response. The role of AMPK in autophagy appears to be more complicated than that of mTOR. On one hand, AMPK has been shown to be a positive regulator of autophagy, especially under energy-depriving, AMPK-activating conditions like glucose starvation. Under glucose starvation, AMPK promotes autophagy by mediating activating phosphorylations on ULK1 at Ser-317 and Ser-777 (118). These phosphorylations promote glucose-starvation-induced autophagy by activating the kinase activity of ULK1 (118). In fact, AMPK can bind the S/T domain of ULK1 and this binding domain does not overlap the binding regions of FIP200 or ATG13. Interestingly, mTOR

can inhibit the interaction between AMPK and ULK1 by phosphorylating the S/T domain of ULK1 at Ser-757, thereby preventing ULK1 activation by AMPK (118). AMPK can additionally phosphorylate ULK1 at Ser-555 and Ser-637 (120). Phosphorylation of ULK1 at Ser-555 is suggested to recruit the phospho-binding protein 14-3-3 (121). These phosphorylations are functionally important in mitochondrial homeostasis, cell survival during starvation, and degradation of p62 an autophagy adaptor (120). Conversely, another study has implicated AMPK as a negative regulator of ULK1. In this instance, nutrient-dependent phosphorylation of ULK1 at Ser-757 by mTOR is required for the ULK1/AMPK interaction. Upon starvation, an ULK1 S757A mutant can induce autophagy much faster compared to the wild-type (119). Overall, the role of the cellular energy sensor (AMPK) in regulating autophagy is less defined than mTORC1.

1.4 Relaying the autophagic signal

In order to further understand the molecular mechanisms that govern autophagy induction and progression, it is imperative that we identify and characterize ULK1 substrates. It is clear that ULK1 substrates must be critical to the progression of autophagy because kinase-dead ULK1 and ULK2 function as dominant-negative mutants by suppressing the formation of ATG16L1 and LC3 punctate (114,122). However, ULK1 may not be essential for all forms of autophagy. In fact, it has been reported that certain forms of selective autophagy proceed without the involvement of the ULK1 complex (87). The identification of biologically relevant

targets will expand our understanding of the autophagic process and the role of ULK1 beyond facilitating autophagy induction.

There have been *bona fide* efforts to identify Atg1/ULK1 substrates. One approach used an arrayed degenerate peptide library to identify the optimal ULK1 consensus motif. ULK1 strongly prefers serine over threonine as the phospho-acceptor site, a Leu or Met residue at the -3 position, hydrophobic residues at the +1 and +2 positions, and is not proline-directed (123). Unfortunately, the identified consensus motif is relatively loose, so it can't be utilized to identify novel proteins that mediate autophagy. However, several known ATG proteins contain the consensus sequence, and the relevant *in vivo* phosphorylations were identified by a subsequent co-overexpression with ULK1 wild-type or kinase-dead followed by mass spectrometry. Multiple ULK1-dependent phosphorylations were identified on Beclin1 Ambra1, ATG101 and VPS34; however, none were demonstrated to be functionally required for autophagy (123). Several reports have identified ATG13 and FIP200 as targets of ULK1. However, the location and function of the ULK1 phosphorylation sites on FIP200 remain unknown. One ULK1-depdent phosphorylation has been described on ATG13: S318. Phosphorylation of ATG13 S318 is though to mediate mitophagy (124). The identification of the mammalian counterparts of the autophagy yeast genes facilitated the modulation of this pathway in animal models, which ultimately uncovered the pivotal role of autophagy in the pathophysiology of disease.

1. 5 Autophagy in the pathophysiology of disease

In unicellular organisms, autophagy evolved to sustain cellular metabolism, under nutrient-deficient conditions. In mammals, the function of autophagy has expanded to encompass other functions that are critical in development and disease. Autophagy was first connected to human diseases by the identification of *Beclin 1,* a tumor suppressor gene, as the mammalian counterpart of *Atg6* (53). *Beclin 1* is located in a tumor susceptibility locus that is mono-allelically deleted in up to 40-75% of ovarian and breast cancers, which results in lower expression of Beclin 1 protein (53,125). The exogenous expression of *Beclin 1* activated autophagy in MCF7 cells, inhibited *in vitro* cellular proliferation and abrogated tumorigenesis in mice (53). This finding was followed by a series of studies connecting autophagy to various pathophysiological conditions, including pathogen infection, neurodegeneration, and cancer.

Pathogen infection

Aside from its ability to degrade intracellular components, autophagy can also mediate the degradation of invading pathogens, including viruses, parasites and bacteria. The first evidence that autophagy is involved in the clearance of bacteria was provided by Nakagawa and colleagues (126). Using *Atg5* -/- embryonic stem cells, autophagy was demonstrated to function as an innate immune defense system, which mediates the degradation of pathogenic bacteria, such as group A Streptococcus (126). The selective degradation of bacteria through autophagy is known as xenophagy. As opposed to bulk degradation,

xenophagy is mediated by a subset of pattern recognition receptors called SQSTM1/p62-like receptors, which include NDP52 and OPTN. These receptors recognize ubiquitinated substrates and facilitate their recruitment to the autophagosome by interacting with LC3 (127). For example, NDP52 facilitates the autophagic degradation of cytoplasmic *S. typhimurium*. Cells lacking this receptor show an accumulation of ubiquitinated bacteria in the cytosol (128). Aside from bacteria, autophagy can also selectively degrade viruses. The first study to implicate autophagy in the selective degradation of viruses used the herpes simplex virus (HSV-1) (129). It quickly became apparent that some bacteria, such as *Coxiella burnetti* and *Legionella pneumophila*, and viruses, such as poliovirus, have co-opted the autophagic process for their own replicative advantage (130). In addition to facilitating the direct degradation of pathogens, autophagy also functions to relay pathogenic ligands to the immune system. In fact, in antigen presenting cells autophagosomes continuously fuse with MHC class-II loading compartments, and in doing so, deliver antigens for presentation to CD4(+) T cells (131). As such, autophagy functions as a multi-pronged defense against pathogen infection.

Neurodegeneration

The hallmark of neurodegenerative disorders is the formation of disease-associated aggregated proteins. For example, Alzheimer's Disease is defined by neurofibrillary tangles and Aβ-amyloid plaques while Parkinson's Disease is defined by Lewy bodies (132). Since proteasome-mediated degradation requires

substrates to be unfolded, these large aggregates are poor substrates. Instead, these aggregates are degraded by the autophagic process. The accumulation of autophagosomes in neurons is associated with neurodegenerative diseases, including Parkinson's disease and Alzheimer's disease (133-135). Neural-specific deletions of ATG genes were used to uncover a central role for autophagy in suppressing neurodegeneration (136). Mice with a neural-specific deletion of *Atg5* accumulate protein aggregates and inclusions, and demonstrate with progressive deficits in motor function. As such, the continuous removal of aggregates through autophagy prevents the accumulation of abnormal proteins, which can disrupt normal neural function (136). These results were mirrored by experiments done using mice lacking *Atg7* in the central nervous system (137). These studies highlight the homeostatic function of autophagy in neurons, and suggests that basal autophagy functions to remove aggregates, which can form even in the absence of aggregate-prone protein variants. The accumulation of autophagosomes in neurodegenerative diseases has prompted questions about autophagy's role in the pathogenesis of these diseases. In an Alzheimer's brain, there is a significant accumulation of immature autophagic vesicles, which suggests that the transport of these vesicles and their fusion to lysosomes is impaired (138,139). These vesicles, which are enriched in APP and PS1, become a major intracellular reservoir of β-amyloid peptides (134). The critical role for autophagy in the Aβ secretion is underscored by the decrease in plaque formation, in APP transgenic mice lacking *Atg7* in forebrain neurons (140). As such, the role of autophagy in neurodegeneration is complex. However, multiple

studies have indicated that the modulation of autophagy can provide therapeutic value (141,142). It is important to note that in diseases with impaired autophagosome clearance, therapeutics that induce autophagy might be more deleterious than beneficial.

Cancer

The role of autophagy in cancer is paradoxical. Autophagy was initially thought to function as a tumor suppressor. This concept was derived from the identification of *Beclin 1* in a tumor susceptibility locus that is mono-allelically deleted in up to 40-75% of ovarian and breast cancers (53,125). The tumor suppressive function of autophagy is mediated by its function in protein and organelle quality control. The removal of damaged mitochondria, and the ensuing reactive oxygen species (ROS) protects cells from oxidative stress, DNA damage and instability, known causes of cancer initiation and progression (143,144). Autophagy sustains metabolism, during metabolic stress, which serves to protect the genome. Conversely, autophagy can function as a tumor promoter. Cancer cells are particularly reliant on autophagy. For example, autophagy is upregulated in hypoxic tumor regions, where it promotes tumor cell survival; inhibition of autophagy under these conditions, promotes tumor cell necrotic death *in vitro* and *in vivo* (145). The role of autophagy in promoting tumorigenesis is underscored by its function in RAS-transformed cancer cells. Deletion of *Atg7* in non-small-cell lung cancer (NSCLC) cells with $KRAS^{G12D}$ activation alters the cell fate from adenomas and carcinomas to oncocytomas, which are benign

neoplasm (146). The dependence of RAS-transformed cancer cells on autophagy to promote tumorigenesis led to the concept of “autophagy addiction” (147,148). The dependence of these cells on autophagy could potentially be exploited for therapeutic benefit. In fact, this theory suggests that the mutation status of RAS in tumors might be used to select patients who might benefit from co-treatment with autophagy-inhibiting drugs. Unfortunately, several studies have shown that the regulation of autophagy and chloroquine sensitivity by oncogenic RAS *in vitro* is context-dependent (149). Clearly, more research is needed. Eventually, in order to fully realize the therapeutic potential of modulation autophagy, there needs to be selective activators and inhibitors of the pathway.

1.6 Thesis goals

In order to functionalize our current knowledge of autophagy in human disease, we have to complete our understanding on how the ULK1 complex senses and relays the autophagic signal downstream to the ATG core machinery. Although mTOR is an established negative regulator of autophagy, the molecular details of this inhibition remain elusive.

In Chapter 2, I identify mTOR- and AMPK-dependent phosphorylations on ATG13, and establish their role in regulating the induction of starvation-induced autophagy. The lack of the dynamic association-dissociation between ULK1 and ATG13 stipulates that mammalian autophagy must be initiated differently from that in yeast. I establish that although these phosphorylations don't regulate the composition of the ULK1 complex, they regulate the localization of the ULK1 complex to punctate and the kinase activity of ULK1.

In Chapter 3, I describe a mass spectrometry quantitative phospho-proteomics study to identify novel substrates of the ULK1 kinase, in starvation-induced autophagy. This study identified sites on FIP200, the ULK1 binding partner. Additionally, I verified two proteins as ULK1 substrates in an *in vitro* kinase assay: GLIPR2 and ARHGEF2. I was able to demonstrate that ARHGEF2 is a novel negative regulator of autophagy.

In Chapter 4, I summarize the unanswered questions raised by the work that I

describe in this dissertation and include some speculation for further experimental research. In addition, I explore the possibility of potentiating the basal rate of autophagy by removing the inhibitory phosphorylations on the ULK1 kinase complex. As we begin to define and understand the molecular mechanisms that define the induction of autophagy, we must consider the pronounced implications of modulating autophagy in human aging and age-related diseases, such as neurodegeneration.

CHAPTER 2. NUTRIENT-REGULATED PHOSPHORYLATION OF ATG13 INHIBITS STARVATION-INDUCED AUTOPHAGY

2.1 Introduction

Recent studies have suggested that mTOR negatively regulates autophagy in mammalian cells by impinging inhibitory phosphorylations on the ULK1 kinase complex. Specifically, mTOR was demonstrated to phosphorylate mouse-derived ULK1 at Ser-637 and Ser-757 (118,119). However, no studies have explored the role of mTOR-driven phosphorylation on the ULK1 binding partners, particularly ATG13, in regulating the induction of autophagy. Studies in yeast have implicated TOR-mediated phosphorylation of Atg13 as the main regulatory component of the initiator complex.

In addition to mTOR, ATG13 is also a substrate of ULK1. Recently, ULK1-dependent phosphorylations on ATG13 were mapped to Ser-318. Phosphorylation of ATG13 at Ser-318 is required for efficient autophagy-mediated clearance of mitochondria (81). However, no ULK1-dependent phosphorylations on ATG13 have been implicated in regulating the induction of starvation-induced autophagy.

ATG13 is phosphorylated by kinases known to have inhibitory and promoting roles in autophagy. Therefore, I hypothesized that mammalian ATG13 might have a vital role in regulating autophagy. However, the phosphorylation residues on mammalian ATG13 by mTOR have not been identified. In this study, I sought

to identify these sites and characterize the function of these phosphorylation events.

2.2 Results

ATG13 is a phospho-protein with two nutrient-regulated phosphorylation sites

Before purifying ATG13, I wanted to confirm its starvation-dependent mobility shift. In cultured mouse embryonic fibroblasts (MEFs), amino acid starvation or pharmacological inhibition of mTOR resulted in the appearance of a fast-migrating form of ATG13 assayed by western blot (Figure 2.1 A). Treatment with calf intestinal alkaline phosphatase (CIP) of cell lysates from cells grown in full-media yielded faster migrating bands; indicating that the gel-shifts are due to altered phosphorylation. This result suggests that ATG13 is phosphorylated when cells are cultured under nutrient-rich condition, likely in an mTOR-dependent manner, and is dephosphorylated upon starvation. Although ATG13 displays a downward mobility shift during starvation, ULK1 is phosphorylating ATG13 during starvation. I generated a MEF cell line stably expressing ATG13 with an N-terminal FLAG and S-tag (F/S-ATG13). I expressed F/S-ATG13 to near endogenous levels. This ectopically expressed F/S-ATG13 retained the ability to undergo a starvation-induced electrophoretic mobility shift (Figure 2.1 B).

A previous effort to identify mTOR-dependent phosphorylations on ATG13 identified one phospho-peptide; however, overall the phosphorylation level of ATG13 did not respond to nutrient availability (74). As such, I purified ATG13 under partially denaturing conditions, in order to better preserve the phosphorylation status. I coupled this strategy with a S/FLAG tandem

immunoprecipitation to improve purity. When I analyzed the tandem immunoprecipitation by western blotting or silver staining, I saw a clear hyper-phosphorylated band for ATG13 during growing conditions, and then a drastic dephosphorylation during starvation (Figure 2.1 C, D). In order to identify these nutrient-regulated phosphorylation sites, we conducted nanoscale liquid chromatography coupled to tandem mass spectrometry (nano-LC-MS/MS). The MS analysis covered nearly 80% of the ATG13 protein sequence.

Under nutrient rich conditions, multiple distinct phosphorylated sites were identified, including Ser-44, Ser-224, Ser-258, Ser-355 and Ser-360 (Figure 2.2 A). These residues correspond to the mouse ATG13 isoform 1 sequence (identifier = Q91YI1-1). I decided not to pursue characterizing the phosphorylation at Ser-44 and Ser-360 because the percent of phosphorylated peptide is low, 1.6% and 5.2%, respectively. I decided not to pursue characterizing the phosphorylation at Ser-355 because the adjacent residue was already reported as a site of ULK1 phosphorylation (81). Since the mass spectrometry data showed ambiguity on the exact phosphorylated residue, I surmised that the site that I identified is known to be phosphorylated by ULK1. However, since ULK1 kinase activity is activated by starvation, a putative ULK1 site should increase in percent phosphorylated with the induction of starvation. In fact, upon starvation, the aforementioned site increases in phosphorylation, as detected by western blotting (81).

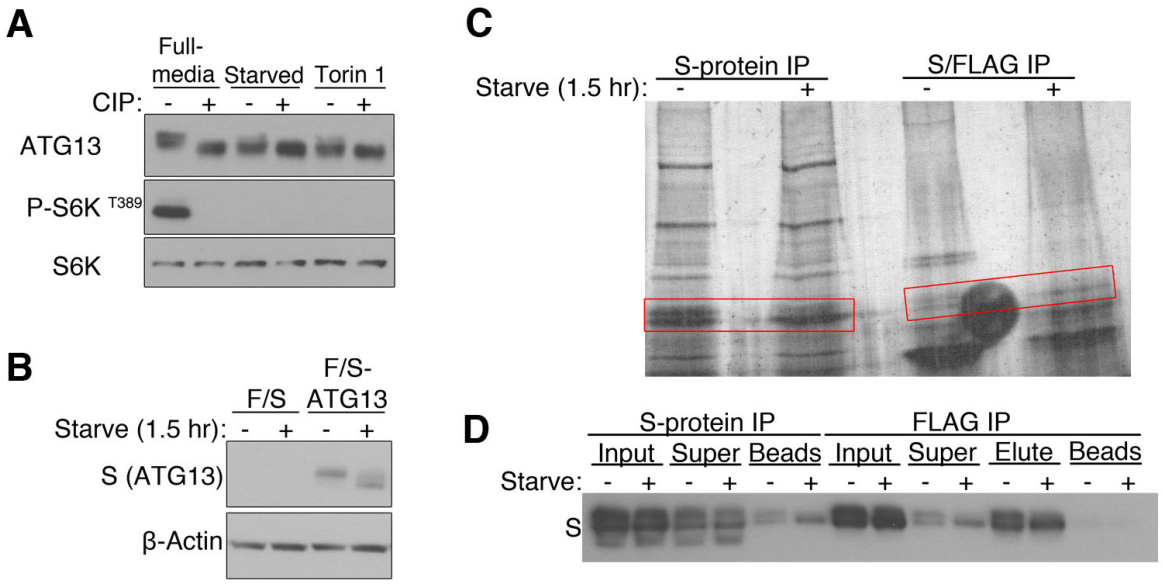

Figure 2.1 Optimizing F/S-ATG13 purification, in order to identify nutrient-regulated phosphorylations. (**A**) mTOR-mediated phosphorylations on ATG13 are dephosphorylated during autophagy. Wild-type MEF cells were placed in full-media, starved of amino acids and serum for 2 hours or treated with 1 μM Torin 1 for 2.5 hours. The lysates were subjected to a phosphatase assay and analyzed by western blotting. (**B**) Exogenously expressed FLAG-S-ATG13 exhibits starvation-induced electrophoretic mobility. F/S-ATG13 was stably expressed in MEF wild-type cells using a retroviral packaging system, followed by puromycin selection. Cells were placed in full-media or starvation media for 1.5 hours. (**C**) F/S-ATG13 was purified using a S-protein IP or a tandem S/FLAG IP. The purity of the elutions and phosphorylation status of ATG13 were analyzed by silver staining. (**D**) The IP efficiency (equal percentage loading) and the phosphorylation status of ATG13 were tracked by western blotting.

Since the phosphorylation at Ser-355 decreases with starvation, it may be possible that some phosphorylation at Ser-355 is independent of ULK1, and is mediated by a kinase that is inactivated by amino acid and serum starvation.

I decided to further characterize phosphorylation at Ser-224 and Ser-258 because a large portion of the identified phospho-peptides were phosphorylated under unstarved conditions, 27% and 85%, respectively (Figure 2.2 A). I further found that Ser-224 and Ser-258 sites are dephosphorylated upon starvation; we compared the integrated selected ion current chromatogram (monoisotopic mass +/- 5 ppm) of phosphorylated peptide versus the integrated selected ion current chromatogram (monoisotopic mass +/- 5 ppm) of the nonphosphorylated peptide under full media or starvation media (an internal ATG13 peptide TVQVIVQAR was used to normalize the integrated peak areas across the different conditions) (Figure 2.2 B, C). In doing so, I detected a 68% reduction in phosphorylated Ser-224 and a 97% reduction in phosphorylated Ser-258, under starvation conditions (Figure 2.2 A).

Although the yeast TOR-mediated Atg13 phosphorylation sites are known, it was not possible to extrapolate that information to higher eukaryotes because of the extremely limited homology between yeast Atg13 and that of mammals. Indeed, using a ClustalW multiple sequence alignment analysis, we failed to detect any yeast serine or threonine conserved with Ser-224 or Ser-258. Both Ser-224 and

Ser-258 are conserved in higher eukaryotes (Figure 2.2 D). Ser-258 is also conserved in *Caenorhabditis elegans*.

To further determine whether the putative sites are nutrient-regulated, I tested whether we could abrogate the starvation-induced increase in gel migration mobility of ATG13 by mutating the residues to alanine. Interestingly, even when cells were cultured in full-media, the Ser-258 alanine mutant migrated as fast as starvation-treated wild-type ATG13, whereas substitution of Ser-224 to alanine had no effect on gel migration shift regardless culture condition (Figure 2.3 A). In fact, I could abrogate the starvation-induced dephosphorylation of ATG13 by mutating Ser-258 to aspartic acid or glutamic acid (Figure 2.3 B). Conversely, mutating Ser-224 to glutamic acid or aspartic acid did not affect the starvation-induced dephosphorylation. These results indicate that the phosphorylation status of Ser-258 but not Ser-224 accounts for the migration shift of ATG13.

ATG13 is a phospho-protein that senses amino acid starvation

To further analyze ATG13 phosphorylation, we generated phospho-antibodies specific for pSer-224 and pSer-258. I validated these antibodies by ectopically expressing ATG13 alanine and glutamic acid mutants and monitoring the phosphorylation under full-media or starved conditions. The pSer-258 and pSer-224 antibodies recognized the wild-type protein under full-media conditions, and showed a drastic decrease in signal upon starvation (Figure 2.4 A).

A

Residue	phospho-peptide	% phosphorylated		% Change
		Unstarved	Starved	
Ser-44	SSSSPTGSDWFNLAIK	1.6	1.6	0
Ser-224	TPPIMGIIIDHFVDRPYPSSSPMHP CNYR	27.2	8.7	-68
Ser-258	TAEDAGVAYPSVEDSQEVCTTSFS TSPPSQLMVPGK	84.7	5.9	- 97
Ser-355	LVMHMPSDGTHCAATPSSSEDTE TVSNSSEGR	34.7	26.3	-24
Ser-360	ASPHDILETIFVR	5.2	3.5	-32

B

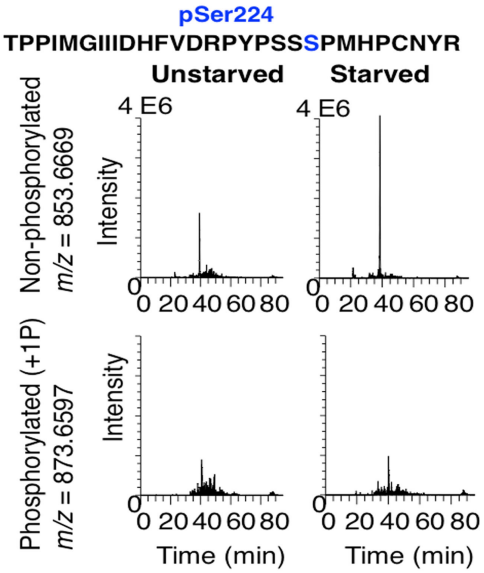

C

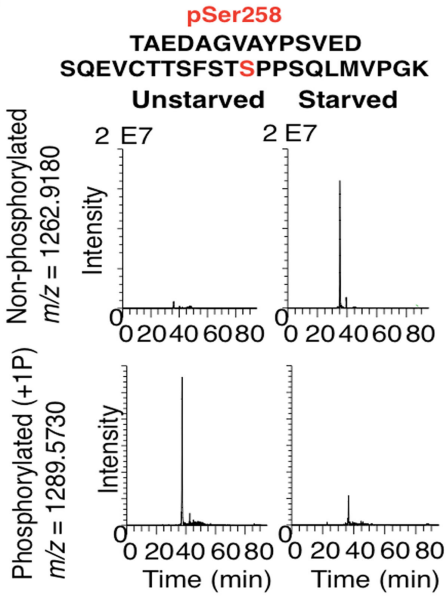

D

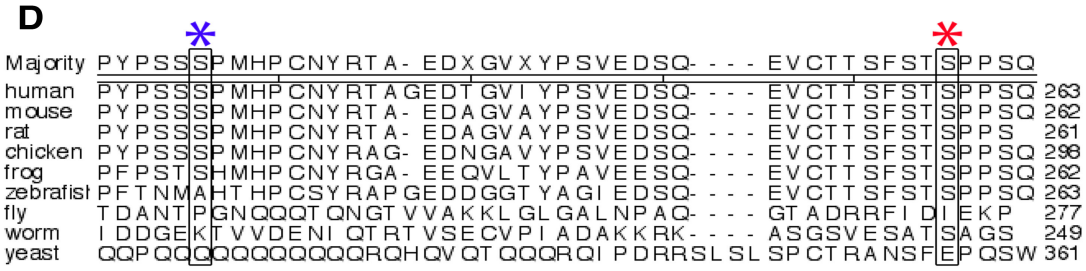

Figure 2.2 ATG13 is a nutrient regulated phospho-protein. (**A**) A summary of the ATG13 phospho-peptides identified. Percent phosphorylated indicates the portion of peptides identified that are phosphorylated over the total number of peptides identified. Percent change indicates the change in the portion of phosphorylated peptides under full-media to starvation conditions. (**B**) and (**C**) Selected ion current chromatograms of putative phosphorylation sites at Ser224 and Ser258. Tandem affinity tag immunoprecipitation and nanoscale liquid chromatography coupled to tandem mass spectrometry (nano-LC-MS/MS) were used to identify ATG13 phosphorylation sites under full media or starvation media. (**D**) ClustalW alignment of ATG13 homologs. The sequences used are: human-NP_001192048.1; mouse-XP_006499950.1; rat-NP_001258141.1; chicken-XP_421116.3; frog-NP_001096420.1; zebrafish-NP_956727.1; fly-NP_649796.1; worm-P34379; yeast-A6ZX59. The blue asterisk denotes Ser-224. The red asterisk denotes Ser-258.

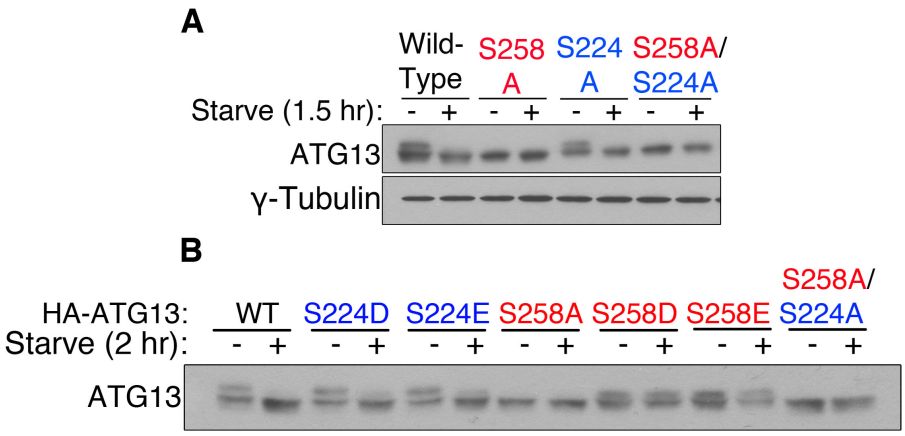

Figure 2.3 Phosphorylation at Ser-258 controls the starvation-induced mobility shift of ATG13. Analyzing the contribution of phosphorylation at Ser-224 and Ser-258 to the electrophoretic mobility of ATG13. *ATG13*-knockout MEFs were stably reconstituted with ATG13 wild-type, (**A**) phospho-mutants and (**B**) phospho-mimetics using a retroviral packaging system. Cells were placed in full-media or starvation media, followed by an analysis of ATG13 shift patterns by western blotting.

Mutation of Ser-258 to alanine or glutamic acid abrogated detection by the pSer-258 antibody. Similarly, mutation of Ser-224 to alanine or glutamic acid abrogated detection by the pSer-224 antibody. Importantly, mutation of Ser-224 did not affect detection by the pSer-258 antibody, and vice versa, indicating that these two phosphorylation events are not inter-dependent. These results validate that ATG13 is phosphorylated *in vivo* at Ser-224 and Ser-258 under full-media conditions, and upon starvation these sites are dephosphorylated. To note, the electrophoretic mobility of ATG13 is drastically different when overexpressed in 293T cells. In this instance, ATG13 does not exhibit starvation-induced dephosphorylation. In addition, mutation of Ser-224 to a phospho-mimetic residue results in a retarded mobility state. In fact, when both phosphorylation sites are mutated to phospho-mimetic residues, ATG13 exhibits a hyper-phosphorylation mobility state(Figure 2.4 A).

To further dissect the trigger that induces dephosphorylation, I performed either serum starvation or amino acid starvation. Both sites demonstrate a drastic dephosphorylation upon amino acid starvation and there is no perceivable dephosphorylation under serum starvation alone (Figure 2.4 B). This indicates these two phosphorylation events are solely dictated by amino acid status but not able to sense growth factor signaling.

To further establish the validity of these sites, I monitored the phosphorylation status of ATG13 stably expressed in *ATG13* knockout MEFs. I monitored

dynamic phosphorylation changes at Ser-224 and Ser-258, in response to nutrient availability (Figure 2.4 C). pSer-258 exhibited an apparent dephosphorylation within only 15 minutes in starvation media, and no phosphorylation was detected by 60 minutes of starvation. On the other hand, pSer-224 exhibited a slower response to nutrient withdrawal. pSer-224 exhibited an apparent dephosphorylation by 60 minutes and there was still some residual phosphorylation by 120 minutes. Similarly, when cells were replenished with full-media, Ser-258 was rapidly phosphorylated starting at 15 minutes while phosphorylation at Ser-224 only increased after 60 minutes. The different kinetics of the phosphorylation between Ser-224 and Ser-258 is suggestive that these two sites are differentially regulated.

ATG13 is phosphorylated on Ser-258 by mTOR and on Ser-224 by the AMPK pathway

Since phosphorylation of Ser-224 and Ser-258 was sensitive to amino acid starvation, I examined whether the sites are phosphorylated by mTOR. We attenuated the mTOR signaling pathway using the following kinase inhibitors, Rapamycin, PI-103 and Torin 1. I found that pSer-258 was sensitive to inhibition by Rapamycin, an allosteric inhibitor of mTORC1, as well as to PI-103 and Torin 1, direct inhibitors of mTOR kinase activity (Figure 2.5 A). Importantly, ATG13 pSer-258 exhibited the same sensitivity to mTOR inhibition as ULK1 pSer-757, another target of mTOR.

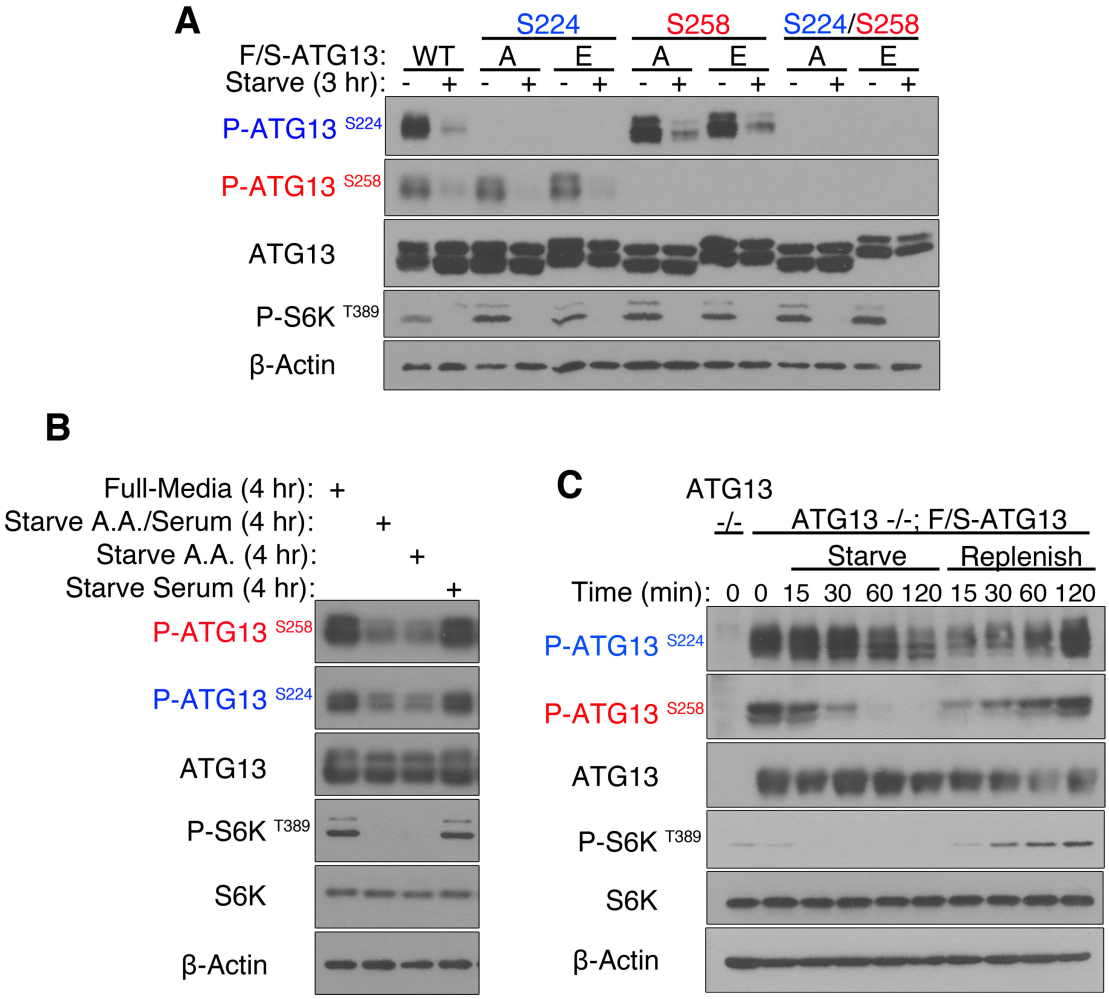

Figure 2.4 ATG13 dynamic phosphorylation at Ser-224 and Ser-258 senses amino acid starvation. (**A**) Phospho-antibodies were generated against ATG13 pSer-224 and pSer-258. To establish their specificity, HEK293T cells were transiently transfected with F/S-ATG13 wild-type, S224A, S224E, S258A, S258E, S224A/S258A or S224E/S258E. The cells were placed in full-media or starvation media for 3 hours. F/S-ATG13 was affinity S-tag immunoprecipitated using S-protein agarose beads and analyzed by western blotting. (**B**) ATG13 is dephosphorylated at Ser-224 and Ser-258 upon amino acid starvation. HEK293T cells were transiently transfected with F/S-ATG13 wild-type. The cells were placed in full-media, amino acid and serum-free media, amino acid-free media or serum-free media for 4 hours. F/S-ATG13 was affinity S-tag immunoprecipitated using S-protein agarose beads and analyzed by western blotting. (**C**) Phosphorylation of ATG13 at Ser-224 and Ser-258 is dynamic. *ATG13* knockout MEF cells were reconstituted by the stable expression of F/S-ATG13. The cells were starved for up to 120 minutes, after which they were replenished by switching to full-media, for the indicated amount of time.

In order to further establish that phosphorylation of Ser-258 is modulated by the mTOR signaling pathway, I compared the phosphorylation level of pSer-258 between TSC2-null ($TSC2^{-/-}$) and wild-type ($TSC2^{+/+}$) MEFs, under starvation or Torin 1 treatment (Figure 2.5 B). I observed that $TSC2^{-/-}$ MEFs, which have increased mTOR signaling, had higher levels of basal pSer-258, which persisted upon starvation. In the $TSC2^{-/-}$ MEFs, dephosphorylation of pSer-258 was only achieved by direct inhibition of mTOR through Torin 1 treatment. In contrast, in $TSC2^{+/+}$ MEFs, pSer-258 was sensitive to both starvation and Torin 1 treatment.

To distinguish if mTOR-regulated sites may be phosphorylated directly by mTOR or by kinases downstream of mTOR, I established an *in vitro* kinase assay. Ectopically overexpressed MYC-mTOR and F/S-ATG13 were immunoprecipitated from HEK293T cells and subjected to an *in vitro* mTOR kinase assay. I demonstrated that ATG13 was directly phosphorylated by mTOR on Ser-258 and this phosphorylation is inhibited by Torin 1 treatment (Figure 2.5 C).

Conversely, pSer-224 was unresponsive to mTOR inhibition. Interestingly, when I treated cells with the AMPK antagonist Compound C, pSer-224 was selectively dephosphorylated while pSer-258 was insensitive (Figure 2.5 A). AMPK functions as a nutrient and energy sensor in the cell. It is known to phosphorylate ULK1 on multiple sites (118,119).

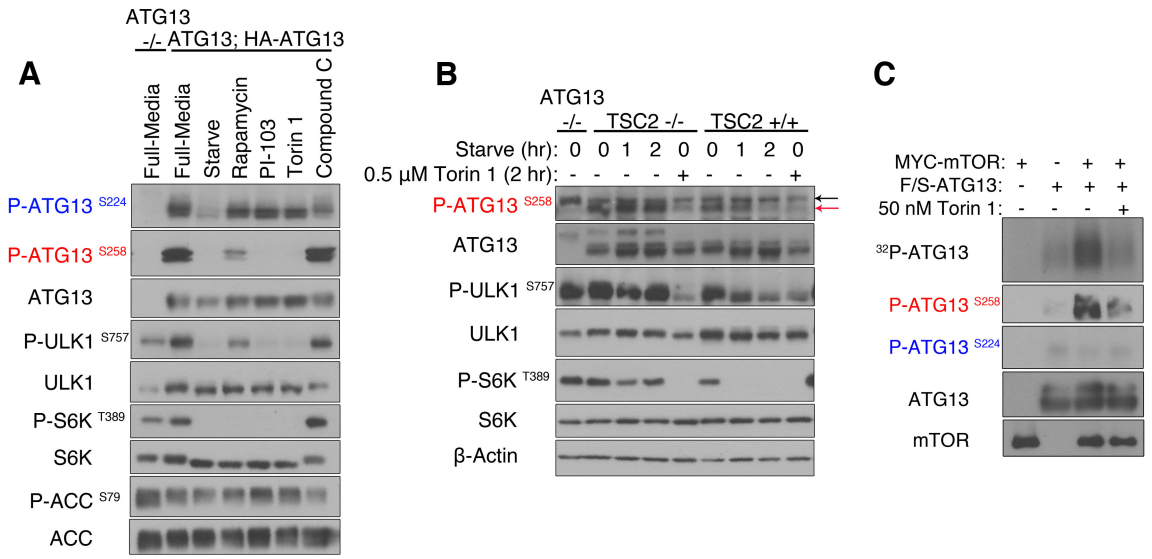

Figure 2.5 ATG13 is directly phosphorylated at Ser-258 by mTOR. (**A**) ATG13 pSer-258 is sensitive to pharmacological inhibition of mTOR. *ATG13* knockout MEF cells were reconstituted by the stable expression of HA-ATG13. The cells were either placed in full-media, starved, or placed in full-media with either 1 μM Rapamycin, 2 μM PI-103, 0.5 μM Torin 1 or 25 μM Compound C. (**B**) Endogenous ATG13 phosphorylation at Ser-258 in TSC2 -/- versus +/+ MEF cells. The black arrow indicates a non-specific band. The red arrow indicates pSer-258. (**C**) mTOR directly phosphorylates ATG13 at Ser-258. MYC-mTOR and F/S-ATG13 were separately transiently transfected in HEK293T cells, after 48 hours, the cells were placed in full-media or 4 hours of starvation media, respectively. The proteins were separately purified by affinity tag immunoprecipitation, and subjected to a mTOR kinase assay.

I then examined whether ATG13 phosphorylation at Ser-224 is modulated by the AMPK pathway. First, I found that upon amino acid and serum starvation, AMPK activity was diminished (Figure 2.6 A). This decrease in AMPK activity correlates with a concomitant decrease in pSer-224. This observation is consistent with previous publications showing that amino acid and serum-starvation cause a decrease of AMPK activity (119). I also modulated AMPK activity with glucose starvation, a known activator of AMPK activity (24). Upon glucose starvation, I observed an increase in phosphorylation of Ser-224 but not Ser-258 (Figure 2.6 B). To directly establish a requirement for the AMPK pathway in modulating the phosphorylation at Ser-224, I overexpressed exogenous ATG13 in AMPKα1/2-null MEFs. We found that immunoprecipitated F/S-ATG13 was phosphorylated at Ser-258 but not at Ser-224 (Figure 2.6 C). Therefore, the AMPK pathway selectively modulates phosphorylation at ATG13 Ser-224. Although ATG13 phosphorylation at Ser-224 is enhanced during glucose starvation, this event is probably not relevant to glucose starvation-induced autophagy. Functionally, starvation-induced autophagy is independent of the ULK1 complex (87,150).

Nutrient-Regulated ATG13 phosphorylations modulate starvation-induced autophagy

In order to assess the functional significance of ATG13 phosphorylation in regulating starvation-induced autophagy, I generated *ATG13*-/- MEFs by CRISPR-CAS9 approach. As expected, the *ATG13*-/- MEFs failed to undergo autophagy upon starvation (Figure 2.7 A).

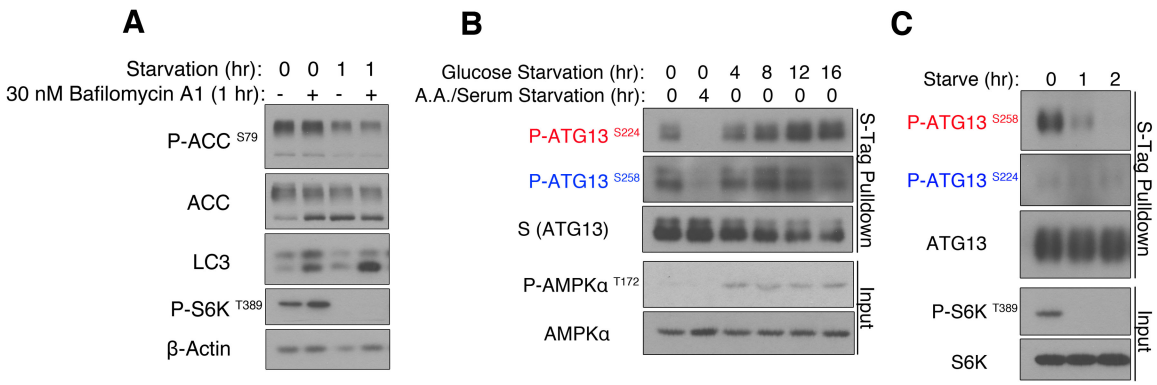

Figure 2.6 Phosphorylation at ATG13 Ser-224 is mediated by the AMPK pathway. (**A**) MEF wild-type cells were placed in full-media or amino acid and serum-starvation media for 1 hour. (**B**) HEK293T cells were transiently transfected with F/S-ATG13 wild-type. The cells were either placed in full-media or the appropriate starvation media for the indicated amount of time. F/S-ATG13 was affinity S-tag immunoprecipitated using S-protein agarose beads and analyzed by western blotting. (**C**) AMPK -/- MEFs were stably transduced with exogenous F/S-ATG13. The cells were placed in full-media or amino acid and serum-starvation media for up to 2 hours. F/S-ATG13 was affinity S-tag immunoprecipitated using S-protein agarose beads and analyzed by western blotting.

I subsequently reconstituted these cells by stably expressing ATG13 wild-type, combined phospho-deficient or phospho-mimetic mutants (Figure 2.7 B). I did not observe any change in the autophagy flux in cells expressing the combined phospho-mimetic mutant, as compared to cells expressing wild-type ATG13. Similarly, reconstitution with single site phospho-mimetic mutations did not alter the autophagy flux, relative to cells reconstituted with ATG13 wild-type (Figure 2.7 C). Since the phospho-antibodies could not recognize their respective phospho-mimetic mutants (Figure 2.4 A), these phospho-mimetic mutants may not recapitulate the properties of the specific phosphorylation events. In sharp contrast, cells expressing the combined alanine mutant induced a more robust autophagy response, relative to cells expressing ATG13 wild-type (Figure 2.7 B).

I decided to further evaluate autophagy induction in cells expressing the combined and single-site alanine mutations at Ser-224 and Ser-258. I observed significantly more GFP-LC3 punctate when both phosphorylation sites were mutated to alanine (Figure 2.8 A). On the other hand, single mutation of either site did not affect the autophagy flux, suggesting that ATG13 integrates signals of nutritional deficiency from multiple pathways into a coordinated autophagic response. These results were corroborated by western blotting for endogenous LC3: a greater depletion of LC3-I was observed when both phosphorylation sites were mutated to alanine whereas single mutation of either site did not appreciably affect the autophagy flux (Figure 2.8 B). I also observed a greater depletion of p62 in cells expressing the combined alanine mutant.

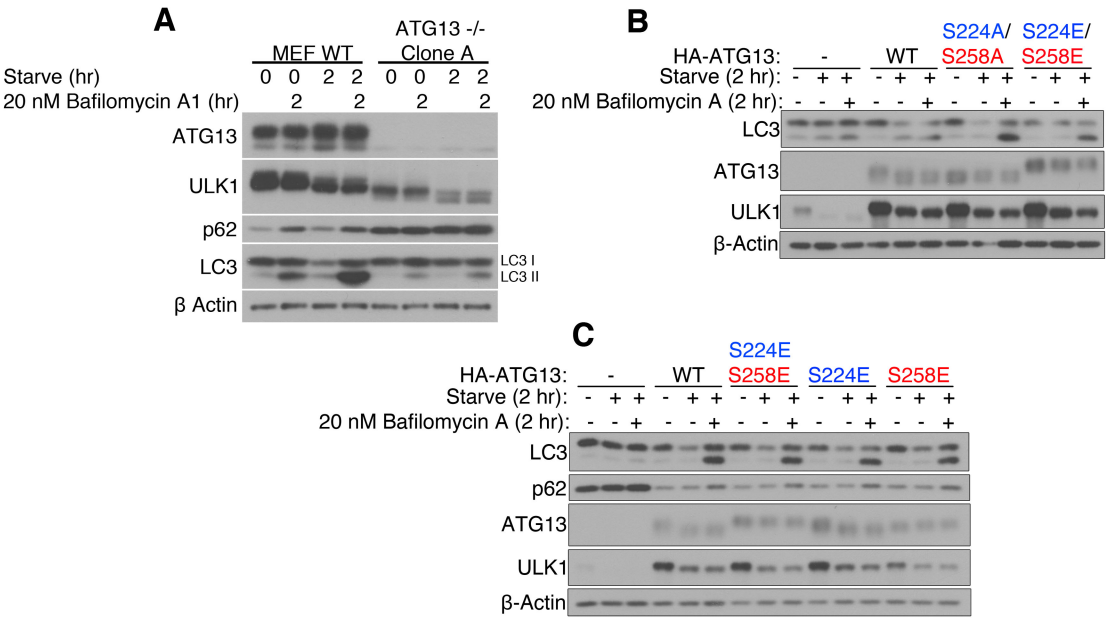

Figure 2.7 Establishing a reconstitution system to analyze the functional relevance of ATG13 phosphorylation at Ser-224 and Ser-258. (**A**) *ATG13* knockout MEFs were generated by CRISPR-CAS9. The cells exhibit a lack of starvation-induced autophagy. (**B**) *ATG13* -/- MEFs were reconstituted by the stable expression of F/S-ATG13 wild-type, S224A/S258A or S224E/S258E. Cells were starved for 2 hours, with or without Bafilomycin A1. (**C**) *ATG13* -/- MEFs were reconstituted by the stable expression of F/S-ATG13 wild-type, S224E/S258E, S224E or S258E. Cells were starved for 2 hours, with or without Bafilomycin A1.

Additionally, I monitored the phosphorylation of ATG13 at Ser-318 with a phospho-antibody. ULK1 phosphorylates ATG13 on Ser-318, thus phosphorylation of this residue can be used as a read-out of ULK1 kinase activity in cells (124,151). Cells expressing the combined alanine mutant had higher levels of ATG13 pSer-318, as compared to cells expressing wild-type or single alanine mutant of ATG13 (Figure 2.8 B). Based on these results, I conclude that phosphorylation of ATG13 on Ser-224 and Ser-258 inhibits autophagy initiation, thus an unphosphorylatable mutant of ATG13 renders the ULK1 kinase complex to be more readily activated upon starvation, instead of waiting for these inhibitory phosphorylations to dissipate.

Interestingly, unlike starvation-induced autophagy, when Torin 1 was used to trigger autophagy, the combined mutant did not further potentiate autophagy compared to wild-type ATG13 (Figure 2.8 C). This result suggests that upon mTOR inhibition, the ATG13 mutant needs to work together with certain additional cellular events to potentiate autophagy, and such events are inducible by amino acid starvation but not by pharmacological inhibition of mTOR. Indeed, it has been recently demonstrated that amino acid starvation triggers both stimulation of protein phosphatase 2A (PP2A) and inhibition of mTOR; these two events coordinately lead to potent activation of ULK1 complex-dependent autophagy (152).

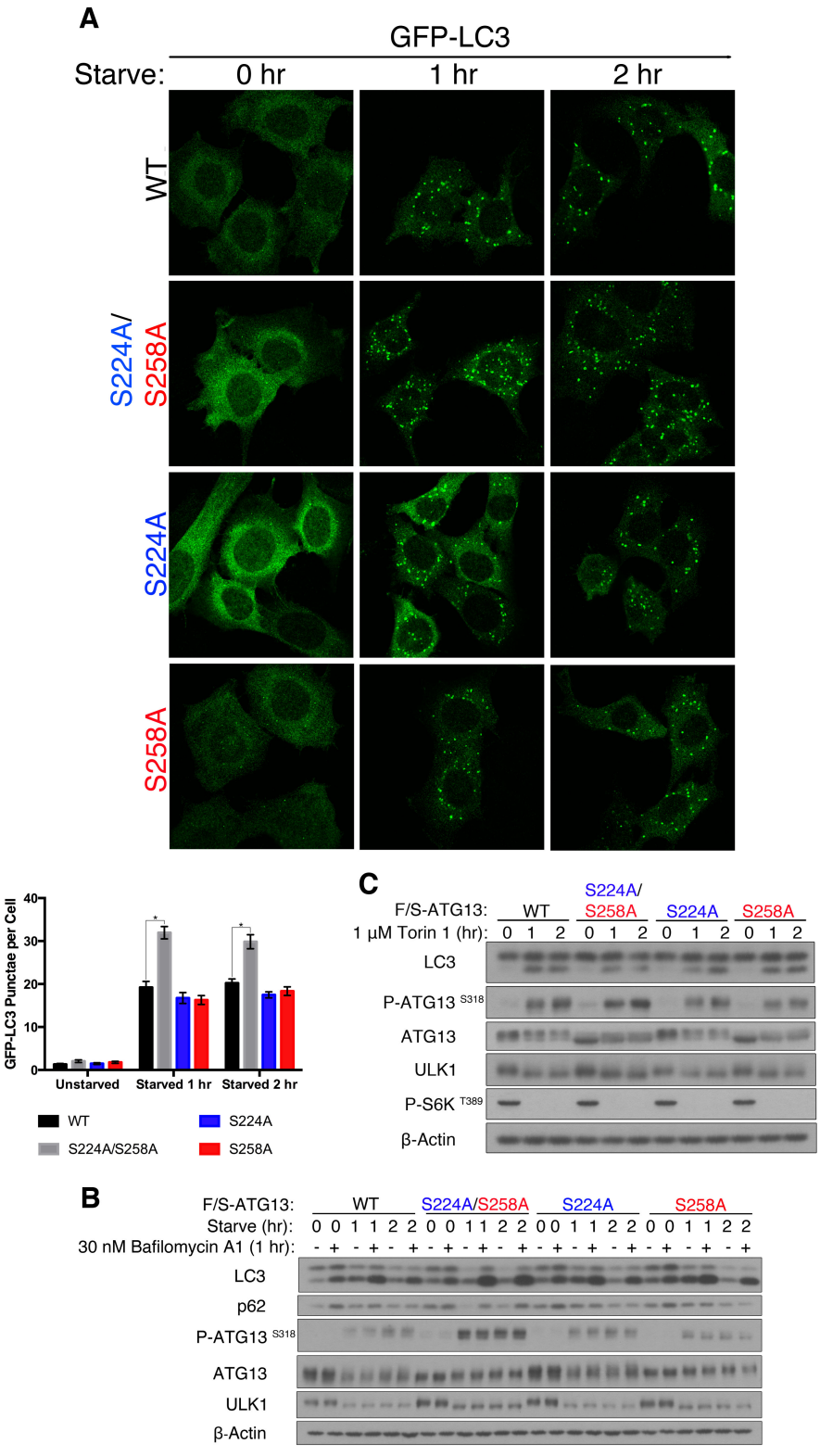
A
GFP-LC3
Starve:
0 hr
1 hr
2 hr
WT
S224A/
S258A
S224A
S258A
GFP-LC3 Punctae per Cell
40
30
20
10
0
Unstarved
Starved 1 hr
Starved 2 hr
WT
S224A
S224A/S258A
S258A
C
F/S-ATG13:
WT
S224A/S258A
S224A
S258A
1 μM Torin 1 (hr):
0 1 2 0 1 2 0 1 2 0 1 2
LC3
P-ATG13 S318
ATG13
ULK1
P-S6K T389
β-Actin
B
F/S-ATG13:
WT
S224A/S258A
S224A
S258A
Starve (hr):
0 0 1 1 2 2 0 0 1 1 2 2 0 0 1 1 2 2 0 0 1 1 2 2
30 nM Bafilomycin A1 (1 hr):
- + - + - + - + - + - + - + - + - + - + - + - +
LC3
p62
P-ATG13 S318
ATG13
ULK1
β-Actin

Figure 2.8 ATG13 phosphorylation at Ser-224 and Ser-258 negatively regulates the induction of autophagy. (**A**) *ATG13* -/- MEFs stably expressing GFP-LC3 were reconstituted by the stable expression of F/S-ATG13 wild-type, S224A/S258A, S224A, or S258A. The cells were placed in full-media or starvation media for 1 to 2 hours. The GFP-LC3 punctae were scored. There are significantly more GFP-LC3 punctae in cells expressing S224A/S258A compared to wild-type at one and two hour starvation, * $p < 0.001$. (**B**) *ATG13* -/- MEFs were reconstituted by the stable expression of F/S-ATG13 wild-type, S224A/S258A, S224A, or S258A. Starvation-induced autophagy was assessed by LC3-I to LC3-II conversion and p62 depletion. *In vivo* ULK1 kinase activity was assessed by phosphorylation of ATG13 at Ser-318. (**C**) Reconstituted *ATG13* -/- MEFs were subjected to 1 μM Torin 1-induced autophagy.

Nutrient-Regulated phosphorylation of ATG13 modulates the autophagic activity of ULK1

In order to understand the molecular mechanism by which nutrient-dependent phosphorylation on ATG13 regulates starvation-induced autophagy, I evaluated distinct properties of ULK1 that are regulated by ATG13, such as protein stability, cellular localization and enzyme activity. ULK1 is destabilized in *ATG13*-/- MEFs. When I reconstituted these cells by expressing wild-type ATG13, or its double-site or single-site alanine mutants, ULK1 was stabilized to comparable levels (Figure 2.8 B). Next, I analyzed the cellular localization of ULK1. Previous work has shown that upon starvation ULK1 translocates to punctae in an ATG13-dependent fashion (81). I analyzed endogenous ULK1 cellular localization using ULK1 immunofluorescence in *ATG13*-/- MEFs reconstituted with either wild-type ATG13 or its mutants. I observed that starvation induced a greater number of ULK1 punctae in cells expressing the double alanine mutant, as compared to cells expressing wild-type or single-site alanine mutants of ATG13 (Figure 2.9). This observation is also mirrored by the translocation pattern of ATG13 (Figure 2.10). Therefore, phosphorylation of ATG13 on Ser-224 and Ser-258 inhibits translocation of the ULK1 kinase complex. To further characterize the role of these phosphorylation events in modulating the ULK1 kinase complex, I evaluated their effect on protein interactions. Phosphorylation at Ser-224 and Ser-258 did not affect binding of ATG13 to ULK1 or ATG101 (Figure 2.11 A, B). This result is expected, as previous work has demonstrated that the ULK1 kinase complex is constitutively formed and insensitive to starvation (18).

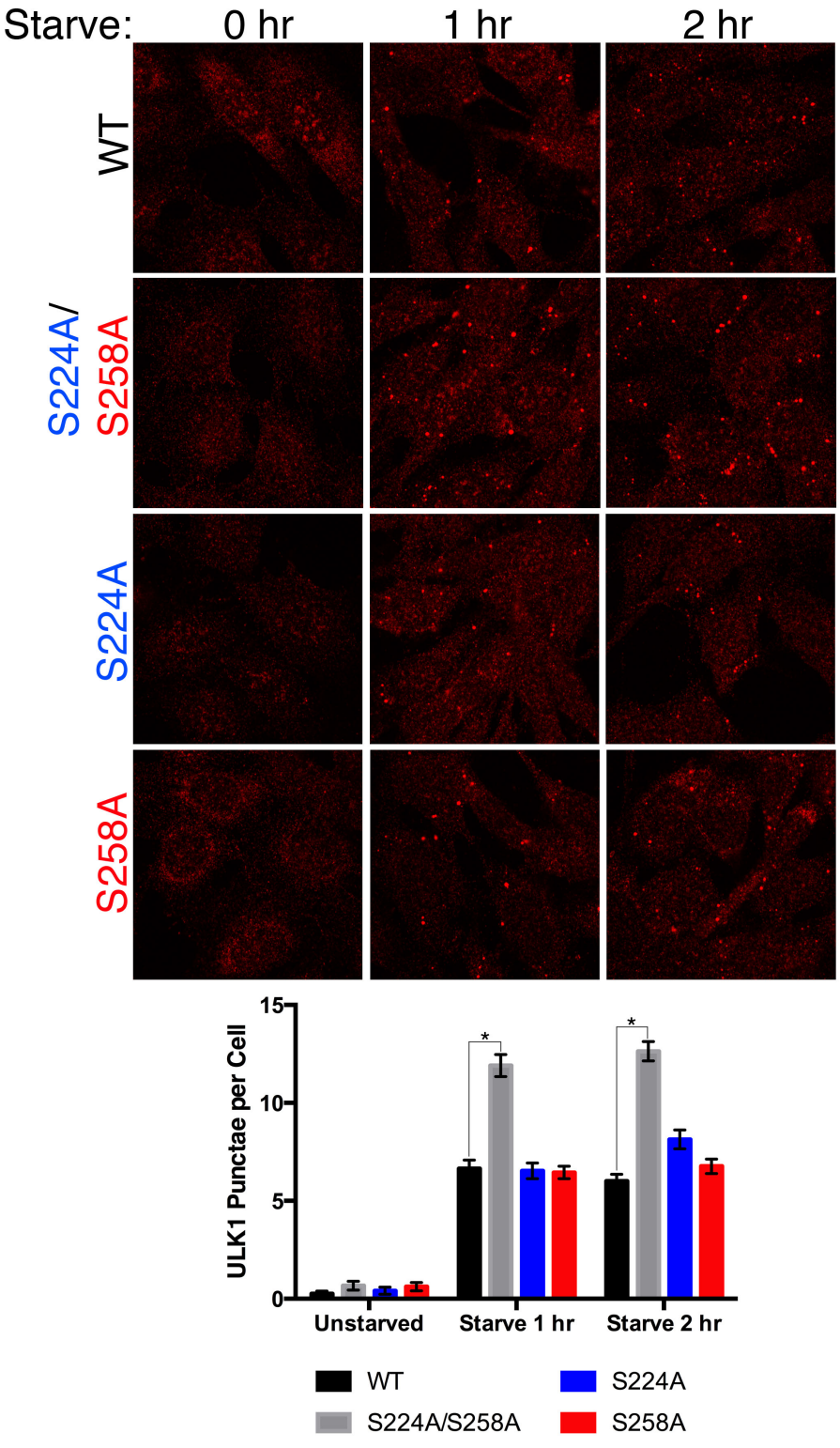
Starve:
0 hr
1 hr
2 hr
WT
S224A/
S258A
S224A
S258A
ULK1 Punctae per Cell
15
10
5
0
*
*
Unstarved
Starve 1 hr
Starve 2 hr
WT
S224A
S224A/S258A
S258A

Figure 2.9 Phosphorylation of ATG13 on Ser-224 and Ser-258 inhibits starvation-induced translocation of ULK1 to punctae. *ATG13* -/- MEFs were reconstituted by the stable expression of F/S-ATG13 wild-type, S224A/S258A, S224A, or S258A. *Top Panel:* The cells were placed in full-media or starvation media for 1 or 2 hours. Endogenous ULK1 immunofluorescence was used to image ULK1 punctae. *Bottom Panel:* There are significantly more ULK1 punctae at one and two hour starvation in cells stably expressing S224A/S258A as compared to wild-type, * $p < 0.001$.

ATG13 is known to stimulate the kinase activity of ULK1 (81). Using ectopically expressed F/S-ATG13 and HA-ULK1 complex affinity-purified by S-tag agarose beads, I confirmed that the complex containing wild-type ULK1 but not K46I (kinase inactive mutant) can phosphorylate the artificial substrate myelin basic protein (MBP) *in vitro* (Figure 2.11 A). To further evaluate the role of ATG13 phosphorylation in regulating ULK1 kinase activity, I compared the activation of ULK1 kinase activity when incubated with ATG13 wild-type or the combined alanine mutant. ULK1 bound with the alanine mutant exhibited higher kinase activity against MBP than ULK1 bound with wild-type ATG13, as determined by the incorporation of ^{32}P gamma phosphate to MBP (Figure 2.12 B). This result and that of cellular Ser-318 ATG13 phosphorylation (Figure 2.8 B) indicate that the nutrient-regulated phosphorylation of ATG13 on Ser-224 and Ser-258 suppresses ULK1 kinase activity.

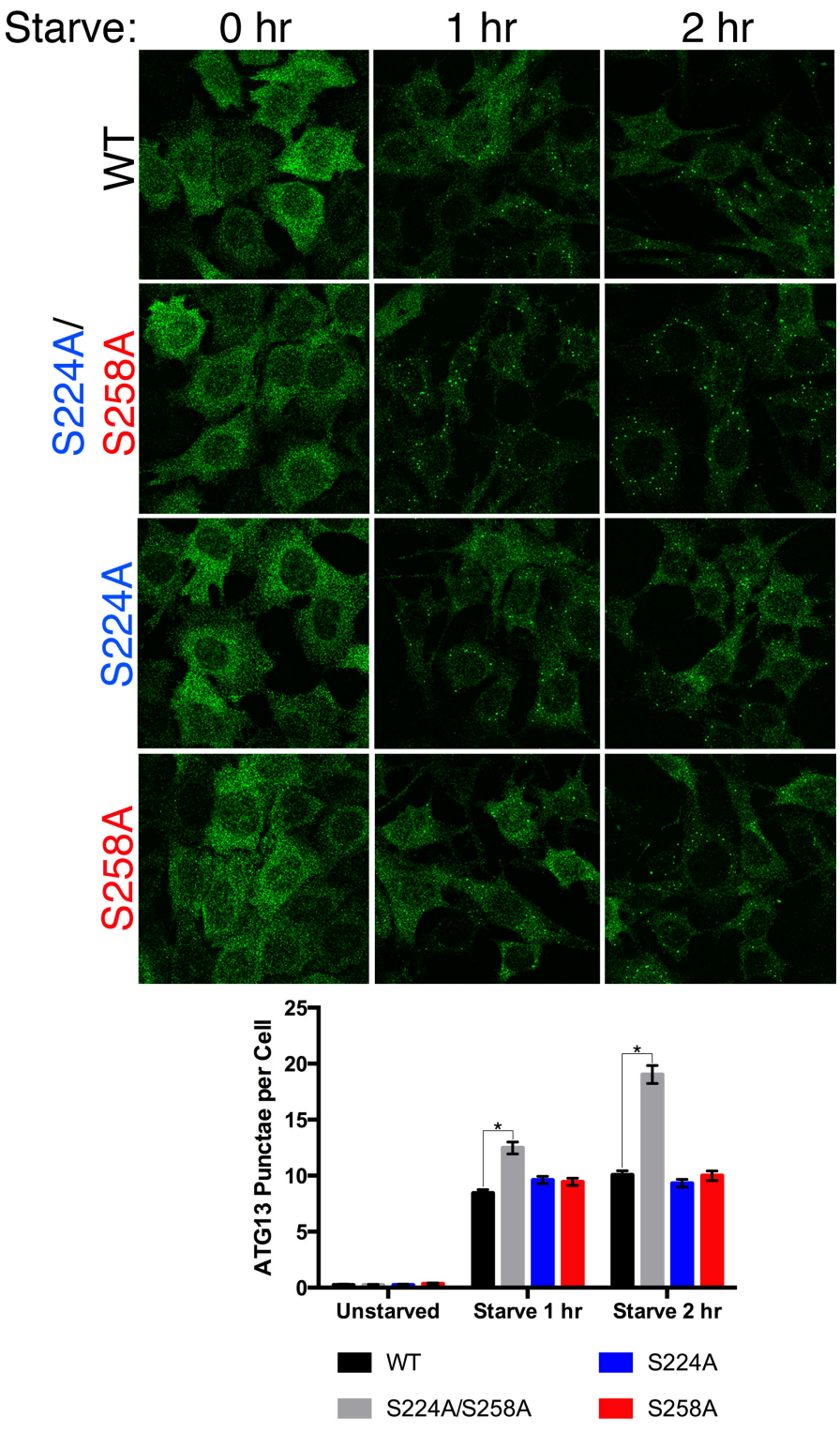
Starve:
0 hr
1 hr
2 hr
WT
S224A/
S258A
S224A
S258A
ATG13 Punctae per Cell
25
20
15
10
5
0
*
*
Unstarved
Starve 1 hr
Starve 2 hr
WT
S224A
S224A/S258A
S258A

Figure 2.10 Phosphorylation of ATG13 on Ser-224 and Ser-258 inhibits starvation-induced translocation of ATG13 to punctae. *ATG13* -/- MEFs were reconstituted by the stable expression of F/S-ATG13 wild-type, S224A/S258A, S224A, or S258A. *Top Panel:* The cells were placed in full-media or starvation media for 1 or 2 hours. S-Tag immunofluorescence was used to image F/S-ATG13 punctae. *Bottom Panel:* There are significantly more ATG13 punctae at one and two hour starvation in cells stably expressing S224A/S258A as compared to wild-type, * $p < 0.001$.

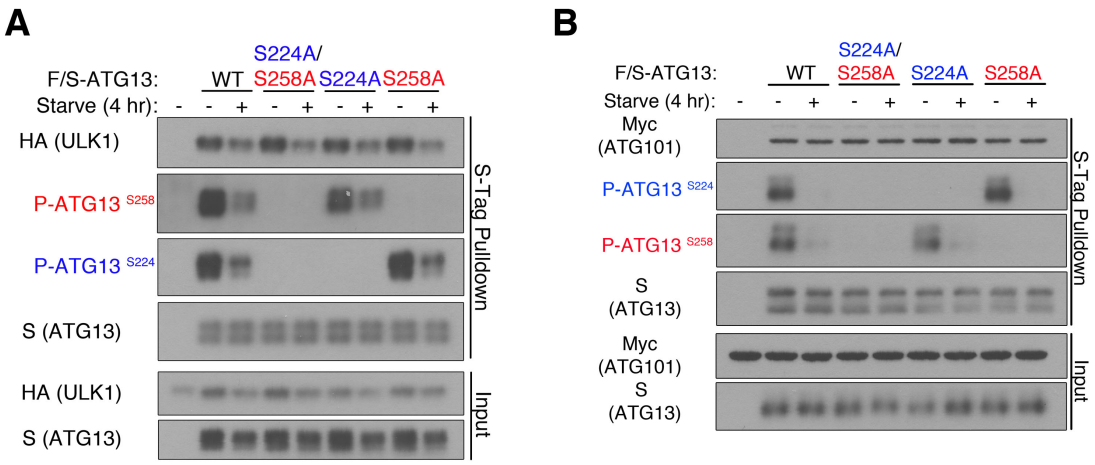

Figure 2.11 ATG13 phosphorylations on Ser-224 and Ser-258 do not modulate the interaction between members of the ULK1 complex. (**A**) F/S-ATG13 was co-transfected in HEK293T alongside HA-ULK1 or (**d**) Myc-ATG101. The cells were placed in full-media or starvation media for 4 hours, then complexes were S-tag immunoprecipitated using S-protein agarose beads and analyzed by western blotting.

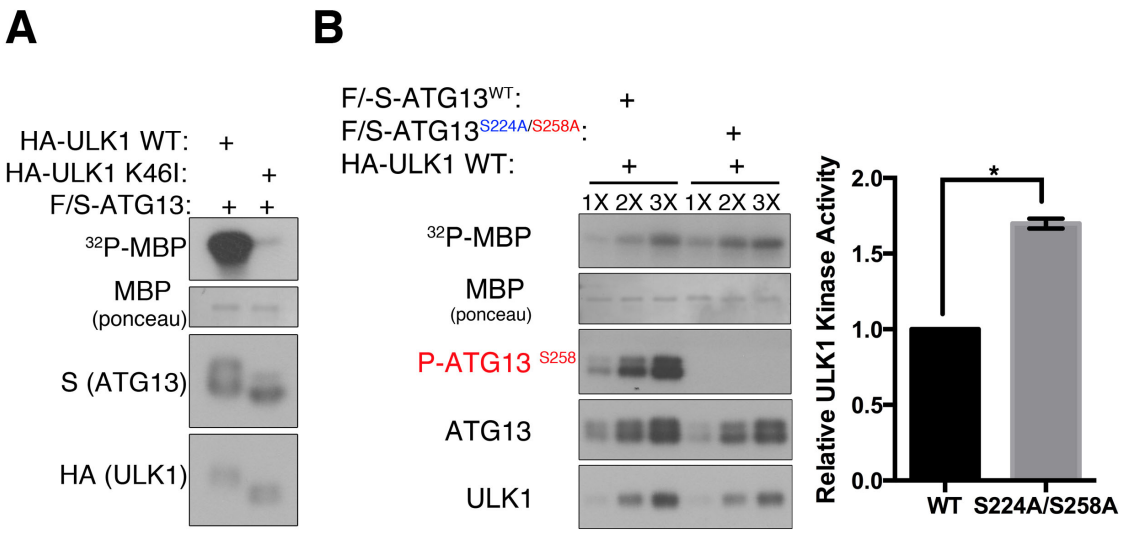

Figure 2.12 ATG13 phosphorylation on Ser-224 and Ser-258 modulates the ULK1 kinase activity. (**A**) FLAG-S-ATG13 was ectopically overexpressed with HA-ULK1 or HA-ULK1-K46I. Complexes were affinity purified by S-protein agarose beads and subjected to an ULK1 kinase assay using ^{32}P-labeled MBP as a readout. (**B**) FLAG-S-ATG13 wild-type or the combined alanine mutant was ectopically overexpressed with HA-ULK1. ULK1 bound to ATG13 S224A/S2458A is significantly more active than when its bound to ATG13 wild-type, * $p < 0.001$.

2.3 Discussion

In this study, I describe the identification and characterization of nutrient-regulated phosphorylation events on ATG13, pSer-224 and pSer-258. These sites are dephosphorylated upon amino acid starvation, with pSer-258 showing faster kinetics. Upon nutrient replenishment, these sites are re-phosphorylated. Interestingly, these sites are differentially regulated with pSer258 being a direct substrate of mTORC1, while pSer-224 is modulated by the AMPK pathway. As such, phosphorylation of Ser-224 and Ser-258 on ATG13 function as molecular sensors of energy and nutrient availability that integrate signals from multiple signaling pathways. Phosphorylation of ATG13 at Ser-224 and Ser-258 exerts an inhibitory effect on the autophagic function of ULK1, as detected by monitoring both ULK1 kinase activity and its cellular translocation.

Although the autophagic process is conversed from yeast to humans, its regulatory mechanisms have diverged. In yeast, TOR negatively regulates the induction of autophagy through regulating the formation of the Atg1-Atg13-Atg17 complex by hyper-phosphorylating Atg13. Upon TOR inactivation, TOR-mediated phosphorylation on Atg13 is inhibited, allowing for the formation of the initiator complex and the subsequent recruitment of downstream players. However, in mammals, although inhibition of mTOR is also sufficient to unleash the autophagy function of the ULK1-ATG13-FIP200 complex (which is the counterpart of the yeast Atg1 complex), the ULK1 complex is always assembled even under nutrient-rich, mTOR-active conditions.

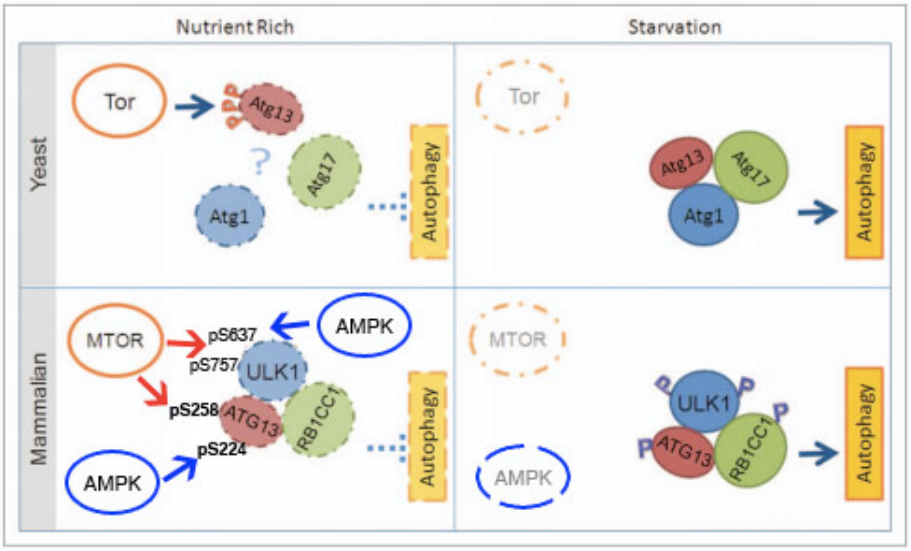

Figure 2.13 Schematic representation of how mTOR and AMPK coordinate to regulate starvation-induced autophagy. My work has added to the current knowledge base of autophagy regulation by identifying ATG13 pSer-224 as a substrate of the AMPK pathway while pSer-258 as a substrate of mTOR. In addition to phosphorylating ATG13, mTOR and AMPK also extend inhibitory phosphorylations onto the ULK1 kinase. Upon starvation, these sites are removed, allowing for the subsequent activation of the ULK1 kinase through auto-phosphorylation and trans-phosphorylation of ATG13 and FIP200. Adapted from Wong, P. M., Puente, C., Ganley, I. G., and Jiang, X. (2013) The ULK1 complex: sensing nutrient signals for autophagy activation. *Autophagy* **9**, 124-137.

The lack of the dynamic association-dissociation between ULK1 and ATG13 stipulates that mammalian autophagy must be initiated differently from that in yeast. How does the phosphorylation status of ULK1 and ATG13 regulate the ULK1 complex without controlling complex assembly? I ruled out the possibility that phosphorylation of ATG13 at Ser-224 and Ser-258 regulates the binding of ATG13 with ATG101, a regulatory protein of the ULK1 complex that has no homologous counterpart in yeast. Other possible mechanisms include that phosphorylation of ULK1 and ATG13 controls the conformation of the ULK1 complex or interaction of the complex with an unknown novel regulator. Further investigation is required to define the precise mechanism by which these phosphorylation events regulate the autophagy function of the ULK1 complex.

Intriguingly, this study also demonstrates that the energy-sensing kinase AMPK can regulate autophagy via phosphorylating ATG13. The role of AMPK in autophagy appears to be more complicated than that of mTOR. On one hand, AMPK has been shown to be a positive regulator of autophagy, especially under energy-depriving, AMPK-stimulating conditions such as glucose starvation (118,153,154). On the other hand, AMPK can also negatively regulate autophagy by phosphorylating ULK1 at Ser-638 site, thus tuning down the autophagy activity of ULK1 (119), Here I show that AMPK phosphorylates ATG13 at Ser-224 and this event also reduces the autophagy activity of the ULK1 complex. Notably, the role of AMPK on the ULK1 complex is dispensable and of a “fine-tuning” nature: regardless of the status of AMPK activity or expression, ULK1 complex-

dependent autophagy can proceed once mTOR activity is suppressed. It is most likely that phosphorylation of ATG13 at Ser-224 by AMPK provides an additional layer of mechanism for controlling autophagy in a more accurate and efficient manner. Ultimately, these novel phosphorylations add to our understanding of how AMPK and mTOR coordinate to regulate the induction of starvation-induced autophagy by impinging phosphorylations on ULK1 and ATG13 (Figure 2.13).

Hierarchy studies have identified the ULK1 complex as the most upstream *ATGs* in the autophagic process (155). Functioning directly downstream is the vacuolar protein sorting mutant 34 (Vps34) complex, which fails to form punctate structures in FIP200 -/- cells (155). This hierarchical relationship is validated by a molecular mechanism. Upon autophagy induction, ULK1 phosphorylates AMBRA1, a component of the Vps34 complex, which facilitates it release from the cytoskeleton and translocation to autophagy initiation sites on the ER (156). The formation of the autophagosome begins with the formation of the omegasome, a phosphatidylinositol (PI) 3-phosphate (PI3P)-enriched membrane that originates from the endoplasmic reticulum (ER) (61). However, what is the protein that designates this structure (Figure 2.14)? Upon autophagy induction, punctate structures containing ULK1 and Vps34 are tightly associated with the ER (155). The current model posits that omegasome structures are defined by Vps34 (157). Upon the induction of autophagy, Vps34 associates with a trimeric complex, composed of Vps15-Beclin1-Atg14L, and translocates to mitochondrial-associated ER membranes (MAM) (62). Also upon autophagy induction, the ULK1 complex translocates to the ER, on sites that are proximal but distinct from

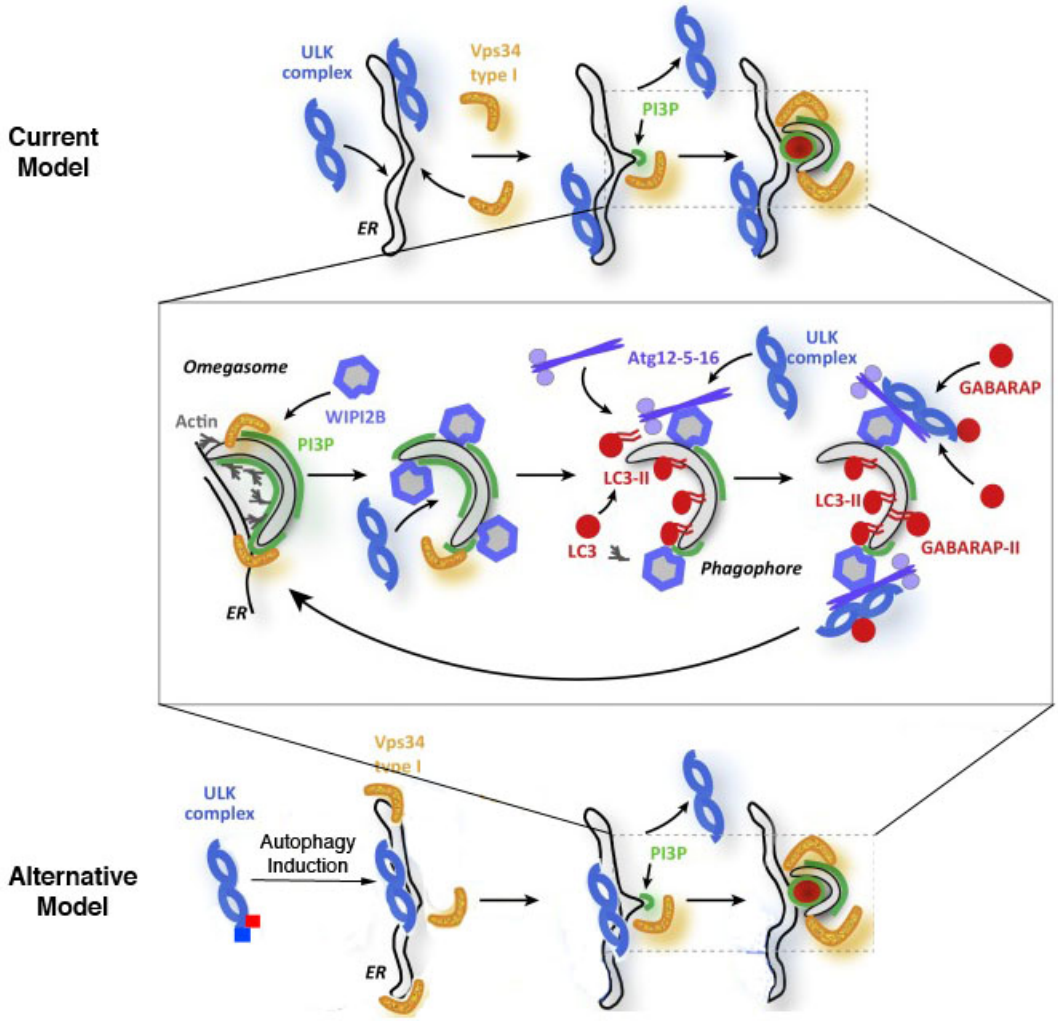

Figure 2.14 Schematic representation of two models describing the function of ULK1 in the formation of the omegasome. *Top Panel:* The current model posits that ULK1 and Vps34 are recruited to the ER. Following activation, Vps34 designates the site of the omegasome by the formation of PI3P. The accumulation of PI3P facilitates the recruitment of effector proteins, such as WIPI and DFCP1. These effectors lead to the stabilization of the ULK1 complex at the omegasome. *Bottom Panel*: In contrast, it is also possible that the site of the omegasome is designated by activated ULK1. Recent findings demonstrate that ULK1-mediated activation of Vps34 is ATG13-dependent. ATG13 binds to ATG14, which facilitates ULK1-dependent phosphorylation, which activates the Vps34 complex. It is possible that the phosphorylations described in this study (illustrated as red and blue squares) modulate the translocation of the ULK1 complex to the ER and/or regulate the interaction between ATG13 and ATG14 (ATG14 not shown). Adapted from Ktistakis, N. T., and Tooze, S. A. (2016) Digesting the Expanding Mechanisms of Autophagy. *Trends in cell biology*

the omegasome, and facilitates the activation of Vps34 (158). The activated Vps34 complex produces PI3P, which subsequently recruits PI3P-effector proteins such as WD-repeat PtdIns(3)P effector protein 2 (WIPI2) the double-FYVE-containing protein 1 (DFCP1) (159,160). The accumulation of DFCP1 generates the omegasome. WIPI2 mediates the recruitment of ATG12-5-16L1, which facilitates the lipidation of LC3 family members. The ULK1 complex is stabilized at the omegasome through a FIP200-ATG16L1 interaction and through LC3-interacting (LIR) domains on each ULK1 complex member (95,150,161). Mutating the mTOR- and AMPK-dependent phosphorylation sites on ATG13 facilitates the formation of a greater number of ULK1 and LC3 punctae. Taking this model into consideration, it is possible that these inhibitory phosphorylations might modulate the binding of the ULK1 complex with LC3 family members or with ATG16L1. Mutating these sites to alanine might probe the ULK1 complex to more readily interact with WIPI and LC3 family members and further support autophagosome biogenesis.

However, an alternative model should also be considered to explain the data presented here (Figure 2.14). Despite the critical function of Vps34 in generating PI3P, the site of autophagy initiation might be designated by ULK1 not Vps34. In support of this model, ATG13 is known to mediate the interaction between ULK1 and ATG14, the autophagy-specific component of the Vps34 complex. This interaction facilitates the ULK1-dependent phosphorylation of ATG14, and is required for the initiation of autophagosome formation (162). As such, by

mediating the local activation of Vps34, ULK1 designates the site of autophagosome nucleation. It will be important to assess whether the phosphorylations described in this study can modulate binding between ATG14 and ATG13. In order to assess the validity of this model, it will be important to ascertain whether ER-localized ULK1 punctate structures persists in ATG14-null cells. Based on published findings, I believe that the current model is correct. First, PI3P synthesis is known to be important for the recruitment and stabilization of the ULK1 complex to punctate. The interplay between these two events, PI3P synthesis and ULK1 translocation is complex. It is probable that PI3P formation creates a feedback loop that promotes the recruitment of ULK1, which further stimulates PI3P synthesis.

2.4 Experimental Procedures

Reagents and Antibodies

The following antibodies were used for western blot analysis: rabbit anti-ATG13 (1:10,000, Sigma, no. SAB4200100); rabbit anti-LC3b (1:3,000, Sigma, no. L7543); rabbit anti-ULK1 (1:3,000, Sigma, no. A7481); mouse anti-β actin clone AC-15 (1:15,000, Sigma, no. A1978); rabbit anti-S6K (1:3,000, Cell Signaling, no. 2708); rabbit anti-phospho-S6K (T389) (1:1,000, Cell Signaling, no. 9205); rabbit anti-p62/SQSTM1 (1:10,000, MBL, no. PM045B); rabbit anti-phospho-ATG13 (S318) (1:1,500, Rockland, no. 600-401-C49); rabbit anti-S-Tag (1:3,000, Bethyl Laboratories, no A190-135A); mouse anti-c-Myc (1:500, Santa Cruz Biotechnology, no. sc-40). Rabbit anti-phospho-ATG13 (S224) and rabbit anti-phospho-ATG13 (S258) were generated through GenScript. Rabbit anti-phospho-ULK1 (S637) and rabbit anti-phospho-ULK1 (S757) were a generous gift from Dr. Xiaodong Wang. Rapamycin was purchased from Enzo Life Sciences (A-275). Torin 1 was purchased from Tocris Bioscience (4247). Bafilomycin A1 was purchased from Sigma (B1793). Compound C was purchased from Tocris (3093). PI-103 was purchased from Cayman Chemical (371935-74-9).

Cell Culture

HEK293T and immortalized MEFs were cultured at 37°C, 5% CO_2 in Dulbecco's modified Eagle's medium (DMEM), supplemented with 10% fetal bovine serum, 2 mM L-glutamine and 1X penicillin-streptomycin. For induction of autophagy, cells

were washed twice in 1X PBS and incubated in DMEM lacking amino acids and serum (starvation medium), or maintained in complete full-media as a control, for the indicated amount of time. We performed amino acid starvation by culturing cells in DMEM without amino acids, and supplemented with 10% dialyzed FBS. We performed serum starvation by culturing cells in DMEM supplemented with 2 mM L-glutamine.

DNA Constructs

ATG13 mouse cDNA was purchased from ATCC (clone ID 5359944). Serine to alanine, aspartic acid, and glutamic acid mutation were generated by PCR-mediated site-directed mutagenesis. The residue of interest was mutated alongside adjacent acceptor residues, in order to prevent compensatory phosphorylation: S224A (S222A/S223A/S224A); S258A (S256A/ T257A/S258A); S224E (S222E/S223E/S224E); S258E (S256E/T257E/S258E). All mutations were subsequently confirmed by direct sequencing. For expression in MEF and HEK293T cells, *ATG13* was subcloned into pBabe/puro containing an N-terminal FLAG-S tag or HA tag.

Tandem Affinity Purification

FLAG-S-ATG13 was stably expressed to near endogenous levels in MEF cells. Cells were either starved in amino acid and serum-free DMEM media for 1.5 hours or kept in full-media and stimulated with insulin at 1 μg/mL for 15 minutes before harvesting. We used 24 x 15-cm plates for each condition. Cells were

lysed in 600 µL of IP lysis buffer (50 mM HEPES pH 7.4, 10 mM KCl, 1 mM EDTA, 1 mM $MgCl_2$, 10% glycerol and 0.5% Triton X-100) per 15-cm plate, supplemented with protease inhibitors and a cocktail of phosphatase inhibitors (Sigma, no P5726 and P0044). Lysates were incubated on ice for 20 minutes and then centrifuged for 15 minutes at 16,000 x g and then followed by an additional spin at 100,000 x g. An 8 M urea solution was added to the clarified lysates to 1.5M. The partially denatured clarified lysate was incubated overnight with 100 µL of S-agarose beads (EMD Millipore, no. 69704-3) at 4 °C. The beads were then washed four times with lysis buffer containing 1 M urea. The bound ATG13 was eluted twice with 250 µL of lysis buffer containing 8M urea. Additional lysis buffer was added to the eluates to dilute urea to 0.25 M and supplemented with protease inhibitors and a cocktail of phosphatase inhibitors. Eluates were further incubated with 150 µL of FLAG beads (Sigma, no. A2220) overnight at 4°C. After four washes in IP lysis buffer, the bound ATG13 was eluted in SDS sample buffer and analyzed by SDS-PAGE and silver staining.

Protein Identification by nano-Liquid Chromatography Coupled to Tandem Mass Spectrometry (LC-MS/MS) Analysis.

Proteins were resolved using SDS-polyacrylamide gel electrophoresis, followed by staining with Coomassie Blue and excision of the separated protein bands; *In situ* trypsin digestion of polypeptides in each gel slice was performed as described (163). The tryptic peptides were purified using a 2-µl bed volume of Poros 50 R2 (Applied Biosystems, CA) reversed-phase beads packed in Eppendorf gel-loading tips (164). The purified peptides were diluted to 0.1%

formic acid and then subjected to nano-liquid chromatography coupled to tandem mass spectrometry (nano-LC-MS/MS) analysis as follows. Peptide mixtures (in 20 µl) were loaded onto a trapping guard column (0.3 x 5 mm Acclaim PepMap 100 C18 cartridge from LC Packings, Sunnyvale, CA) using an Eksigent nano MDLC system (Eksigent Technologies, Inc. Dublin, CA) at a flow rate of 20 µl/min. After washing, the flow was reversed through the guard column and the peptides eluted with a 5-45% acetonitrile gradient over 85 min at a flow rate of 200 nl/min, onto and over a 75-micron x 15-cm fused silica capillary PepMap 100 C18 column (LC Packings, Sunnyvale, CA). The eluent was directed to a 75-micron (with 10-micron orifice) fused silica nano-electrospray needle (New Objective, Woburn, MA). The electrospray ionization needle was set at 1800 V. A linear ion quadrupole trap-Orbitrap hybrid analyzer (LTQ-Orbitrap, ThermoFisher, San Jose, CA) was operated in automatic, data-dependent MS/MS acquisition mode with one MS full scan (450-2000 m/z) in the Orbitrap analyzer at 60,000 mass resolution and up to ten concurrent MS/MS scans in the LTQ for the ten most intense peaks selected from each survey scan. Survey scans were acquired in profile mode and MS/MS scans were acquired in centroid mode. The collision energy was automatically adjusted in accordance with the experimental mass (m/z) value of the precursor ions selected for MS/MS. Minimum ion intensity of 2000 counts was required to trigger an MS/MS spectrum; dynamic exclusion duration was set at 60 s.

Initial protein/peptide identifications from the LC-MS/MS data were performed using the Mascot search engine (Matrix Science, version 2.3.02; www.matrixscience.com) with the Xenopus segment of Uniprot protein database (3,363 sequences; European Bioinformatics Institute, Swiss Institute of Bioinformatics and Protein Information Resource). The search parameters were as follows: (i) two missed cleavage tryptic sites were allowed; (ii) precursor ion mass tolerance = 10 ppm; (iii) fragment ion mass tolerance = 0.8Da; and (iv) variable protein modifications were allowed for methionine oxidation, cysteine acrylamide derivatization and protein N-terminal acetylation, mono- and di-methylated Lysine and Arginine, and tri-methylated Lysine. MudPit scoring was typically applied using significance threshold score $p<0.01$. Decoy database search was always activated and, in general, for merged LS-MS/MS analysis of a gel lane with $p<0.01$, false discovery rate averaged around 1%.

Scaffold (Proteome Software Inc., Portland, OR), version 3_6_1 was used to further validate and cross-tabulate the tandem mass spectrometry (MS/MS) based peptide and protein identifications. Protein and peptide probability was set at 95% with a minimum peptide requirement of 1.

CRISPR-CAS9 Knockout MEF Cell Line

CRISPR-CAS9 system of RNA-guided genome editing was used to generate *ATG13* -/- MEFs. The targeting sequence 5'-ACTGTCCAAGTGATT GTCC-3' was incorporated into a 60mer oligo, as described previously (165). The forward

and reverse oligos were annealed to make a 100bp double-stranded DNA fragment using Phusion polymerase (NEB, no. M0530S). The DNA fragment was fused by Gibson assembly (NEB, no. E2611S) to an AflII-linearized U6 target gRNA expression vector (Addgene, no. 41824). The targeting sequence was confirmed by sequencing. MEF cells were then electroporated using the Amaxa MEF2 nucleofector kit (VAPD-1005), as per manufacturer's instructions. Cells were electroporated in three consecutive days and then plated for single clones.

Preparation of Cell Lysates and Immunoprecipitation

Cells were washed with ice-cold 1X PBS buffer and then lysed in RIPA buffer (10 mM Tris.HCl, pH 7.5, 100 mM NaCl, 1.0% Triton X-100, 0.5% sodium deoxycholate, 0.1% sodium dodecyl sulfate, 10% glycerol, 1 mM EDTA/EGTA) or IP lysis buffer, supplemented with protease inhibitors and a cocktail of phosphatase inhibitors. The lysates were incubated on ice for 20 minutes and then centrifuged at 12,000 x g for 15 minutes. For IP, lysate were incubated with 10 µL of S-protein agarose beads for 4 hours at 4 °C. The beads were then washed four times in IP lysis buffer and eluted by boiling in SDS sample buffer. The precipitated proteins were resolved by SDS-PAGE and analyzed by western blotting.

Microscopy

For fluorescence analysis, cells were either stably transfected with GFP-LC3 or processed for ULK1(1:400, Sigma, no. A7481) or F/S-ATG13 (1:400, EMD

Millipore, no. 71549) immunofluorescence. Cells were plated on coverslips in a six-well plate format. The subsequent day, cells were either placed in full-media or starvation media for the indicated amount of time. Coverslips were then fixed with 3.7% paraformaldehyde in 20 mM HEPES pH 7.5 for 20 minutes at room temperature. For immunofluorescence, the fixed cells were permeabilized with 0.1% Triton X-100 in 1X PBS for 5 minutes. After washing, the coverslips were then incubated with ULK1 antibody or S-Tag antibody in blocking buffer (1% BSA/1X PBS) for 30 minutes at room temperature. After washing three times for 10 minute intervals, slides were incubated with Alexa Fluor secondary antibody (1:1,000, ThermoFisher, no. A11012 or A11029) for 30 minutes at room temperature. After washing, coverslips were mounted on microscope slides using ProLong Gold antifade reagent with DAPI (Life Technologies, no. P36935). GFP-LC3, ATG13 and ULK1 punctae were visualized with a Nikon Eclipse TE2000-U confocal microscope using the 60X objective. Images were acquired using Nikon EZ-C1 image acquisition software. Subsequently, the images were processed using Photoshop.

ULK1 Kinase Assay

FLAG-S-ATG13 (WT or S224A/S258A) and HA-ULK1 were co-transfected in HEK293T cells with Lipofectamine 2000, as per manufacturer's instructions. We transfected 2 x 10-cm plates for each ATG13. After 48 hours, cells were lysed in lysis buffer (50 mM Tris, pH 7.5, 150 mM NaCl, 10% glycerol, 1% Triton X-100, 1 mM EDTA/EGTA, 0.5 mM DTT) supplemented with protease inhibitors and

phosphatase inhibitors (Sigma, P0044 and P5726). Lysates were centrifuged at 20,000 x g for 15 minutes. An equal amount of total protein was then incubated with 15 µL of S-protein agarose beads (EMD Millipore, 69704-3) overnight with rotation at 4°C. After washing with lysis buffer, the S-protein agarose beads were resuspended in ULK1 kinase buffer (25 mM HEPES, pH 7.5, 50 mM NaCl, 10 mM $MgCl_2$, 0.1% Tween-20, 1 mM DTT, 0.5 mg/ml BSA 10 µM cold ATP, 0.5 µCi of [γ^{32}-P] ATP (PerkinElmer, BLU002A250UC) and 0.25 mg/ml myelin basic protein (MBP) (EMD Millipore, 13-110). The reaction was incubated at 30 °C for 30 minutes. The reaction was terminated by the addition of sample buffer. The samples were run in a 15% SDS-PAGE gel, transferred to nitrocellulose and signal was acquired with X-ray film.

mTOR Kinase Assay

For the kinase assay, Myc-mTOR and FLAG-S-ATG13 were separately transfected into HEK293T cells using Lipofectamine 2000, as per manufacturer's instructions. Cells transfected with Myc-mTOR were maintained in full-media while cells transfected with F/S-ATG13 were starved for 4 hours prior to harvesting, in order to remove any phosphorylations mediated by endogenous mTOR. Myc-mTOR and F/S-ATG13 were immunoprecipitated using c-Myc agarose beads (Clontech, no. 631208) or S-protein agarose beads (EMD Millipore, 69704-3), respectively. Cells were lysed in lysis buffer and incubated with 20 µl of beads while rotating at 4°C for 5 hours. The beads were washed 4 times with lysis buffer, aliquoted and then resuspended in mTOR kinase buffer

(20 mM HEPES, pH7.5, 100 mM NaCl, 5 mM $MnCl_2$, 1 mM DTT, 0.5 mg/ml BSA, 20 μM cold ATP and 0.5 μCi of [γ^{32}-P] ATP). This reaction was performed on the beads. The reaction was incubated at 30°C for 45 minutes. The reaction was terminated by the addition of sample buffer. The samples were run in a 7% SDS-PAGE gel, transferred to nitrocellulose and signal was acquired with X-ray film.

In vitro Phosphatase Assay

Cells were lysed in RIPA buffer supplemented with protease with or without phosphatase inhibitors. A total of 60 μg of lysate was incubated in 1X NEB3 buffer and with or without 10 U of calf intestinal phosphatase (CIP) (New England BioLabs, M0290S) for 1 hour at 37°C. The reaction was terminated by the addition of sample buffer and analyzed by immunoblotting.

Statistical Analysis

The statistical significance of differences between means was calculated by two-tailed student t-test. Values of $p < 0.05$ were considered significant.

CHAPTER 3. RELAYING THE AUTOPHAGIC SIGNAL DOWNSTREAM: IDENTIFYING SUBSTRATES OF ULK1

3.1 Introduction

The ULK1 kinase plays a vital role in the regulation of autophagy. However, only a few direct substrates have been identified. In an effort to understand how the ULK1 complex relays the autophagy induction signal downstream to the ATG core machinery, I undertook to identify novel substrates of the ULK1 kinase. I generated and optimized two separate systems to identify substrates. In both scenarios, I started with ULK1/2 -/- MEF which I then reconstituted with either (1) wild-type or shokat kinase ULK1 (2) wild-type or kinase-dead ULK1. Ultimately, my approach exploited the use of an ULK1 kinase dead mutant, ULK1 K46I, and a quantitative phospho-proteomic approach. I selected to use stable isotope labeling with amino acids in cell culture (SILAC) to facilitate a quantitative analysis. This method exploits the principle that peptides, which are labeled with different stable isotopes, are chemically identical but differ in their mass.

While some candidates are obvious, such as ATG proteins, other predicted substrates point to novel links between autophagy and certain other cellular processes or structures. I was able to verify two putative substrates as *in vitro* substrates of ULK1: GLIPR2 and ARHGEF2. GLIPR2 is described as a negative regulator of autophagy, through the sequestration of Beclin 1. ARHGEF2 had never been implicated in autophagy.

3.2 Results

Setting up a system to identify ULK1 substrates: ULK1 shokat kinase

In order to identify prospective substrates of ULK1, I generated and optimized a cellular system where I could modulate the activity of the ULK1 kinase. A previous post-doctoral fellow, Dr. Ian Ganley, generated an analog sensitive mutant of ULK1, ULK1 M92G. The analog-sensitive mutant of ULK1 is based on the shokat kinase principles developed by Dr. Shokat and colleagues (166-170). By mutating the gatekeeper residue, identified as M92, to a small residue such as glycine, the ATP-binding pocket is enlarged. This expanded ATP-binding pocket can accommodate ATP competitive inhibitors with bulky steric groups. As such, bulky ATP inhibitors selectively target the genetically modified kinase and not the native kinases. Importantly, mutation of the gatekeeper residue does not affect the protein substrate specificity of kinases. This property allows for the specific inhibition of ULK1 shokat mutant in cells.

Dr. Ganley attempted to use this kinase; however, an *in vitro* kinase assay demonstrated that the shokat mutant is putatively inactive. In fact, it was reported that roughly 30% of kinases tested do not tolerate the shokat mutation (171). In an attempt to reactivate the kinase, I introduced and tested several second-site suppressor mutations (171). Surprisingly, when I reconstituted ULK1/2 -/- MEF with the shokat kinase mutant and the second-site suppressor mutants, the shokat kinase was able to support starvation-induced autophagy (Figure 3.1 A). However, the electrophoretic mobility of the ULK1 M92G mutant, relative to ULK1

wild-type, indicates a hypo-phosphorylation state. Hypo-phosphorylated ULK1 is thought to be less active, which was reflected in the hypo-phosphorylated state of ATG13 during starvation. ATG13 is a known substrate of ULK during starvation; as such its phosphorylation state can be used as a read-out for ULK1 kinase activity. Under normal starvation conditions, ATG13 is dephosphorylated at mTOR sites and phosphorylated at ULK1 sites, as such, a starvation-induced electrophoretic mobility is not always obvious. However, if the ULK1 sites are not phosphorylated as efficiently, ATG13 appears in a hypo-phosphorylated state. As per the ATG13 phosphorylation state, no second-site suppressor mutants seemed to further activate the shokat kinase, except for ULK1 M92GL110I. However, this second-site suppressor could not activate autophagy more efficiently than the original shokat mutant (Figure 3.1 A). As such, I decided to continue characterizing the ULK1 shokat kinase, M92G.

I tested several bulky ATP analogs for their ability to specifically block autophagy in cells expressing the shokat kinase but not wild-type ULK1. The 1NA-PP1 ATP analog could not abrogate starvation-induced autophagy. However, I was able to achieve specific inhibition using 3MB-PP1 and 1NM-PP1 (Figure 3.1 B). I continued characterizing the specific inhibition by 3MB-PP1. I was able to demonstrate that at 4 μM 3MB-PP1, I could nearly completely inhibit starvation-induced autophagy and block ATG13 phosphorylation, as evident by its hypo-phosphorylated state (Figure 3.1 C).

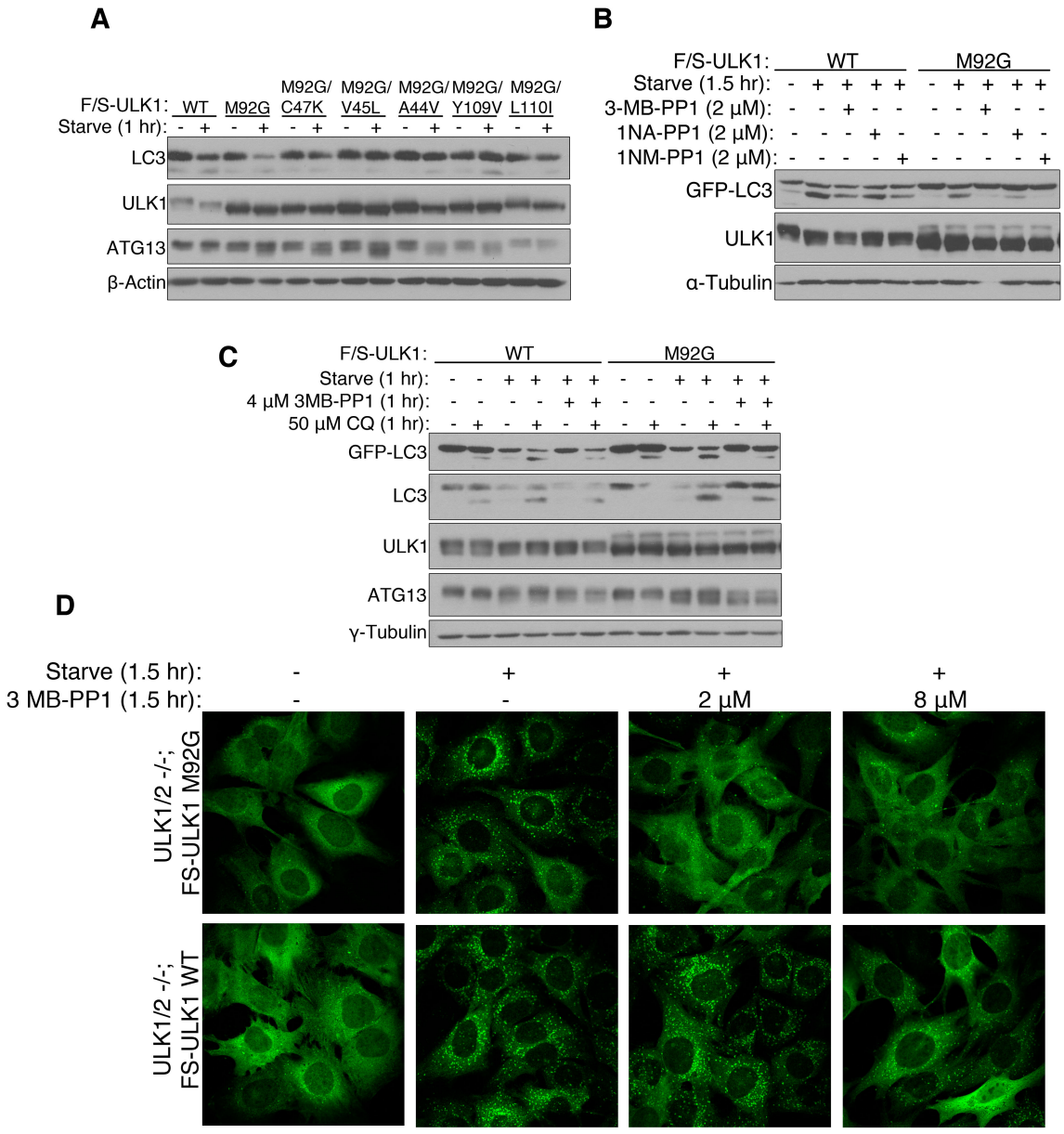

Figure 3.1 Modulating starvation-induced autophagy using an ULK1 shokat kinase. (**A**) ULK1/2 -/- MEF were reconstituted by the stable expression of FLAG-S-ULK1 (F/S-ULK1) wild-type, shokat kinase (M92G) or second-site suppressor mutants. Autophagy was assessed by western blotting of LC3. (**B**) Reconstituted ULK1/2 -/- MEF were stably transduced with GFP-LC3 and treated with the bulky ATP analogs 3MB-PP1, 1NA-PP1 and 1NM-PP1 or just (**C**) 3MB-PP1, and monitored for autophagy inhibition by LC3 western blotting. (**D**) Confocal microscopy imaging of reconstituted ULK1/2 -/- MEFs expressing GFP-LC3, and treated with 3MB-PP1.

However, the dynamic range for specific inhibition by 3MB-PP1 is very limited, as slightly higher concentrations of inhibitor also inhibit autophagy in cells expressing wild-type ULK1 (Figure 3.1 D). Although the ULK1 M92G shokat kinase is partially active in cells, can sustain starvation-induced autophagy, and can be selectively targeted by the 3MB-PP1 inhibitor, I felt that the system was not sufficiently robust to be the base of a large phospho-proteomic analysis for ULK1 substrates. As such, I established and characterized another reconstitution system in the ULK1/2 -/- MEF.

Setting up a system to identify ULK1 substrates: ULK1 kinase-dead

Since the ULK1 kinase activity is required for starvation-induced autophagy, I set up a two-cell line system to identify ULK1 substrates. In this case, ULK1/2 -/- MEF were reconstituted by the stable expression of F/S-ULK1 wild-type or kinase-dead, ULK1 K46I. I observed a near complete block in starvation-induced autophagy, in cells expressing ULK1-K46I, as indicative by the block in LC3 conversion. In addition, ATG13 appeared hypo-phosphorylated, in cells expressing ULK1 K46I. As such, in cells expressing ULK1 K46I, ULK1 substrates are not phosphorylated.

I decided to compare the starvation-induced phospho-proteome of these cell lines using stable isotope labeling with amino acids in cell culture (SILAC). Since the two cell lines are virtually identical, except for ULK1 kinase activity, phospho-peptides identified in cells expressing ULK1 wild-type but not K46I are potential

ULK1 substrates. This approach entails the *in vivo* metabolic incorporation of "heavy" ^{13}C- or ^{15}N-labeled amino acids into one proteome and the incorporation of "light" amino acids into the other proteome.

The phospho-proteomic SILAC experiment

I utilized two heavy amino acids [$^{13}C_6$, $^{15}N_4$]-L-Arginine and [$^{13}C_6$]-L-Lysine. The incorporation of one [$^{13}C_6$, $^{15}N_4$]-L-Arginine heavy amino acid results in a 10-Da mass shift compared to peptides generated with light arginine. The incorporation of one [$^{13}C_6$]-L-Lysine heavy amino acid results in a 6-Da mass shift relative to peptides generated with light lysine. I performed the SILAC experiment twice. In the first experiment, which I will refer to as the "forward" experiment, the cells expressing ULK1 wild-type were labeled with the heavy amino acids, while the cells expressing ULK1 kinase-dead were labeled with the light amino acids. In the second experiment, which I will refer to as the "reverse" experiment, the heavy label was inversed. For both experiments, equal amounts of the cell lysates were combined and then treated as a single sample in all subsequent steps, which prevents introducing any errors. In order to enrich for phospho-peptides and reduce the sample complexity, the sample workflow included titanium dioxide (TiO_2) and strong cation exchange chromatography (SCX), respectively.

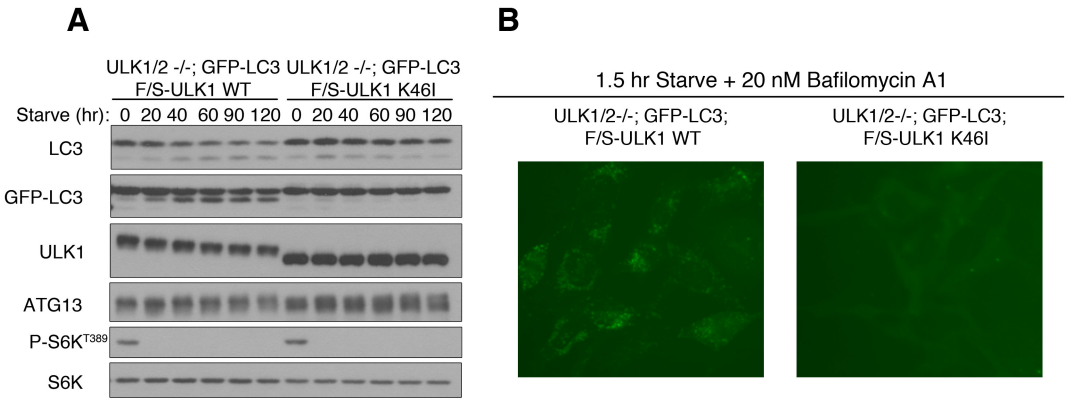

Figure 3.2 A two-cell line system to identify ULK1 substrates. ULK1/2 -/- MEF were reconstituted by the stable expression of ULK1 wild-type or kinase-dead. (**A**) Autophagy was monitored by LC3 western or (**B**) GFP-LC3 imaging

In order to compare the presence of phospho-peptides in heavy and light conditions, the Heavy/Light (H/L) ratio was calculated. Most phospho-peptides will not be modulated by ULK1, as so will display H/L ratios close to 1. In the forward experiment, where cells expressing ULK1 wild-type are labeled with the heavy amino acid, putative ULK1 substrates will have a very high H/L ratio or have no reported H/L ratio. In the perfect system, ULK1 substrates will be phosphorylated when ULK1 wild-type is present but will not be phosphorylated in cells expressing the kinase-dead mutant. In such as case, the H/L ratio cannot be reported because the divisor is zero, or close to zero. Importantly, in this scenario we assume that the kinase activity of ULK1 K46I is null, when in fact there may be residual activity. Taking into consideration the increased sensitivity of MS instrumentation, complete presence or absence of a phospho-peptide should be rarely seen.

The complete lack of a light phospho-peptide would strongly indicate that a phosphorylation site is directly and exclusively regulated by the ULK1 kinase. However, it is hard to follow up on this subset of putative ULK1 substrates because the absence of a light peptide can also indicate that the light peptide was not selected from the elution profile for subsequent fragmentation. In order to confirm that the absence of the light peptide is a not a technical artifact, we would have to review the raw data and check the elution profiles at the correct retention time and specific m/z values corresponding to the phospho-peptides in question. This manual validation would also have to consider additional factors of

the heavy phospho-peptide such as the number of total spectra, peptide identification probability and protein identification probability. After all, what is the likelihood of a protein being an ULK1 substrate if only one phospho-peptide spectra was identified, with a protein identification probability of 70%.

John Philip, our collaborator at the mass spectrometry core facility at MSKCC, manually verified the H/L ratios for 18 phospho-peptides, of which two had no corresponding light peptide, these phospho-peptides corresponded to UVRAG and ATG14. I decided to evaluate UVRAG and ATG14 along with putative substrates with designated H/L ratios from the forward and the reverse SILAC experiment. In order to facilitate this analysis, I did a log2 transformation of the data to fit the data to a standard curve and calculated the standard deviation. In order to assess significant putative substrates, I only evaluated putative substrates with H/L ratios greater than three standard deviations away from the mean (Table 3.1). In the forward experiment, there were 30 phospho-peptides with an H/L ratio greater than 5.19. In the reverse experiment, there were 27 phospho-peptides with an H/L ratio lower than 0.15. In total, we had a list of 59 putative substrates to evaluate (Table 3.1). I believe that our list captured real ULK1 substrates because both the forward and the reverse experiment identified FIP200 phospho-peptides (Table 3.2, left panel). FIP200, is a binding partner and a known substrate of ULK1. Unfortunately, besides FIP200 there was no overlap between the 60 putative substrates in the forward and reverse SILAC experiments.

	Forward	Reverse**
Cells with Heavy label	ULK1 WT	ULK1 K46I
Phospho-peptides with H/L ratio	8,172	7,445
Total phospho-peptides	10,597	10,074
Average H/L ratio	0.899	1.251
H/L ratio ≥ 2 SD away from mean	2.89	0.2725
H/L ratio ≥ 3 SD away from mean	5.19	0.1504
Phospho-peptides with H/L ratio ≥ 3 SD away from mean	30	27
Manually-verified heavy phospho-peptides with no corresponding light	2	NC*
Total putative targets	59	

Table 3.1 Summary of the forward and reverse SILAC experiments. In order prioritize the assessment of putative ULK1 targets, I relied on the H/L ratio. In the reverse** experiment, in which cells expressing the ULK1 K46I mutant are labeled with the heavy amino acid, this ratio is actually represented as an L/H ratio; hence the ratio is less than one. Also, in the reverse experiment, I did not manually verify the true absence of a corresponding heavy peptide for a light phospho-peptides with no reported H/L ratio (NC*= not calculated).

This lack of reproducibility is most likely the result of several factors, which I will address in the discussion section. Regardless of this limitation, both the forward and the reverse SILAC experiment also identified known regulators of autophagy. The forward experiment identified a phospho-peptide belonging to GLIPR2 (H/L ratio = 6.2054), a protein that binds to and inhibits the autophagic functions of Beclin 1 (172). The reverse experiment identified a phospho-peptide belonging to TRIM28 (H/L ratio = 0.10671) (Table 3.2, left panel). TRIM28 functions as a positive regulator of autophagy by mediating the SUMOlytion of VPS34, which is associated with an increase in the lipid kinase activity of VPS34 as well as binding to Beclin 1 (173).

In order to gain a greater understanding of the proteins in my list of putative ULK1 substrates, I conducted a pathway analysis (Table 3.2, right panel). I identified 9 proteins with lipid binding capacity, a function that is crucial for ATG proteins. I identified 6 proteins that regulate and mediate the autophagic process. Interestingly, I also identified several proteins that function at the centrosome and in ciliogenesis. Recent studies have identified the bidirectional interplay between cilia and autophagy. Autophagy can regulate cilia formation by degrading the ciliary proteins IFT20 and OFD1, while cilia can enhance the autophagy flux through cilia-related Shh (174,175).

	Forward SILAC		Reverse SILAC	
	Protein	H/L Ratio	Protein	H/L Ratio*
1	Olfr1123	1325.8	Isyna1	0.0037453
2	Dcaf12l1	181.7	Arhgef2	0.049218
3	Lect2	89.611	Mprip	0.075029
4	Myo18a	58.888	Unc119	0.078461
5	Dmxl2	48.401	Cyp2b10	0.010542
6	Ap2a2	44.046	Dcun1d4	0.023588
7	Slc26a11	35.605	Vmn1r171	0.028425
8	Comp	25.522	Olfr1222	0.0383
9	Camlg	22.227	Dzank1	0.042986
10	Dis3	14.902	Bai1	0.045884
11	Nipbl	14.511	Pdk2	0.0668
12	Wdr47	10.306	Dars2	0.074971
13	Fam120b	9.4631	F2	0.077685
14	Srgap2	9.3221	Rb1cc1	0.079656 0.11533, 0.1294
15	Smchd1	9.2062	Synpo	0.083551 0.13457
16	Rpl18a	8.7135	Rrm1	0.086719
17	Bcl9l	8.5702	Glis3	0.090752 0.12752
18	Rapgefl1	8.0676	Rab3b	0.093671
19	Pcnt	8.0499	Ccdc121	0.098127
20	Rb1cc1	8.0299, 7.9384, 6.5883	Arsg	0.10324
21	Nestin	6.2933	Trim28	0.10671
22	Glipr2	6.2054	Dkk3	0.1238
23	Stard9	6.107	Atp8b2	0.12407
24	Cars	5.4416	Hoxc12	0.12414
25	Snx13	5.4237	Cc2d1b	0.13147
26	Celsr2	5.3973	Lrrc49	0.14264
27	Slmap	5.3805		
28	Kirrel	5.3703		
29	Tns1	5.2553		
30	Numb	5.2489		

Function	#	Protein Names
Lipid binding	9	Ap2a2, Srgap2, Glipr2, Stard9, Snx13, Atp8b2, Arhgef2, Unc119, Mprip
Cytoskeleton	9	Myo18a, Arhgef2, Mprip, Lrrc49, Synpo, Nes, Pcnt, Srgap2, Wdr47
Autophagy	6	Rb1cc1, Glipr2, Trim28, Uvrag, Atg14, Ulk1
G-protein coupled receptor activity	6	Olfr1123, Snx13, Celsr2, Vmn1r171, Olfr1222, Bai1, Fam120b
Regulation of transcription	6	Trim28, Cc2d1b, Hoxc12, Glis3, Bcl9l,
Endocytosis	5	Ap2a2, Snx13, Numb, Atp8b2, Unc119
Wnt Pathway	4	Lect2, Bcl9l, Celsr2, Dkk3
Centrosome	4	Unc119, Slmap, Stard9, Pcnt
Cilium Assembly	3	Celsr2, Glis3, Unc119
GEF activity	2	Arhgef2, Rapgefl1
Endosome	2	Cc2d1b, Unc119
Notch Pathway	2	Dmxl2, Numb
Synaptic vesicle exocytosis	2	Dmxl2, Rab3b
Cell-cell adhesion	2	Kirrel, Bai1
Motor activity	2	Myo18a, Stard9
Olfactory Receptor Activity	2	Olfr1123, Olfr1222
Small GTPase mediated signal transduction	1	Rab3b
Chemotaxis	1	Lect2
Ion Transport	1	Slc26a11
Apoptosis	1	Comp
rRNA processing	1	Dis3
Chromatin binding	1	Nipbl
Filopodium assembly	1	Srgap2
Phospholipid biosynthetic process	1	Isyna1
Phagocytosis	1	Bai1
Angiogenesis	1	Bai1
Glucose homeostasis	1	Pdk2
DNA replication	1	Rrm1
Sulfuric ester hydrolase activity	1	Arsg
ATPase activity	1	Atp8b2
Lysosome	1	Arsg
Unknown	4	Dcaf12l1, Dcun1d4, 6330439K17Rik, Ccdc121

Table 3.2 Summary of putative ULK1 substrates and their biological functions. *Left Panel:* Table of putative ULK1 substrates with H/L ratios greater than three standard deviations away from the mean, in both the forward and the reverse SILAC experiment. *Right Panel:* Pathway analysis for these substrates

Putative ULK1 consensus motif

In order to gain a deeper understanding of the ULK1 kinase and identify additional substrates that may be important for the control of autophagy, I defined a preliminary consensus motif (Figure 3.3). It quickly became evident that ULK1 strongly prefers serine as the phospho-acceptor residue and is not a proline-directed Ser/Thr kinase. Additionally, the +1 position selected for aliphatic hydrophobic residues, such as valine, leucine and alanine. Conversely, the +2 position partially selected for acidic amino acids, such as aspartic acid and glutamic acid, or serine. This loose motif has significant overlap with an ULK1 motif generated *in vitro* using an arrayed degenerate peptide library (123). This motif also noted the prevalence for serine over threonine as the phosphorylated residue and the lack of proline at the +1 position. However, this motif additionally noted a strong preference for leucine or methionine at position -3 and hydrophobic residues at both +1 and +2 positions.

Validating the SILAC list of putative substrates: FIP200

In order to establish the credibility of our list of putative ULK1 substrates, I first attempted to validate the ULK1-dependent phosphorylations on FIP200. Although FIP200 is a known substrate of ULK1, ULK1-dependent phosphorylation sites have not been validated and their functional relevance in regulation starvation-induced autophagy is unknown. I was able to identify five phospho-peptides (Table 3.3).

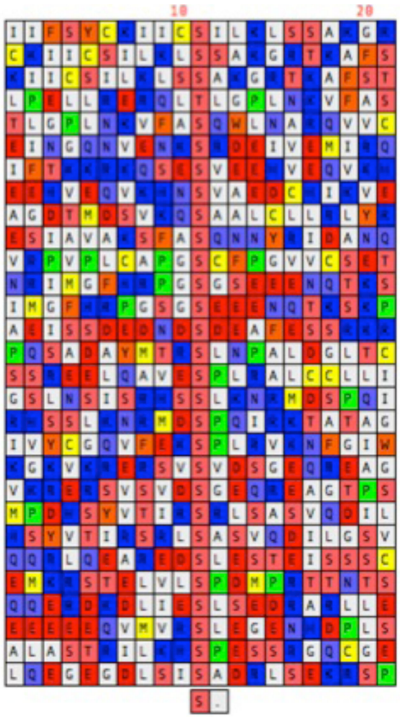

Figure 3.3 A preliminary ULK1 consensus motif. I overlapped the residues spanning position -10 to +10, relative to the phospho-acceptor residue, from putative substrates in the forward SILAC experiment.

I was able to identify two phospho-peptides in both the forward and the reverse SILAC experiment, while the other three only appeared in the reverse SILAC experiment.These putative phosphorylations do not overlap with previously reported putative phosphorylation sites (123). Previous reports demonstrated that co-expression with ULK1 can retard the electrophoretic mobility of FIP200 (82). This change in mobility is mediated by the ULK1-dependent phosphorylations on FIP200. I decided to assess the physiological relevance of the identified phosphorylation sites by assessing their affect on FIP200 mobility. I generated single-site alanine mutations at each putative phospho-acceptor residue. However, single-site mutation to alanine of any site had no perceivable effect on the mobility of FIP200 (Figure 3.4 A). However, when I combined the M1 and M3 mutations, the ULK1-dependent mobility shift was slightly abrogated. As such, I then continued to combine all of the alanine mutations into one mutant (FIP200 M1-M5) (Figure 3.4 B). Unfortunately, the combined alanine mutant still exhibits an ULK1-dependent mobility shift. However, FIP200 M1-M5 expressed alone migrates perceivably faster than FIP200 wild-type expressed alone. Demonstrating that these phosphorylations can in fact alter the mobility of FIP200 and suggesting that the co-overexpression system allows for superfluous phosphorylation of FIP200 by ULK1. As such, it was not surprising when the combined alanine mutant was phosphorylated to the same extent as FIP200 wild-type in an *in vitro* ULK1 kinase assay (Figure 3.4 C).

Phospho-peptide	Forward H/L Ratio	Reverse H/L Ratio	Mutant Name
AEMKRSTELVLSPDMPR	8.0299	0.079656	M1
DLIESLSEDR_	7.9384	0.20032	M2
SMEHVAPDPTGTER		0.11533	M3
AAQSLDEMSQTITDLLNEQK		0.1294	M4
LRTSSFLSSAPVAAAPELYG ACAPELPGEPER		0.15896	M5

Table 3.3 Summary of putative ULK1-dependent phosphorylations on FIP200 identified in the forward and the reverse SILAC. Two phospho-peptides were identified in both experiments, while the remaining were only identified in the reverse experiment. Mutant name designates the name of the corresponding alanine mutant.

Since conclusions drawn from both the mobility shift assay and the *in vitro* kinase assay are limited by the possibility of secondary phosphorylation sites, which can result from the overexpression of a substrate and kinase, I decided to evaluate the putative ULK1-dependent phosphorylations in a more physiologically relevant condition. With the help of Dr. Junru Wang, I generated FIP200 -/- MEF by CRISPR-CAS9. The aim was to reconstitute these cells by the stable expression of FIP200 wild-type, single-site mutants or the combined alanine mutant, and assess their ability to support starvation-induced autophagy. However, I did not foresee the difficulty with viral packaging of the FIP200 coding sequence. The coding sequence of FIP200 is exceedingly large, about 5,000 bases. Unfortunately, the size of this insert exceeds the cloning capacity of retroviral expression vectors and leads to lower virus titer. I attempted to circumnavigate this problem by concentrating the virus by ultracentrifugation. However, I was still unable to reconstitute the cells. As such, I was unable to ascertain the functional relevance of the putative ULK1-dependent phosphorylations in modulating starvation-induced autophagy. In the discussion, I identify how to address this problem.

Validating the SILAC list of putative substrates: ARHGEF2 and GLIPR2

I continued to validate the list of putative ULK1 substrates. My approach was similar to that of trying to validate the sites on FIP200. First, I analyzed the mobility shift of the putative substrates when overexpressed with ULK1.

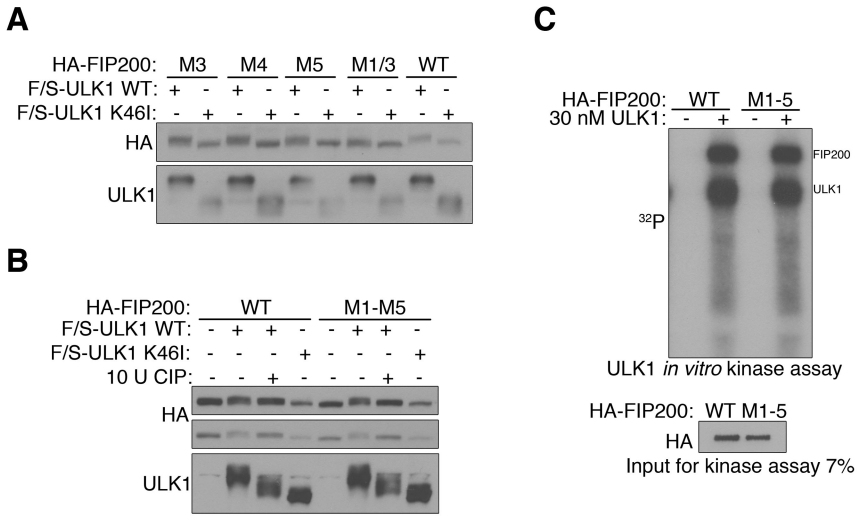

Figure 3.4 Assessing putative ULK1-dependent phosphorylations on FIP200. FIP200 (**A**) single-site alanine mutants and a (**B**) a combined alanine mutant, FIP200 M1-M5, were analyzed by the mobility shift assay. (**C**) The combined alanine mutant, FIP200 M1-M5 is evaluated in an ULK1 *in vitro* kinase assay.

Then I performed an ULK1 *in vitro* kinase assay to determine whether ULK1 can mediate a direct phosphorylation. Finally, I analyzed the corresponding knockout MEF cell lines for their capacity to undergo starvation-induced autophagy.

To facilitate the mobility shift analysis of the putative ULK1 substrates, I cloned the respective coding sequences into a retroviral expression construct. I performed the cloning and mobility shift assays in collaboration with fellow graduate student Helen Kang and Yogesh Nagaraj Huliuraiah, a volunteer student. We could not obtain any protein expression for SNX13, DARS2 and SRGAP2. We did not detect any mobility shift for ISYNA-1, UNC-119, RAB3B, TRIM28 or GLIPR2. I observed a clear upward mobility shift for ATG14, UVRAG and ARHGEF2 when they were co-overexpressed with ULK1 wild-type (Figure 3.5 A, B). This mobility shift was reverted by the use of calf intestinal phosphatase (CIP), indicating that the mobility change is attributed to phosphorylation. However, when I mutated the putative phospho-acceptor residues in UVRAG, it did not prevent the ULK1-dependent mobility shift (Figure 3.5 C). Although I observed a decrease in the ULK1-dependent mobility shift for a combined alanine mutant or ARHGEF2, which I termed ARHGEF2 M1, this mutation also resulted in a decrease in overall protein levels, relative to ARHGEF2 wild-type. As such, it was unclear whether the putative phosphorylations mediated on M1 in fact modulate the mobility shift of ARHGEF2.

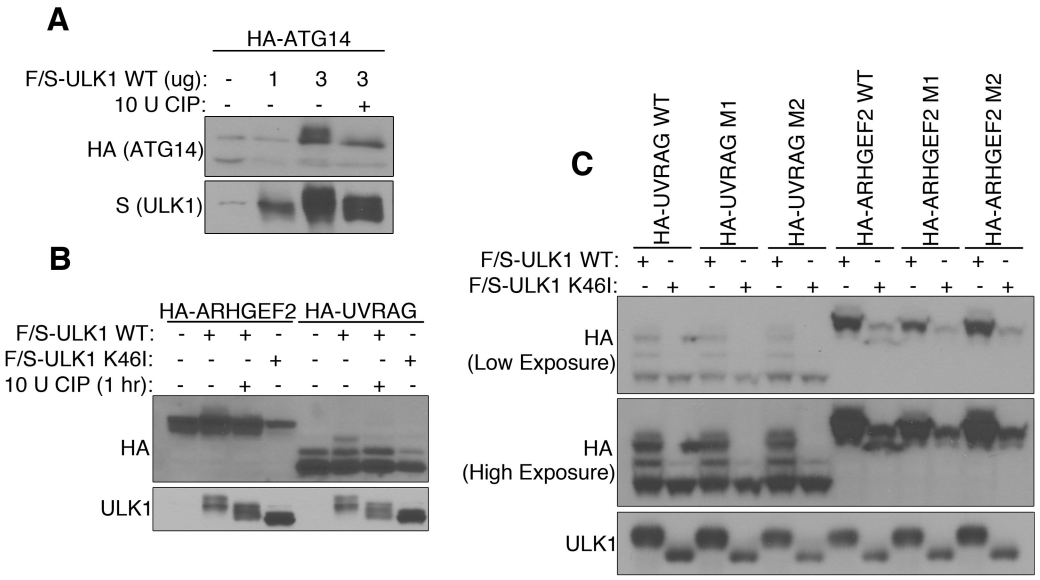

Figure 3.5 Co-expression with ULK1 alters the electrophoretic mobility of ATG14, UVRAG and ARHGEF2. Co-expression with ULK1 wild-type leads to an upward mobility shift, which can be reversed by the phosphatase CIP, for (**A**) ATG14 and (**B**) ARHEGF2 and UVRAG. (**C**) Assessing alanine mutants of UVRAG and ARHGEF2 for their ability to inhibit the ULK1-dependent mobility shift.

Since the mobility shift assay was largely inconclusive, I decided to evaluate the putative substrates in an ULK1 *in vitro* kinase assay for their ability to function as direct substrates. I was able to demonstrate that ARHGEF2 and GLIPR2 are direct *in vitro* substrates of the ULK1 kinase (Figure 3.6). Unfortunately, no other putative substrates were phosphorylated in this assay, including ATG14, UVRAG, TRIM28. Using alanine mutants, I was able to demonstrate that ULK1 directly phosphorylates GLIPR2 at Ser-55, as predicted by the forward SILAC experiment (Figure 3.6 B).

The reverse SILAC experiment identified two putative phospho-acceptor sites on ARHGEF2. However, the probability of phosphorylation was divided into multiple residues, as such I generated two combined alanine mutants for ARHGEF2. The ARHGEF2 M1 combined mutant compromises a S939A and S940A mutation, which I further dissected into single mutants M3 (S939A) and M4 (S940A). The ARHGEF2 M2 combined mutant compromises a S951A, S952A and S955A mutation. Using these alanine mutants, I was able to demonstrate that ULK1 directly phosphorylates ARHGEF2 on S939 (Figure 3.6 C). I had to employ the ARHGEF2 M1 and M4 mutants because the M3 mutation severely compromises protein expression.

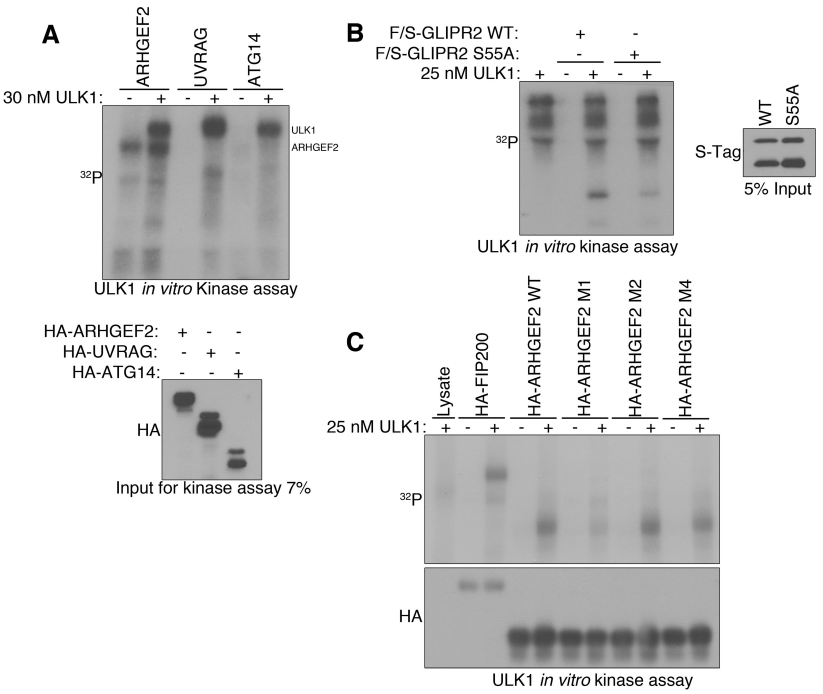

Figure 3.6 ULK1 directly phosphorylates GLIPR2 and ARHGEF2. (**A**) ARHGEF2, UVRAG and ATG14 are subjected to an ULK1 in vitro kinase assay. In this experiment, co-purifying impurities in the substrate IP lead to non-specific phosphorylation of ARHGEF2 in the absence of ULK1. The bottom panel is the input for the kinase assay. (**B**) GLIPR2 wild-type or S55A mutant were subjected to an ULK1 *in vitro* kinase assay. Alanine mutation of Ser-55 abrogates direct phosphorylation by ULK1. The panel on the right represents the input for the kinase assay. (**C**) ARHGEF2 wild-type, combined alanine mutants M1 and M2, and the single-site mutant M4, were subjected to an ULK1 *in vitro* kinase assay. The top panel is the autoradiograph. The bottom panel is a western comparing the relative levels of the substrates.

Since ARHGEF2 and GLIPR2 proved to be direct substrates of ULK1, Helen Kang and I continued characterizing them. Helen is currently collaborating with an antibody company to generate phospho-specific antibodies for GLIPR2 pSer-55. She is also generating a GLIPR2 -/- MEF cell line, in order to determine whether GLIPR2 can modulate starvation-induced autophagy. Ultimately, she will query whether the ULK1-dependent phosphorylations on GLIPR2 are functionally relevant in regulating starvation-induced autophagy.

I have taken on the role to further characterize ARHGEF2. I generated ARHGEF2 -/- MEF cell lines using CRISPR-CAS9. I noticed that clones with residual expression of ARHGEF2 showed a slight increase in LC3 conversion, relative to the wild-type MEF parental cell line used to generate the knockout. Interestingly, a clone completely lacking ARHGEF2 expression showed a dramatic increase in LC3 conversion, an indicator for autophagy induction (Figure 3.7 A). However, when I evaluated a panel of ARHGEF2 knockout cell lines, against the wild-type MEF parental cell line, I did not see such a dramatic activation of starvation-induced autophagy, as per LC3 conversion (Figure 3.7 B). It was difficult to analyze the effect of ARHGEF2 because the knockout cell lines had a drastically different level of basal LC3-I and p62. As such, I reconstituted the ARHGEF2 -/- MEF cell line with an empty vector or the wild-type protein, in order to facilitate a more equal comparison. I was able to demonstrate that reconstituting the ARHGEF2 -/- cell line with the wild-type protein resulted in a slower autophagic response, as per LC3 conversion (Figure 3.7 C). As such, it

seems that ARHGEF2 is functioning as a negative regulator of starvation-induced autophagy. I also reconstituted the ARHGEF2 -/- cell line with the combined alanine mutant M1; however, the result is inconclusive (Figure 3.7 D).

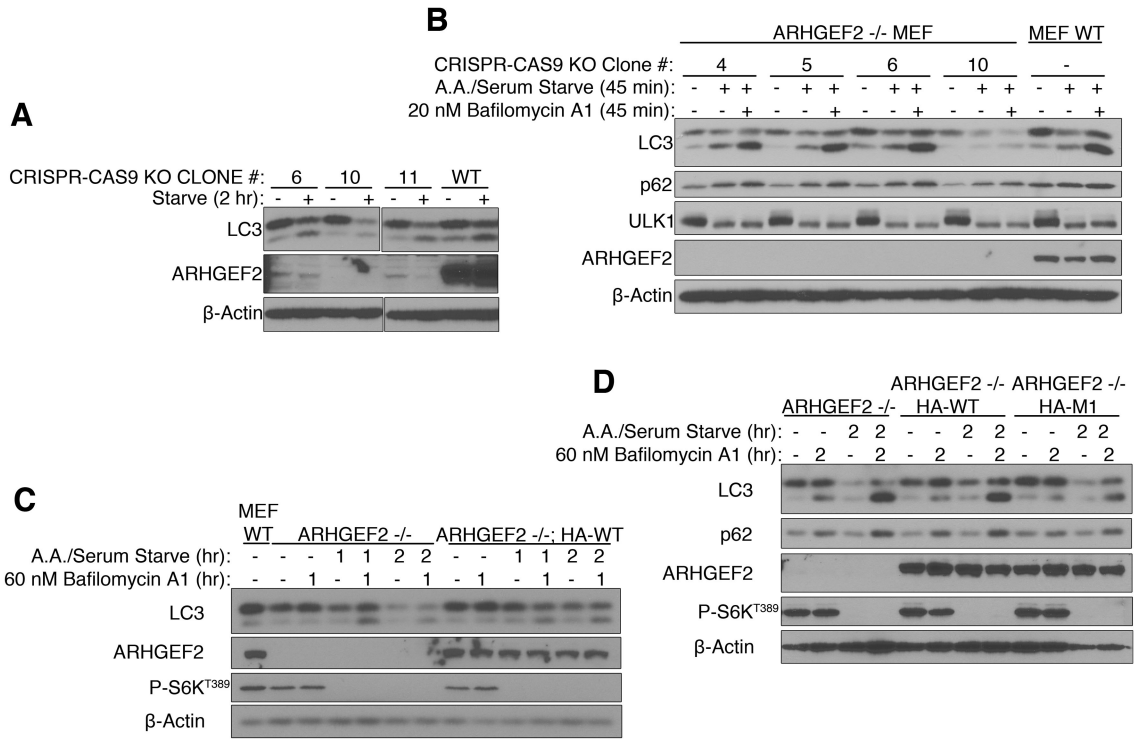

Figure 3.7 ARHGEF2 expression modulates starvation-induced autophagy. (**A**) and (**B**) *ARHGEF2* -/- single clones are evaluated for their capacity of starvation-induced autophagy. (**C**) *ARHGEF2* -/- single clone #5, is reconstituted by the stable expression of ARHGEF2 wild-type or (**D**) the M1 mutant, and evaluated for their capacity to undergo starvation-induced autophagy.

3.3 Discussion

The goal of this project was to identify novel substrates of the ULK1 kinase, in order to facilitate a deeper understanding of the molecular mechanisms that govern starvation-induced autophagy. My approach utilized a two-cell line reconstitution system that relied on the ULK1 kinase activity to promote or, lack thereof, to dampen autophagy. We then compared the phospho-proteome between these two cell lines using SILAC, a quantitative phospho-proteomics approach. Our analysis generated a list of nearly 60 putative ULK1 targets. The value of this list is underscored by the reproducible presence of FIP200 phospho-peptides. FIP200 is a member of the ULK1 kinase complex and a known substrate of ULK1.

The validation process of these putative substrates involved a three-step process. First, we evaluated the electrophoretic mobility of the substrates when co-overexpressed with ULK1. This assessment relied on the fact that known substrates of ULK1, such as ATG13 and FIP200, demonstrate a mobility retardation that is mediated by the ULK1-dependent phosphorylations. Second, I evaluated the substrates for direct phosphorylation by ULK1 in an *in vitro* kinase assay. Third, I evaluated the functional relevance of the ULK1 substrate by generating a knockout cell line and assessing the capacity for starvation-induced autophagy. Although I recognized the limitations of the first two assessments, I narrowed my focus to two specific proteins, GLIPR2 and ARHGEF2, because I demonstrated that they could function as *in vitro* substrates to the ULK1 kinase. I was able to demonstrate that expression of ARHGEF2 does in fact negatively

modulate the starvation-induced autophagic response. My assessment suggests that ARHEGF2 is a negative regulator of autophagy. The functional significance of the ULK1-dependent phosphorylation still needs to be established. This assessment will necessitate the use of phospho-specific antibodies. I began the process of generating the ARHGEF2 phospho-specific antibodies. I ordered the phospho-peptide, then conjugated it to KLH and performed a subsequent purification. The conjugated phospho-peptide was then used by a vendor (Pocono Rabbit Farm) to inject rabbits and generate serum containing the pertinent polyclocal phospho-specific antibodies. The polyclonal phospho-specific antibodies now need to be purified using reiterative peptide affinity purification, which includes a phospho-peptide column and a non-phospho-peptide column. As for GLIPR2, my fellow graduate student Helen Kang is overseeing the characterization of the knockout cell line and evaluating the physiological relevance of the ULK1-dependent phosphorylations. In order to strengthen our in vitro observations, we will have to continue to demonstrate that these phosphorylation sites are present in cells and that ULK1 can interact with GLIPR2 and ARHEGF2.

Overall, this study is the first to generate a phosphomap of ULK1-dependent phosphorylations. It identifies proteins potentially regulated by ULK1 phosphorylation and identifies the specific phospho-acceptor residue. As more of these putative substrates are implicated in autophagy, it will be important to determine whether these putative phosphorylation sites are functionally relevant

to the autophagic process. Case and point, there was a recent publication that identified the Drosophila protein Gyf as a positive regulator of autophagy (176). The mammalian homologue *GIGYF2* was identified in the reverse SILAC experiment with an H/L ratio of 0.219. It will be in important to determine whether GIGYF2 can also modulate mammalian autophagy and whether the putative ULK1-dependent phosphorylations are functionally important.

Assessing the 2-cell line system and SILAC approach

Although I was able to confirm two novel *in vitro* substrates of the ULK1 kinase, I feel that I must critically analyze my approach, in order to help prioritize the assessment of other putative substrates. I performed the SILAC experiment twice, with the aid of the mass spectrometry core facility at MSKCC. Since we alternated the heavy label in these two experiments, we expected to see a list of proteins with reciprocal H/L ratios. However, there was very limited overlap between the phospho-peptides (greater than three standard deviations from the mean) identified in the two experiments. The only protein that was reproducible and had a reciprocal H/L ratio was FIP200. This limited reproducibility might be the results of several factors. First, our samples were used to optimize the sample preparation and processing protocols for SILAC experiments, at the mass spectrometry core facility at MSKCC, and so unless all sample-prep steps are uniformly consistent and reproducible, small technical discrepancies can lead to large result output biases. Second, the total amount of protein that was processed for the two experiments was different. This is important because mass

spectrometers have a limited capacity to detect low abundance peptides, as such, less total protein might have resulted in undersampling. Third, we did not extensively manually verify phospho-peptides derived from ULK1 wild-type cells, with no H/L ratio, for the lack of the corresponding phospho-peptide derived from cells expressing ULK1 K46I. If we assume that the ULK1 K46I mutant is completely kinase-activity deficient, then a phospho-peptide that is solely phosphorylated by the ULK1 kinase cannot be designated an H/L ratio, in our system. An H/L ratio is only designated when a phospho-peptide is detected both in heavy-labeled and light-labeled cells. As such, we largely overlooked a group of proteins that had the highest potential to be ULK1 substrates. However, the ULK1 K46I mutant most likely has some residual kinase activity and so we could potentially obtain H/L ratios for ULK1 substrates. Since the kinase activity of the ULK1 K46I mutant is not sufficient to promote the activation of downstream autophagy, this set up could never identify ULK1 substrates that function further downstream. ULK1 substrates that could obtain an H/L ratio would most likely be limited to proteins that function at the beginning of the autophagic process. Perhaps, this explains why FIP200 is identified in both SILAC experiments. If ULK1 K46I does in fact have residual kinase activity, it would most efficiently phosphorylate its' binding partner. The decision to focus on phospho-peptides with H/L ratios was a result of the extensive manual validation that would otherwise be required. Although if I had the resources, it would be a valuable investment of effort and time.

Assessing the substrate validation approach

Our approach to validate the putative ULK1 substrates had several limitations. I started the validation process by looking for an electrophoretic mobility with co-overexpression with ULK1, which could be reverted by phosphatase treatment. The rationale behind this approach was that several known substrates of ULK1 experience a clear upward mobility shift when co-overexpressed with ULK1. However, not all phosphorylation events alter the electrophoretic mobility of a protein. Assessing the substrates by direct phosphorylation in an *in vitro* ULK1 kinase assay also had several limitations. Mainly that a substrate might have to be presented in the context of a complex or a specific binding partner. Additionally, the *in vitro* kinase assay dissolves the physical boundaries between proteins, as such a direct phosphorylation may not translate to be physiologically relevant. Lastly, I evaluated putative substrates for their ability to modulate starvation-induced autophagy, when in reality this is not an absolute requirement. The ULK1 complex integrates signals of nutritional deficiency from the mTOR and the AMPK pathway and then translates that signal to the downstream core autophagy machinery. It is also quite conceivable that ULK1 regulates complimentary pathways, in order to facilitate a coordinated response in the face of nutritional starvation. In that case, it would be interesting to probe whether, in different starvation stimuli, ULK1 can phosphorylate a different set of proteins.

Evaluating the putative ULK1 substrates: FIP200

Although the SILAC experiment identified a total of five novel ULK1-mediated phosphorylations on FIP200, this project necessitates the additional investment of phospho-specific antibodies. The phospho-specific antibodies would confirm the requirement of the ULK1 kinase and confirm their presence *in vivo*. In addition, I was unable to assess the functional significance of these phosphorylations in regulating starvation-induced autophagy because I couldn't reconstitute the FIP200 -/- cells. The FIP200 coding sequence is so large that it exceeds the capacity of the retroviral vector. In order to facilitate expression, I would transfer the FIP200 coding sequences to a lentiviral vector, which have a higher capacity.

In speculating the function of the ULK1-dependent phosphorylations on FIP200, I wondered whether they might mediate the interaction between FIP200 and ATG16L1, which facilitates targeting of ATG16L1 to the isolation membrane. Although the interacting domain on FIP200 (amino acids 1315-1413) encompasses an ULK1-dependent phosphorylation site (amino acid 1367), the interaction between ATG16L1 and FIP200 is largely insensitive to nutrient conditions and ULK1/2 deletion (150,177). Aside from its role in autophagy, FIP200 interacts with many proteins and is involved in the regulation of various cellular functions, such as proliferation, cell size control, cell migration and apoptosis (178). It will be important to query whether the phosphorylation events that I identified can modulate any of these autophagy-independent processes.

Addressing this question might bring more clarity as to how FIP200 can function to coordinate various signaling pathways.

Evaluating the putative ULK1 substrates: GLIPR2

In this phospho-proteomic study, I identified GLIPR2 as a direct substrate of the ULK1 kinase at Ser-55. I am particularly interested in further characterizing the role of this phosphorylation in regulating starvation-induced autophagy because GLIPR2 has been previously been implicated as a negative regulator of autophagy. GLIPR2, also known as Golgi-associated pathogenesis-related protein 1 (GAPR-1), is a protein that associates with lipid rafts at the cytosolic leaflet of the Golgi membrane (179). It was recently identified as a Beclin 1-interacting protein (172). This interaction functions to tether Beclin 1, in the Golgi apparatus, where it cannot support autophagy. Inhibition of the GLIPR2-Beclin 1 interaction results in enhanced early autophagosome formation. Also, knockdown of GLIPR2 potentiates the autophagic flux. As such, it will be important to determine whether this novel phosphorylation can somehow modulate the binding to Beclin 1.

Evaluating the putative ULK1 substrates: ARHGEF2

In this phospho-proteomic study, I identified two putative phosphorylation sites on ARHGEF2 and validated Ser-939 as a direct phosphorylation site for ULK1 in an *in vitro* kinase assay. ARHGEF2 is a microtubule-associated guanine nucleotide exchange factor (GEF) for the RHO family of small GTPases (180). ARHGEF2

can activate the RhoA GTPase to regulate exocytosis vesicle trafficking and fusion with the plasma membrane (181). This function relies on the direct interaction between ARHGEF2 and components of the exocyst complex, specifically Sec5. This ARHGEF2-Sec5 interaction affects the stability of an exocyst subcomplex and localization of the exocyst components. This finding is interesting because it raises the possibility that the ARHGEF2-RhoA pathway can coordinate the cytoskeleton with membrane trafficking and fusion. Beyond functioning to regulate the exocyst complex to regulate exocytosis, ARHGEF2 has also been implicated as a critical signaling intermediate for innate immune signaling through the STING pathway (182). Strikingly, core innate immune signaling through TBK1 and STING is also supported by the Sec5 subunit of the exocyst complex (183). In addition, the exocyst complex functions as a platform for components of the autophagy machinery and has been shown to regulate autophagy induction during metabolic stress (184,185). During starvation, the ULK1 and PI3K complexes bind to the Exo84 exocyst subcomplex to form an autophagy-active complex. In contrast, during nutrient-rich conditions, these complexes bind the Sec5 exocyst subcomplex to create an autophagy-inactive complex.

Since the Sec5 exocyst complex and ARHGEF2 seem intersect in several functions, it will be important to determine the exact role of ARHGEF2 in regulating autophagy. In order to gain further insight into the role of ARHGEF2 in autophagy, it will first be important to determine whether its function is GEF-

activity dependent. This query can be addressed by reconstituting the *ARHGEF2* -/- cells with ARHGEF2 wild-type, a dominant-negative mutant (Y393A) or a constitutively active mutant (C53R), and then assessing the autophagy flux. Additionally, the *in vivo* phosphorylation at Ser-939 and its dependence on ULK1-mediated phosphorylation needs to be confirmed with the use of phospho-antibodies.

Reassessment of putative ULK1 substrates: ATG14, UVRAG, TRIM28

The SILAC experiment is particularly "bottom-heavy" and so I didn't have sufficient time and resources to further pursue other high-value putative ULK1 substrates. In my opinion, several proteins that I analyzed should be reassessed including ATG14, UVRAG, TRIM28 and ISYNA-1. Also, some proteins, which I did not have the time to analyze, should be further investigated as putative ULK1 substrates, including SNX13, ARSG and DARS2.

The phospho-peptides for both ATG14 and UVRAG did not have a designated H/L ratio because they were manually verified as not having a corresponding light peptide, in the forward experiment. As such, these sites are high-value putative ULK1 substrates. Both ATG14 and UVRAG demonstrated an electrophoretic mobility shift when they were co-overexpressed with ULK1. However, when I mutated the corresponding site to alanine, in UVRAG (phospho-acceptor restricted to amino acids 303-316), I could not inhibit the ULK1-mediated shift. Also, neither UVRAG nor ATG14 could be directly

phosphorylated by ULK1 in an *in vitro* kinase assay. ATG14 was recently identified as a substrate of ULK1 on Ser-29; however, the site that I identified is restricted to amino acids 2-20 in ATG14. The literature suggests that this putative phosphorylation is functionally meaningful because ATG13 Ser3 was identified as a site of mTOR phosphorylation. *ATG14*-null cells reconstituted with an alanine mutant for these mTOR sites demonstrated increased autophagy under nutrient-rich conditions (186). The only way to further assess these phosphorylation sites is to generate phospho-specific antibodies.

I am particularly interested in further characterizing TRIM28 and ISYNA-1. TRIM28 is known to mediate Lys840 SUMOylation on Vps34, which increases its lipid kinase activity (173). This phospho-proteomic experiment identified three putative ULK1-mediated phosphorylations restricted to a single phospho-peptide spanning amino acids 592-629. When I co-overexpressed TRIM28 along with ULK1, I did not observe a mobility shift. Also, TRIM28 could not be phosphorylated by ULK1 in an *in vitro* kinase assay. However, these results do not guarantee that TRIM28 is not an ULK1 substrate. To make a conclusive decision on whether these sites are ULK1-depedent, there would need to be an investment into phospho-specific antibodies. I am interested in Inositol-3-phosphate synthase (ISYNA1) because it catalyzes the synthesis of D-inositol-3-phophate from glucose-6-phosphate, which then feeds into the many pathways of phosphoinositide metabolism (187). Since phosphoinositides are such master

regulators of autophagy (188), I would want to determine whether the function of ISYNA1 is required to replenish their availability during autophagy.

In addition, based on a review of the literature, the following putative substrates merit an assessment for their involvement in autophagy, SNX13, Dars2 and ARSG. SNX13 is involved in endolysosomal trafficking and contains a PX domain, which acts as a sensor of membrane phosphoinositide lipids (189,190). In addition, *SNX13*-null mice are embryonic lethal and endoderm-derived cells show numerous large autophagic vacuoles (191). Arylsulfatase G (ARSG) is a lysosomal sulfatase that functions in the lysosomal degradation pathway of glucosamine residues in heparin sulfate (192). Deficiency in ARSG causes a subclass of lysosomal storage disorders called mucupolysaccharidoses (193). I highlight ARSG because it's interesting to consider that ULK1 may modulate the lysosomal degradation capacity by regulating key proteins. This possibility does not seem so unreasonable when we consider that mTOR also indirectly regulates autophagy by controlling lysosomal biogenesis through the regulation of TFEB (194,195).

DARS2 encodes a mitochondrial aspartyl-tRNA synthetase (mtAspRS), and as its name suggests functions to aminoacylate $tRNA^{Asp}$. Mutation of DARS2 is known to result in a condition known as leukoencephalopathy with brain stem and spinal cord involvement and lactate elevation (LBSL) (196). Described mutations decrease the catalytic activity of DARS2 and result in the

compromised incorporation of aspartic acid into mitochondrial-DNA-encoded proteins. The end result is compromised oxidative phosphorylation and an accumulation of lactate. The putative ULK1-mediated phosphorylation on DARS2 in on Ser-45. Interestingly, Ser45 is located in the predicted mitochondrial targeting sequence of DARS2 and a Ser^{45} to Gly^{45} mutation is known to impair the import of DARS2 into the mitochondria and lead to LBSL (197). As such, this putative phosphorylation has the potential to coordinate the nutritional status of the cell, autophagy and mitochondrial activity.

3.4 Experimental Procedures

Cell culture, Lysis and In-Solution Digestion

ULK1/2 -/- MEF cells were reconstituted by the stable expression of FLAG-S-ULK1 wild-type or K46I. Cells were grown in DMEM media supplemented with 10% dialyzed FBS and penicillin and streptomycin either unlabeled L-arginine (Arg0) and L-lysine (Lys0) at 50 mg/liter or equimolar amounts of the isotopic variants [U-^{13}C6, $^{15}N_4$]-L- Arginine (Arg10) and [U-$^{13}C_6$]-L–Lysine (Lys6), (Cambridge Isotope Laboratories). After ten cell doublings, cells were >99% labeled with the isotopes. Cells were expanded to 8 x 15-cm plates. Cells were starved in amino acid and serum free media for 1.5 hours. Cells were collected, washed with ice cold 1X PBS and frozen in liquid nitrogen. For lysis, cells were thawed on ice and lysed in lysis buffer (8 M urea, 25 mM Tris-HCl, 150 mM NaCl, phosphatase inhibitor 2 and 3 (Sigma) and protease inhibitors. (1 mini-Complete EDTA-free tablet per 10ml lysis buffer; Roche). Lysates were sonicated three times at 30 – 40% power for 15 sec each with intermittent cooling on ice, followed by centrifugation at 14000 rpm for 30 min at 4 °C. The supernatant were transferred to a new tube and the protein concentration was determined using a BCA assay (Pierce). 10mg of total protein from each light and heavy labeled cells mixed and total 20 mg protein was reduced with 5 mM DTT at 56 °C for 30 min. Afterwards, lysates were thoroughly cooled to room temperate (~21 °C) and alkylated with 11 mM iodoacetamide (IAA) at room temperature for 30 min. The alkylation was then quenched by the addition of an additional 5 mM DTT.

Samples were digested sequentially, first samples were diluted 4 fold with 50 mM ammonium bicarbonate and digested with lys-C 1:100 at 37 °C for 4 hours. Afterward, samples were further diluted 2 fold with 50 mM ammonium bicarbonate and 1 mM $CaCl_2$, and digested overnight at 37 °C with trypsin 1:50. The next day, the digestion was stopped by the addition of 0.25% TFA (final v/v), centrifuged at 10000 rpm for 10 min at room temperature to pellet precipitated lipids, and cleared supernatant desalted on a SepPak C_{18} cartridge 500mg (Waters). Desalted peptides were lyophilized and stored at -80 °C until further use.

Phospho-peptide Enrichment

For phospho-peptide enrichment, 20 mg of lyophilized peptides were resuspended in 1 mL of binding buffer (2 M lactic acid in 50% acetonitrile). Resuspended peptides were incubated with 80 mg of titanium dioxide microspheres for one hour, by an air thermostat vortex mixer on the highest speed setting at room temperature (~ 21 °C). Afterwards, the beads were washed twice with 200µl of the binding solution and three times with 200 µl 50% ACN / 0.1% TFA, and phospho-peptides were eluted sequentially with 100 µl of 5% ammonium hydroxide, 5% piperdine and 5% pyrrolidine solution. Peptide elutions were combined, quenched with 150 µl 50% ACN / 5% formic acid, dried and desalted on a SepPak C_{18} cartridge 500mg (Waters). Desalted peptides were dried down by speed-vac and stored at -80 °C until further use.

Strong Cation Exchange Chromatography (SCX)

Dried phospho-peptides were resuspended in 1 mL of SCX buffer A (7 mM KH_2PO_4, pH 2.65 / 30% ACN) and separated per injection on a SCX column (PolySULFOETHYL A 200 x 9.4 mm, 5 µm 200 Å pore, item# 209SE0502; PolyLC Inc, Columbia, MD) using a gradient of 0 to 10 % SCX buffer B (350 mM KCl / 7 mM KH_2PO_4, pH 2.65 / 30% ACN) over 10 minutes, 10% to 17% SCX buffer B over 17 minutes, 17% to 32% SCX buffer B over 13 minutes, 32% to 60% SCX buffer B over 10 minutes, 60% to 100% SCX buffer B over 2 minutes, holding at 100% SCX buffer B for 5 minutes, from 100% to 0% SCX buffer B over 2 minutes, and equilibration at 0% SCX buffer B for 65 minutes, all at a flow rate of 2.5 ml/min, after a full blank injection of the same program was run to equilibrate the column. 15 fractions were collected from the onset of the void volume (2.2 minutes) until the elution of strongly basic peptides in the 100% SCX buffer B wash (52 minutes), at 2.075-minute intervals. After separation, the SCX fractions were lyophilized and desalted using a 50-mg SepPak C_{18} cartridge (Waters). Desalted peptides were dried down by speed -vac and dissolved in 3% acetonitrile/0.1% formic acid and were injected onto a C18 capillary column on a nano ACQUITY UPLC system (Water) which was coupled to the Q Exactive mass spectrometer (Thermo Scientific).

Antibodies

Purified anti-HA.11 epitope tag antibody (1:3,000, Covance no. MMS-101P). ARHEGF2/GEF-H1 antibody (1:3,000, Bethyl Laboratories no. A301-928A-T)

DNA Constructs

Full-length mouse cDNA clones of putative ULK1 substrates were ordered through the Mammalian Gene Collection (MGC) at GE Dharmacon. cDNAs were then cloned into pBabe/puro containing an N-terminal HA tag. Serine to alanine mutations were generated by PCR-mediated site-directed mutagenesis. All mutations were subsequently confirmed by direct sequencing.

In vitro Phosphatase Assay

Cells were lysed in RIPA buffer supplemented with protease with or without phosphatase inhibitors. A total of 60 µg of lysate was incubated in 1X NEB3 buffer and with or without 10 U of calf intestinal phosphatase (CIP) (New England BioLabs, M0290S) for 1 hour at 37°C. The reaction was terminated by the addition of sample buffer and analyzed by immunoblotting.

ULK1 Kinase Assay

HA-tagged putative substrates were transiently over-expressed in HEK293T cells with Lipofectamine 2000, as per manufacturer's instructions. I transfected 2 x 10-cm plates for each substrate. After 48 hours, cells were lysed in lysis buffer (50 mM Tris, pH 7.5, 150 mM NaCl, 10% glycerol, 1% Triton X-100, 1 mM

EDTA/EGTA, 0.5 mM DTT) supplemented with protease inhibitors and phosphatase inhibitors (Sigma, P0044 and P5726). Lysates were centrifuged at 20,000 x g for 15 minutes. Substrates were immunoprecipitated with 15 µL of S-protein agarose beads (EMD Millipore, 69704-3) with rotation at 4°C for 6 hours. After washing with lysis buffer, the S-protein agarose beads were resuspended in ULK1 kinase buffer (25 mM HEPES, pH 7.5, 50 mM NaCl, 10 mM $MgCl_2$, 0.1% Tween-20, 1 mM DTT, 0.5 mg/ml BSA 10 µM cold ATP, 0.5 µCi of [γ^{32}-P] ATP (PerkinElmer, BLU002A250UC). Recombinant SF-9 purified ULK1 was added to the reaction at a final concentration range of 20 nM – 40 nM. The reaction was incubated at 30 °C for 40 minutes. The reaction was terminated by the addition of sample buffer. The samples were run in a SDS-PAGE gel, transferred to nitrocellulose and signal was acquired with X-ray film.

CRISPR-CAS9 Knockout MEF Cell Line

CRISPR-CAS9 system of RNA-guided genome editing was used to generate *ARHGEF2* -/- MEFs. The targeting sequence 5'-CACATGGTCATGCCGGAGA-3' was incorporated into a 60mer oligo, as described previously (165). The forward and reverse oligos were annealed to make a 100bp double-stranded DNA fragment using Phusion polymerase (NEB, no. M0530S). The DNA fragment was fused by Gibson assembly (NEB, no. E2611S) to an AflII-linearized U6 target gRNA expression vector (Addgene, no. 41824). The targeting sequence was confirmed by sequencing. MEF cells were then electroporated using the Amaxa

MEF2 nucleofector kit (VAPD-1005), as per manufacturer's instructions. Cells were electroporated in three consecutive days and then plated for single clones.

CHAPTER 4. PERSPECTIVES

4.1 Exploring phosphorylation-dependent conformational changes

We have begun to understand how the ULK1 kinase complex is regulated to induce autophagy. Since autophagy induction is not regulated by the formation of the initiation complex, as it is in yeast, I have defined inhibitory phosphorylations that impinge on the complex. Based on my results, I propose that mTOR and AMPK can regulate the induction of autophagy by mediating phosphorylations on ATG13 that inhibit ULK1 kinase activity and translocation to the isolation membrane. However, further investigation is required to define the precise molecular mechanism by which phosphorylation events regulate the autophagy induction function of the ULK1 complex

One possibility is that these phosphorylations on ATG13 might be occluding binding sites for ULK1 substrates. I tried to address this possibility by overexpressing ATG13 wild-type or a combined alanine mutant, under nutrient-rich conditions, and analyzing the binding partners by SDS-PAGE and silver staining. However, I did not see any changes. However, this experiment has a few limitations. First, binding of a putative target to ATG13 might have to take place in the context of the ULK1 kinase complex. Second, binding of a putative ULK1 substrate to ATG13 might necessitate a positive signal that is provided by nutritional starvation and cannot be replicated by simply removing a phosphorylation on ATG13 to make binding accessible. As such, a better

experiment to test the involvement of these phosphorylation sites on recruiting ULK1 substrates would be to overexpress ATG13 wild-type or a phospho-mimetic mutant, along with FIP200 and ULK1, under amino acid/serum starvation. Putative substrates would be able to bind wild-type ATG13 because it can be dephosphorylated upon starvation while the phospho-mimetic mutant would not bind the substrates. Conversely, the binding of putative ULK1 substrates might be mediated by the activating phosphorylations mediated on ULK1, ATG13 and FIP200.

Another possibility is that the inhibitory phosphorylations on the ULK1 complex maintain a steady-state level of the complex that can be readily activated upon nutritional deficiency. The activation of autophagy is marked by a concurrent decreased in ULK1 and ATG13 protein levels. The role and mechanism of this starvation-induced degradation is not understood. However, it might function to efficiently tune autophagy to the nutritional status of a cell. Further research needs to explore whether this starvation-induced decrease in protein levels is mediated through the proteasome pathway, and if so, also identify the relevant E3 ligases.

Another possibility is that the inhibitory phosphorylations on the ULK1 complex mediate the lipid-binding capacity of ULK1 and ATG13. The extreme N-terminus of ATG13 contains four conserved basic residues that mediate binding to acidic phospholipids, mainly phosphatidic acid, PtdIns3P and PtdIns4P (99). A mutant

for these sites exhibited reduced *in vitro* affinity for all three phospholipids and also 50% fewer GFP-ATG13 punctae during starvation (99). The C-terminal domain of ULK1 has also been reported to direct membrane binding (122). Chan *et al* 2009, proposed a working model in which phosphorylation-dependent conformational changes would facilitate interaction between the C-terminal and N-terminal domains, in order to maintain ULK1 in a closed conformation (122). In addition, the structure of the ATG13 HORMA domain contains a positively charged sulfate-binding pocket. Since a HORMA domain can exist in two distinct conformations, this indicates that the N-terminus of ATG13 may undergo a conformational change upon phosphorylation, which alternates between a phospho-binding and a nonphospho-binding state (96,198). However, the structure of the ATG13 HORMA domain adopts a C-MAD2 state and it is unknown if ATG13 is indeed able to adopt an additional conformation. Since phosphorylation of ATG13 Ser-258 is responsible for the electrophoretic mobility during starvation, it is interesting to posit that the HORMA domain might bind this phosphorylated residue. As such, the phosphorylation status of the ULK1 complex may regulate conformational changes involving the exposure of membrane-binding domains.

4.2 ULK1 activating phosphorylations on the ULK1 kinase complex

The phosphorylations that ULK1 mediates on its own complex have largely remained unexplored. Recently, an ULK1-depdent phosphorylation on ATG13 was reported on Ser-318 (124). The role of this phosphorylation in regulating

autophagy induction is unknown. My phospho-proteomic study identified a potential ULK1-mediated phosphorylation on ATG13 (amino acid 172-199). In the forward experiment, this phospho-peptide had no designated H/L ratio and I manually verified that it was only present in cells expressing ULK1 wild-type. Another group was able to identify five ULK1-dependent phospho-sites *in vitro* (corresponding to amino acids S48, T170, T331, T428 and T478 in the ATG13 human isoform 2) (199). Their *in vivo* relevance also awaits further clarification.

Another study used mass spectrometry to identify Ser-1047 as a putative site of ULK1 auto-phosphorylation by comparing the phosphorylation status of ULK1 wild-type and the kinase-dead mutant ULK1 K46R (200). However, this site has not been validated by *in vivo* studies or phospho-specific antibodies. My phospho-proteomic analysis identified two phospho-peptides as putative auto-phosphorylation sites on ULK1 (amino acid 137-154 and 162-201). In the forward experiment, these phospho-peptides had no designated H/L ratio and I manually verified that they were only present in cells expressing ULK1 wild-type.

In addition to the putative ULK1-mediated phosphorylations that I described in Table 3.3, my phospho-proteomic analysis also identified three additional phospho-peptides on FIP200 (amino acid 89-117, 277-296, 1420-1450). These phospho-peptides have no designated H/L ratio and I manually verified that they don't have a corresponding phospho-peptide from cells expressing ULK1 K46I. Since these sites represent high-value putative ULK1-mediated sites, if I mutate

them to alanine, I might abrogate phosphorylation by ULK1 in the *in vitro* kinase assay.

4.3 Topics for exploration: ATG13

As a member of the ULK1 kinase complex, ATG13 has proven to be essential for the autophagy flux and it's phosphorylations have proven to function in regulating the induction of starvation-induced autophagy. Hitherto, ATG13 has only been reported to function through the ULK1 kinase. However, does ATG13 have ULK-independent functions in autophagy or non-autophagic functions?

The first indication that ATG13 might possess additional functions in autophagy, which are independent of ULK1, comes from experiments in the yeast system. Kraft *et al*., 2012 demonstrated that the autophagy-deficient phenotype of *Atg13*-null strains could be partially rescued by expression of an Atg13 mutant that cannot bind Atg1 (161). Similarly, in mammalian cells, expression of an ULK1/2 binding-deficient ATG13 variant in *ATG13*-null cells could partially reconstitute the autophagic flux (201). Consequently, ATG13 possess ULK-dependent and independent functions that promote autophagy.

Unlike ULK, the vertebrate genome only possesses one *ATG13* gene. However, alternative splicing of the ATG13 pre-mRNA results in the generation of multiple splice variants, with potentially different functions. There are at least 5 different isoforms reported at the protein level, in human cells, and 7 different isoforms

reported at the mRNA, in DT40 cells (82,199). Notably, the human isoform 2 has a truncated ULK1 binding domain. Also, the human isoform 3 lacks ULK1-binding capacity, the LIR (LC3-interacting region) motif but retains the FIP200-binding site and encodes an alternative C-terminus (82). It will be important to establish whether these variants do in fact lack ULK1-binding capacity and then probe their ability to reconstitute autophagy in *ATG13*-null cells. Additionally, are these variants constitutively produced or induced upon the induction of starvation? If these variants are constitutively produced, then that might indicate legitimate ULK1-indepdent functions. If these variants are induced upon starvation then that might indicate that these splice variants function as a feedback mechanism to dampen autophagy.

Recent studies indicate that ATG13 does in fact have non-autophagic functions. Like *FIP200*-null mice, *ATG13*-null mice die *in utero*, which is in sharp contrast to all the other *ATG*-deficient mice, which die shortly after birth. Also, *ATG13*-null mice show growth retardation and a myocardial growth defect (202). Thus indicating that ATG13 has a non-autophagic function essential for post-implantation embryonic development. Other members of the ULK1 kinase complex possess non-autophagic functions. ULK1 has been implicated in neuronal functions while FIP200 is involved in various signaling pathways including p53, focal adhesion kinase (FAK), Pyk2, tumor necrosis factor alpha (TNF-α) and Jun N-terminal protein kinase (JNK) (178,203).

4.4 Topics for exploration: ULK1

The yeast *Atg1* has multiple homologues in the mammalian system. Although an RNAi-based screen identified ULK1, but not ULK2, as essential for starvation-induced autophagy, later studies indicated that these proteins have redundant functions (80,84,204). Suggesting that their requirement in autophagy might be a function of their expression profile. In fact, the general consensus in the autophagy field is that ULK1 and ULK2 are the functional equivalents responsible for mediating the autophagy initiation (101). Consistently, mice with a single targeted deletion of the *ULK1* or *ULK2* gene are viable, whereas the double deletion results in the canonical neonatal death phenotype (83,87). However, the amino acid identity between these two proteins is only 79%, in the kinase domain, and 56%, in the C-terminal domain. Since the presence of two separate ULK complexes suggests a higher order of complexity, as compared to cells with just one Atg1, it is important to consider whether ULK1 and ULK2 have distinct functions in autophagy regulation, sensitivity to different starvation stimuli and a different specificity for downstream substrates. For example, ULK1 but not ULK2 is required for the autophagic clearance of mitochondria in reticulocytes (83). Another study reported that ULK1 but not ULK2, is critical to induced the autophagic response of cerebellar granule neurons (CGN) to low potassium in serum-free starvation (204). In order to tease apart the differences between ULK1 and ULK2, it will be important to establish their relative expression in different cell types and tissues and relative activation intensity to different nutritional starvation stimuli. These distinctions are vital for the future application

of ULK inhibitors (123,151,205). In certain physiological instances in which autophagy is ULK1- and ULK2-dependent, compounds, which target both kinases, will have a greater therapeutic potential.

4.5 Functional application of autophagy induction in human disease

My study and that of others indicate that, in eukaryotes, autophagy induction is regulated by nutrient availability and cellular energy through the direct regulation of the ULK1 complex by mTOR and AMPK. mTOR can phosphorylate ULK1 on Ser-757 and this phosphorylation mediates binding of AMPK, which can mediate its own phosphorylation on ULK1 Ser-638 (119). In fact expression of an alanine mutation of ULK1 Ser-757 primes cells for a faster response to starvation-induced autophagy. Additional AMPK-dependent phosphorylations on ULK1 have been described (Ser-467 and Ser-555); however, they were described as activating the ULK1 kinase (120). The contradictory reports on AMPK function in autophagy may be a function of the different starvation conditions used in these reports. I identified mTOR- and AMPK-dependent phosphorylations on ATG13, Ser-258 and Ser-224, respectively, and established that their mutation potentiates starvation-induced autophagy (206).

If these phosphorylation events represent the gatekeepers of autophagy induction, can we generate a system with constitutively active autophagy? In order to query this question, I could generate a triple knockout cell line, ULK1$^{-/-}$-ULK2$^{-/-}$-ATG13$^{-/-}$, and reconstitute it with the combined alanine mutants of ULK1

(S638A/S757A) and ATG13 (S224A/S258A). In this scenario, we may be able to observe an activate autophagy flux, without necessitating the inhibition of mTOR. Perhaps, I could intensify this “constitutive autophagy” by also including mutations in ATG14. mTOR also extends inhibitory phosphorylations onto the VPS34 complex through direct phosphorylation of ATG14 (Ser3, Ser223, Thr233, Ser383, and Ser440). In fact ATG14-null cells stably reconstituted with a combined alanine mutant for these sites can increase the activity of the VPS34 kinase and ultimately also autophagy, under nutrient-rich conditions (186). By removing these inhibitory phosphorylations, we might prime the ULK1 kinase to activate by auto-phosphorylation and trans-phosphorylation of its binding partners, ATG13 and FIP200.

As we begin to define and understand the molecular mechanisms that define the induction of autophagy, we must consider the pronounced implications of modulating autophagy in human diseases. Aberrant autophagy activation and inhibition are implicated in a plethora of human diseases. As such, there is a clear therapeutic need in modulating autophagy. Recently, several ULK1 small molecule inhibitors were developed, and they’re capable of inhibiting autophagy. The ultimate goal for these inhibitors is to use them in conjunction with approved therapies that are known to induce an autophagic response, which has been shown to limit the therapeutic potential (207). For example, in response to therapeutic and oncogenic stress, cancer cells upregulate and demonstrate an increased dependence on autophagy (207).

Although there are many known activators of autophagy; however, many also target the mTOR pathway or lysosomal function. Specific activation of autophagy was recently described by the Tat-Beclin 1 peptide, which functions by releasing Beclin 1 from inhibition by GLIPR2 (172). Modulating autophagy activation is particularly important in human longevity and age-related disorders, such as neurodegeneration.

Autophagy promotes cellar homeostasis by facilitating quality control, cellular source of energy and cellular defense. This indelible versatility is particularly crucial in terminally differentiated cells. As the autophagy capacity decreases with age, these cells experience an accumulation of damaged proteins and organelles that ultimately manifest in cellular functional decline (208). As such, autophagy inhibition is thought to be a major contributor to organismal aging. In fact, many regimens that are implicated in longevity, such as TOR inhibition, calorie restriction and sirtuin activation, led to the activation of autophagy (209,210). This relationship between autophagy and aging is more than just a correlation, since the attributable life-span extension is absent in autophagy-deficient animals (211). In addition, studies in *Drosophila melanogaster* indicate that activating autophagy increases lifespan, while decreasing autophagy shortens lifespan (212,213).

A hallmark of neurodegenerative disorders is the accumulation of aggregate-prone mutant proteins, such as polyglutamine tract-containing proteins in

Hungtington's disease, mutant alpha-synucleins in familial Parkinson's disease and mutant tau proteins in frontotemporal dementia (213,214). These aggregates cannot efficiently unfold, and so cannot be degraded through the proteasome pathway, as such, they serve as substrates for autophagy. However, once they overload the degradation capacity of autophagy, they accumulate and lead to cellular toxicity. The theory that compromised autophagy contributes to the development of neruodegeneration is underscored by the dramatic phenotype of tissue-specific knockouts for ATG genes. For example, mice deficient for *ATG5* or *ATG7* in neural cells develop a neurodegenerative disease marked by the accumulation of protein aggregates into inclusion bodies and progressive deterioration in motor function (136,137). The promise of autophagy enhancement is underscored my multiple studies, which showed that autophagy upregulation can enhance the clearance of aggregate-prone proteins and attenuate neural toxicity (215-217). However, the development of any future therapy must reconcile one glaring limitation. Previous treatments, which have cured Alzheimer's in mouse models, failed to improve symptoms in humans. Most likely because the drugs were administered in patients with advanced disease, and any benefit could not have a measurable effect. As such, patients with neurodegeneration need to be identified at the early-stages of the disease. However, the cost-effectiveness of this approach would need to be examined because it would necessitate the use of expensive imaging techniques, such as MRI and fluorodeoxyglucose PET.

By facilitating a constitutive hyper-activation of autophagy, possibly through the future application of gene targeting, we might be able to establish a sort of "whole-body rejuvenation." In this scenario, ageing and neurodegeneration could be delayed. However, we must also remain vigilant of the detrimental effects of over-activated autophagy. Although autophagy is general viewed as facilitating cell survival through stress adaptation, it can also constitute an alternative cell death pathway (218). Ultimately, the potential of autophagy enhancement as a therapeutic strategy will necessitate a careful investigation of its complex role in cell survival and cell death, in different physiological conditions.

REFERENCES

1. Guggenheim, K. Y. (1991) Rudolf Schoenheimer and the concept of the dynamic state of body constituents. *The Journal of nutrition* **121**, 1701-1704
2. Schoenheimer, R., Ratner, S., and Rittenberg, D. (1939) The Process of Continuous Deamination and Reamination of Amino Acids in the Proteins of Normal Animals. *Science* **89**, 272-273
3. Levine, B., and Klionsky, D. J. (2004) Development by self-digestion: molecular mechanisms and biological functions of autophagy. *Developmental cell* **6**, 463-477
4. Mizushima, N. (2007) Autophagy: process and function. *Genes & development* **21**, 2861-2873
5. Mizushima, N., and Levine, B. (2010) Autophagy in mammalian development and differentiation. *Nature cell biology* **12**, 823-830
6. Li, W., Yang, Q., and Mao, Z. (2011) Chaperone-mediated autophagy: machinery, regulation and biological consequences. *Cellular and molecular life sciences : CMLS* **68**, 749-763
7. Li, W. W., Li, J., and Bao, J. K. (2012) Microautophagy: lesser-known self-eating. *Cellular and molecular life sciences : CMLS* **69**, 1125-1136
8. Melendez, A., and Neufeld, T. P. (2008) The cell biology of autophagy in metazoans: a developing story. *Development* **135**, 2347-2360
9. Sabatini, D. D., and Adesnik, M. (2013) Christian de Duve: Explorer of the cell who discovered new organelles by using a centrifuge. *Proceedings of the National Academy of Sciences of the United States of America* **110**, 13234-13235
10. De Duve, C. (1963) The lysosome. *Scientific American* **208**, 64-72
11. Clark, S. L., Jr. (1957) Cellular differentiation in the kidneys of newborn mice studies with the electron microscope. *The Journal of biophysical and biochemical cytology* **3**, 349-362
12. Novikoff, A. B. (1959) The proximal tubule cell in experimental hydronephrosis. *The Journal of biophysical and biochemical cytology* **6**, 136-138
13. Hruban, Z., Spargo, B., Swift, H., Wissler, R. W., and Kleinfeld, R. G. (1963) Focal cytoplasmic degradation. *The American journal of pathology* **42**, 657-683
14. De Duve, C., and Wattiaux, R. (1966) Functions of lysosomes. *Annual review of physiology* **28**, 435-492
15. Ashford, T. P., and Porter, K. R. (1962) Cytoplasmic components in hepatic cell lysosomes. *The Journal of cell biology* **12**, 198-202
16. Ericsson, J. L., and Trump, B. F. (1965) Observations on the application to electron microscopy on the lead phosphate technique for the demonstration of acid phosphatase. *Histochemie. Histochemistry. Histochimie* **4**, 470-487
17. Glinsmann, W. H., and Ericsson, J. L. (1966) Observations on the subcellular organization of hepatic parenchymal cells. II. Evolution of reversible alterations induced by hypoxia. *Laboratory investigation; a journal of technical methods and pathology* **15**, 762-777

18. Brandes, D., and Bertini, F. (1964) Role of Golgi Apparatus in the Formation of Cytolysomes. *Experimental cell research* **35**, 194-197
19. Seglen, P. O., Gordon, P. B., Tolleshaug, H., and Hoyvik, H. (1986) Use of [3H]raffinose as a specific probe of autophagic sequestration. *Experimental cell research* **162**, 273-277
20. Marzella, L., and Glaumann, H. (1980) Increased degradation in rat liver induced by vinblastine. II. Morphologic characterization. *Laboratory investigation; a journal of technical methods and pathology* **42**, 18-27
21. Mizushima, N., Ohsumi, Y., and Yoshimori, T. (2002) Autophagosome formation in mammalian cells. *Cell structure and function* **27**, 421-429
22. Glaumann, H., Ericsson, J. L., and Marzella, L. (1981) Mechanisms of intralysosomal degradation with special reference to autophagocytosis and heterophagocytosis of cell organelles. *International review of cytology* **73**, 149-182
23. Amenta, J. S., and Brocher, S. C. (1981) Mechanisms of protein turnover in cultured cells. *Life sciences* **28**, 1195-1208
24. Pfeifer, U. (1978) Inhibition by insulin of the formation of autophagic vacuoles in rat liver. A morphometric approach to the kinetics of intracellular degradation by autophagy. *The Journal of cell biology* **78**, 152-167
25. Seglen, P. O., and Bohley, P. (1992) Autophagy and other vacuolar protein degradation mechanisms. *Experientia* **48**, 158-172
26. Mortimore, G. E., and Mondon, C. E. (1970) Inhibition by insulin of valine turnover in liver. Evidence for a general control of proteolysis. *The Journal of biological chemistry* **245**, 2375-2383
27. Deter, R. L., Baudhuin, P., and De Duve, C. (1967) Participation of lysosomes in cellular autophagy induced in rat liver by glucagon. *The Journal of cell biology* **35**, C11-16
28. Mortimore, G. E., and Schworer, C. M. (1977) Induction of autophagy by amino-acid deprivation in perfused rat liver. *Nature* **270**, 174-176
29. Mortimore, G. E., and Poso, A. R. (1987) Intracellular protein catabolism and its control during nutrient deprivation and supply. *Annual review of nutrition* **7**, 539-564
30. Novikoff, A. B., Essner, E., and Quintana, N. (1964) Golgi Apparatus and Lysosomes. *Federation proceedings* **23**, 1010-1022
31. Gordon, P. B., and Seglen, P. O. (1988) Prelysosomal convergence of autophagic and endocytic pathways. *Biochemical and biophysical research communications* **151**, 40-47
32. Lee, H. K., Myers, R. A., and Marzella, L. (1989) Stimulation of autophagic protein degradation by nutrient deprivation in a differentiated murine teratocarcinoma (F9 12-1a) cell line. *Experimental and molecular pathology* **50**, 139-146
33. Tooze, J., Hollinshead, M., Ludwig, T., Howell, K., Hoflack, B., and Kern, H. (1990) In exocrine pancreas, the basolateral endocytic pathway converges with the autophagic pathway immediately after the early endosome. *The Journal of cell biology* **111**, 329-345

34. Ericsson, J. L. (1969) Studies on induced cellular autophagy. II. Characterization of the membranes bordering autophagosomes in parenchymal liver cells. *Experimental cell research* **56**, 393-405
35. Ericsson, J. L. (1969) Studies on induced cellular autophagy. I. Electron microscopy of cells with in vivo labelled lysosomes. *Experimental cell research* **55**, 95-106
36. Lawrence, B. P., and Brown, W. J. (1992) Autophagic vacuoles rapidly fuse with pre-existing lysosomes in cultured hepatocytes. *Journal of cell science* **102 (Pt 3)**, 515-526
37. Marzella, L., and Glaumann, H. (1981) Effects of in vivo liver ischemia on microsomes and lysosomes. *Virchows Archiv. B, Cell pathology including molecular pathology* **36**, 1-25
38. Bolender, R. P., and Weibel, E. R. (1973) A morphometric study of the removal of phenobarbital-induced membranes from hepatocytes after cessation of threatment. *The Journal of cell biology* **56**, 746-761
39. Beaulaton, J., and Lockshin, R. A. (1977) Ultrastructural study of the normal degeneration of the intersegmental muscles of Anthereae polyphemus and Manduca sexta (Insecta, Lepidoptera) with particular reference of cellular autophagy. *Journal of morphology* **154**, 39-57
40. Veenhuis, M., Douma, A., Harder, W., and Osumi, M. (1983) Degradation and turnover of peroxisomes in the yeast Hansenula polymorpha induced by selective inactivation of peroxisomal enzymes. *Archives of microbiology* **134**, 193-203
41. Klionsky, D. J. (2007) Autophagy: from phenomenology to molecular understanding in less than a decade. *Nature reviews. Molecular cell biology* **8**, 931-937
42. Moe, H., and Behnke, O. (1962) Cytoplasmic bodies containing mitochondria, ribosomes, and rough surfaced endoplasmic membranes in the epithelium of the small intestine of newborn rats. *The Journal of cell biology* **13**, 168-171
43. Helminen, H. J., and Ericsson, J. L. (1968) Studies on mammary gland involution. 3. Alterations outside auto- and heterophagocytic pathways for cytoplasmic degradation. *Journal of ultrastructure research* **25**, 228-239
44. Helminen, H. J., and Ericsson, J. L. (1968) Studies on mammary gland involution. II. Ultrastructural evidence for auto- and heterophagocytosis. *Journal of ultrastructure research* **25**, 214-227
45. Hamberg, H., Brunk, U., Ericsson, J. L., and Jung, B. (1977) Cytoplasmic effects of X-irradiation on cultured cells 2. Alterations in lysosomes, plasma membrane, Golgi apparatus, and related structures. *Acta pathologica et microbiologica Scandinavica. Section A, Pathology* **85**, 625-639
46. Takeshige, K., Baba, M., Tsuboi, S., Noda, T., and Ohsumi, Y. (1992) Autophagy in yeast demonstrated with proteinase-deficient mutants and conditions for its induction. *The Journal of cell biology* **119**, 301-311
47. Tsukada, M., and Ohsumi, Y. (1993) Isolation and characterization of autophagy-defective mutants of Saccharomyces cerevisiae. *FEBS letters* **333**, 169-174

48. Straub, M., Bredschneider, M., and Thumm, M. (1997) AUT3, a serine/threonine kinase gene, is essential for autophagocytosis in Saccharomyces cerevisiae. *Journal of bacteriology* **179**, 3875-3883
49. Harding, T. M., Morano, K. A., Scott, S. V., and Klionsky, D. J. (1995) Isolation and characterization of yeast mutants in the cytoplasm to vacuole protein targeting pathway. *The Journal of cell biology* **131**, 591-602
50. Thumm, M., Egner, R., Koch, B., Schlumpberger, M., Straub, M., Veenhuis, M., and Wolf, D. H. (1994) Isolation of autophagocytosis mutants of Saccharomyces cerevisiae. *FEBS letters* **349**, 275-280
51. Noda, T., Matsuura, A., Wada, Y., and Ohsumi, Y. (1995) Novel system for monitoring autophagy in the yeast Saccharomyces cerevisiae. *Biochemical and biophysical research communications* **210**, 126-132
52. Mizushima, N., Sugita, H., Yoshimori, T., and Ohsumi, Y. (1998) A new protein conjugation system in human. The counterpart of the yeast Apg12p conjugation system essential for autophagy. *The Journal of biological chemistry* **273**, 33889-33892
53. Liang, X. H., Jackson, S., Seaman, M., Brown, K., Kempkes, B., Hibshoosh, H., and Levine, B. (1999) Induction of autophagy and inhibition of tumorigenesis by beclin 1. *Nature* **402**, 672-676
54. Tian, Y., Li, Z., Hu, W., Ren, H., Tian, E., Zhao, Y., Lu, Q., Huang, X., Yang, P., Li, X., Wang, X., Kovacs, A. L., Yu, L., and Zhang, H. (2010) C. elegans screen identifies autophagy genes specific to multicellular organisms. *Cell* **141**, 1042-1055
55. Behrends, C., Sowa, M. E., Gygi, S. P., and Harper, J. W. (2010) Network organization of the human autophagy system. *Nature* **466**, 68-76
56. Lipinski, M. M., Hoffman, G., Ng, A., Zhou, W., Py, B. F., Hsu, E., Liu, X., Eisenberg, J., Liu, J., Blenis, J., Xavier, R. J., and Yuan, J. (2010) A genome-wide siRNA screen reveals multiple mTORC1 independent signaling pathways regulating autophagy under normal nutritional conditions. *Developmental cell* **18**, 1041-1052
57. Johansen, T., and Lamark, T. (2011) Selective autophagy mediated by autophagic adapter proteins. *Autophagy* **7**, 279-296
58. Birgisdottir, A. B., Lamark, T., and Johansen, T. (2013) The LIR motif - crucial for selective autophagy. *Journal of cell science* **126**, 3237-3247
59. Mizushima, N. (2009) Physiological functions of autophagy. *Current topics in microbiology and immunology* **335**, 71-84
60. Yang, C., Kaushal, V., Shah, S. V., and Kaushal, G. P. (2008) Autophagy is associated with apoptosis in cisplatin injury to renal tubular epithelial cells. *American journal of physiology. Renal physiology* **294**, F777-787
61. Axe, E. L., Walker, S. A., Manifava, M., Chandra, P., Roderick, H. L., Habermann, A., Griffiths, G., and Ktistakis, N. T. (2008) Autophagosome formation from membrane compartments enriched in phosphatidylinositol 3-phosphate and dynamically connected to the endoplasmic reticulum. *The Journal of cell biology* **182**, 685-701
62. Hamasaki, M., Furuta, N., Matsuda, A., Nezu, A., Yamamoto, A., Fujita, N., Oomori, H., Noda, T., Haraguchi, T., Hiraoka, Y., Amano, A., and Yoshimori, T.

(2013) Autophagosomes form at ER-mitochondria contact sites. *Nature* **495**, 389-393
63. Wirawan, E., Lippens, S., Vanden Berghe, T., Romagnoli, A., Fimia, G. M., Piacentini, M., and Vandenabeele, P. (2012) Beclin1: a role in membrane dynamics and beyond. *Autophagy* **8**, 6-17
64. Simonsen, A., and Stenmark, H. (2008) Self-eating from an ER-associated cup. *The Journal of cell biology* **182**, 621-622
65. Hanada, T., Noda, N. N., Satomi, Y., Ichimura, Y., Fujioka, Y., Takao, T., Inagaki, F., and Ohsumi, Y. (2007) The Atg12-Atg5 conjugate has a novel E3-like activity for protein lipidation in autophagy. *The Journal of biological chemistry* **282**, 37298-37302
66. Ichimura, Y., Kirisako, T., Takao, T., Satomi, Y., Shimonishi, Y., Ishihara, N., Mizushima, N., Tanida, I., Kominami, E., Ohsumi, M., Noda, T., and Ohsumi, Y. (2000) A ubiquitin-like system mediates protein lipidation. *Nature* **408**, 488-492
67. Kirisako, T., Baba, M., Ishihara, N., Miyazawa, K., Ohsumi, M., Yoshimori, T., Noda, T., and Ohsumi, Y. (1999) Formation process of autophagosome is traced with Apg8/Aut7p in yeast. *The Journal of cell biology* **147**, 435-446
68. Fujita, N., Hayashi-Nishino, M., Fukumoto, H., Omori, H., Yamamoto, A., Noda, T., and Yoshimori, T. (2008) An Atg4B mutant hampers the lipidation of LC3 paralogues and causes defects in autophagosome closure. *Molecular biology of the cell* **19**, 4651-4659
69. Liang, C., Lee, J. S., Inn, K. S., Gack, M. U., Li, Q., Roberts, E. A., Vergne, I., Deretic, V., Feng, P., Akazawa, C., and Jung, J. U. (2008) Beclin1-binding UVRAG targets the class C Vps complex to coordinate autophagosome maturation and endocytic trafficking. *Nature cell biology* **10**, 776-787
70. Matsunaga, K., Saitoh, T., Tabata, K., Omori, H., Satoh, T., Kurotori, N., Maejima, I., Shirahama-Noda, K., Ichimura, T., Isobe, T., Akira, S., Noda, T., and Yoshimori, T. (2009) Two Beclin 1-binding proteins, Atg14L and Rubicon, reciprocally regulate autophagy at different stages. *Nature cell biology* **11**, 385-396
71. Furuta, N., Fujita, N., Noda, T., Yoshimori, T., and Amano, A. (2010) Combinational soluble N-ethylmaleimide-sensitive factor attachment protein receptor proteins VAMP8 and Vti1b mediate fusion of antimicrobial and canonical autophagosomes with lysosomes. *Molecular biology of the cell* **21**, 1001-1010
72. Furuta, N., Yoshimori, T., and Amano, A. (2010) Mediatory molecules that fuse autophagosomes and lysosomes. *Autophagy* **6**, 417-418
73. Matsuura, A., Tsukada, M., Wada, Y., and Ohsumi, Y. (1997) Apg1p, a novel protein kinase required for the autophagic process in Saccharomyces cerevisiae. *Gene* **192**, 245-250
74. Ogura, K., Wicky, C., Magnenat, L., Tobler, H., Mori, I., Muller, F., and Ohshima, Y. (1994) Caenorhabditis elegans unc-51 gene required for axonal elongation encodes a novel serine/threonine kinase. *Genes & development* **8**, 2389-2400

75. Scott, R. C., Juhasz, G., and Neufeld, T. P. (2007) Direct induction of autophagy by Atg1 inhibits cell growth and induces apoptotic cell death. *Current biology : CB* **17**, 1-11
76. Toda, H., Mochizuki, H., Flores, R., 3rd, Josowitz, R., Krasieva, T. B., Lamorte, V. J., Suzuki, E., Gindhart, J. G., Furukubo-Tokunaga, K., and Tomoda, T. (2008) UNC-51/ATG1 kinase regulates axonal transport by mediating motor-cargo assembly. *Genes & development* **22**, 3292-3307
77. Kuroyanagi, H., Yan, J., Seki, N., Yamanouchi, Y., Suzuki, Y., Takano, T., Muramatsu, M., and Shirasawa, T. (1998) Human ULK1, a novel serine/threonine kinase related to UNC-51 kinase of Caenorhabditis elegans: cDNA cloning, expression, and chromosomal assignment. *Genomics* **51**, 76-85
78. Yan, J., Kuroyanagi, H., Kuroiwa, A., Matsuda, Y., Tokumitsu, H., Tomoda, T., Shirasawa, T., and Muramatsu, M. (1998) Identification of mouse ULK1, a novel protein kinase structurally related to C. elegans UNC-51. *Biochemical and biophysical research communications* **246**, 222-227
79. Jung, C. H., Ro, S. H., Cao, J., Otto, N. M., and Kim, D. H. (2010) mTOR regulation of autophagy. *FEBS letters* **584**, 1287-1295
80. Yan, J., Kuroyanagi, H., Tomemori, T., Okazaki, N., Asato, K., Matsuda, Y., Suzuki, Y., Ohshima, Y., Mitani, S., Masuho, Y., Shirasawa, T., and Muramatsu, M. (1999) Mouse ULK2, a novel member of the UNC-51-like protein kinases: unique features of functional domains. *Oncogene* **18**, 5850-5859
81. Ganley, I. G., Lam du, H., Wang, J., Ding, X., Chen, S., and Jiang, X. (2009) ULK1.ATG13.FIP200 complex mediates mTOR signaling and is essential for autophagy. *The Journal of biological chemistry* **284**, 12297-12305
82. Jung, C. H., Jun, C. B., Ro, S. H., Kim, Y. M., Otto, N. M., Cao, J., Kundu, M., and Kim, D. H. (2009) ULK-Atg13-FIP200 complexes mediate mTOR signaling to the autophagy machinery. *Molecular biology of the cell* **20**, 1992-2003
83. Kundu, M., Lindsten, T., Yang, C. Y., Wu, J., Zhao, F., Zhang, J., Selak, M. A., Ney, P. A., and Thompson, C. B. (2008) Ulk1 plays a critical role in the autophagic clearance of mitochondria and ribosomes during reticulocyte maturation. *Blood* **112**, 1493-1502
84. Chan, E. Y., Kir, S., and Tooze, S. A. (2007) siRNA screening of the kinome identifies ULK1 as a multidomain modulator of autophagy. *The Journal of biological chemistry* **282**, 25464-25474
85. Komatsu, M., Waguri, S., Ueno, T., Iwata, J., Murata, S., Tanida, I., Ezaki, J., Mizushima, N., Ohsumi, Y., Uchiyama, Y., Kominami, E., Tanaka, K., and Chiba, T. (2005) Impairment of starvation-induced and constitutive autophagy in Atg7-deficient mice. *The Journal of cell biology* **169**, 425-434
86. Sou, Y. S., Waguri, S., Iwata, J., Ueno, T., Fujimura, T., Hara, T., Sawada, N., Yamada, A., Mizushima, N., Uchiyama, Y., Kominami, E., Tanaka, K., and Komatsu, M. (2008) The Atg8 conjugation system is indispensable for proper development of autophagic isolation membranes in mice. *Molecular biology of the cell* **19**, 4762-4775
87. Cheong, H., Lindsten, T., Wu, J., Lu, C., and Thompson, C. B. (2011) Ammonia-induced autophagy is independent of ULK1/ULK2 kinases. *Proceedings of the*

National Academy of Sciences of the United States of America **108**, 11121-11126
88. Funakoshi, T., Matsuura, A., Noda, T., and Ohsumi, Y. (1997) Analyses of APG13 gene involved in autophagy in yeast, Saccharomyces cerevisiae. *Gene* **192**, 207-213
89. Kamada, Y., Funakoshi, T., Shintani, T., Nagano, K., Ohsumi, M., and Ohsumi, Y. (2000) Tor-mediated induction of autophagy via an Apg1 protein kinase complex. *The Journal of cell biology* **150**, 1507-1513
90. Tian, E., Wang, F., Han, J., and Zhang, H. (2009) epg-1 functions in autophagy-regulated processes and may encode a highly divergent Atg13 homolog in C. elegans. *Autophagy* **5**, 608-615
91. Chang, Y. Y., and Neufeld, T. P. (2009) An Atg1/Atg13 complex with multiple roles in TOR-mediated autophagy regulation. *Molecular biology of the cell* **20**, 2004-2014
92. Meijer, W. H., van der Klei, I. J., Veenhuis, M., and Kiel, J. A. (2007) ATG genes involved in non-selective autophagy are conserved from yeast to man, but the selective Cvt and pexophagy pathways also require organism-specific genes. *Autophagy* **3**, 106-116
93. Kabeya, Y., Kamada, Y., Baba, M., Takikawa, H., Sasaki, M., and Ohsumi, Y. (2005) Atg17 functions in cooperation with Atg1 and Atg13 in yeast autophagy. *Molecular biology of the cell* **16**, 2544-2553
94. Ragusa, M. J., Stanley, R. E., and Hurley, J. H. (2012) Architecture of the Atg17 complex as a scaffold for autophagosome biogenesis. *Cell* **151**, 1501-1512
95. Alemu, E. A., Lamark, T., Torgersen, K. M., Birgisdottir, A. B., Larsen, K. B., Jain, A., Olsvik, H., Overvatn, A., Kirkin, V., and Johansen, T. (2012) ATG8 family proteins act as scaffolds for assembly of the ULK complex: sequence requirements for LC3-interacting region (LIR) motifs. *The Journal of biological chemistry* **287**, 39275-39290
96. Jao, C. C., Ragusa, M. J., Stanley, R. E., and Hurley, J. H. (2013) A HORMA domain in Atg13 mediates PI 3-kinase recruitment in autophagy. *Proceedings of the National Academy of Sciences of the United States of America* **110**, 5486-5491
97. Suzuki, S. W., Yamamoto, H., Oikawa, Y., Kondo-Kakuta, C., Kimura, Y., Hirano, H., and Ohsumi, Y. (2015) Atg13 HORMA domain recruits Atg9 vesicles during autophagosome formation. *Proceedings of the National Academy of Sciences of the United States of America* **112**, 3350-3355
98. Qi, S., Kim do, J., Stjepanovic, G., and Hurley, J. H. (2015) Structure of the Human Atg13-Atg101 HORMA Heterodimer: an Interaction Hub within the ULK1 Complex. *Structure* **23**, 1848-1857
99. Karanasios, E., Stapleton, E., Manifava, M., Kaizuka, T., Mizushima, N., Walker, S. A., and Ktistakis, N. T. (2013) Dynamic association of the ULK1 complex with omegasomes during autophagy induction. *Journal of cell science* **126**, 5224-5238
100. Mizushima, N. (2010) The role of the Atg1/ULK1 complex in autophagy regulation. *Current opinion in cell biology* **22**, 132-139

101. Wong, P. M., Puente, C., Ganley, I. G., and Jiang, X. (2013) The ULK1 complex: sensing nutrient signals for autophagy activation. *Autophagy* **9**, 124-137
102. Kabeya, Y., Noda, N. N., Fujioka, Y., Suzuki, K., Inagaki, F., and Ohsumi, Y. (2009) Characterization of the Atg17-Atg29-Atg31 complex specifically required for starvation-induced autophagy in Saccharomyces cerevisiae. *Biochemical and biophysical research communications* **389**, 612-615
103. Cheong, H., Yorimitsu, T., Reggiori, F., Legakis, J. E., Wang, C. W., and Klionsky, D. J. (2005) Atg17 regulates the magnitude of the autophagic response. *Molecular biology of the cell* **16**, 3438-3453
104. Suzuki, K., Kubota, Y., Sekito, T., and Ohsumi, Y. (2007) Hierarchy of Atg proteins in pre-autophagosomal structure organization. *Genes to cells : devoted to molecular & cellular mechanisms* **12**, 209-218
105. Cheong, H., Nair, U., Geng, J., and Klionsky, D. J. (2008) The Atg1 kinase complex is involved in the regulation of protein recruitment to initiate sequestering vesicle formation for nonspecific autophagy in Saccharomyces cerevisiae. *Molecular biology of the cell* **19**, 668-681
106. Mercer, C. A., Kaliappan, A., and Dennis, P. B. (2009) A novel, human Atg13 binding protein, Atg101, interacts with ULK1 and is essential for macroautophagy. *Autophagy* **5**, 649-662
107. Kawamata, T., Kamada, Y., Kabeya, Y., Sekito, T., and Ohsumi, Y. (2008) Organization of the pre-autophagosomal structure responsible for autophagosome formation. *Molecular biology of the cell* **19**, 2039-2050
108. Kamada, Y., Yoshino, K., Kondo, C., Kawamata, T., Oshiro, N., Yonezawa, K., and Ohsumi, Y. (2010) Tor directly controls the Atg1 kinase complex to regulate autophagy. *Molecular and cellular biology* **30**, 1049-1058
109. Fujioka, Y., Suzuki, S. W., Yamamoto, H., Kondo-Kakuta, C., Kimura, Y., Hirano, H., Akada, R., Inagaki, F., Ohsumi, Y., and Noda, N. N. (2014) Structural basis of starvation-induced assembly of the autophagy initiation complex. *Nature structural & molecular biology* **21**, 513-521
110. Stephan, J. S., Yeh, Y. Y., Ramachandran, V., Deminoff, S. J., and Herman, P. K. (2009) The Tor and PKA signaling pathways independently target the Atg1/Atg13 protein kinase complex to control autophagy. *Proceedings of the National Academy of Sciences of the United States of America* **106**, 17049-17054
111. Budovskaya, Y. V., Stephan, J. S., Reggiori, F., Klionsky, D. J., and Herman, P. K. (2004) The Ras/cAMP-dependent protein kinase signaling pathway regulates an early step of the autophagy process in Saccharomyces cerevisiae. *The Journal of biological chemistry* **279**, 20663-20671
112. Alers, S., Wesselborg, S., and Stork, B. (2014) ATG13: just a companion, or an executor of the autophagic program? *Autophagy* **10**, 944-956
113. Kim, D. H., Sarbassov, D. D., Ali, S. M., King, J. E., Latek, R. R., Erdjument-Bromage, H., Tempst, P., and Sabatini, D. M. (2002) mTOR interacts with raptor to form a nutrient-sensitive complex that signals to the cell growth machinery. *Cell* **110**, 163-175
114. Hara, T., Takamura, A., Kishi, C., Iemura, S., Natsume, T., Guan, J. L., and Mizushima, N. (2008) FIP200, a ULK-interacting protein, is required for

autophagosome formation in mammalian cells. *The Journal of cell biology* **181**, 497-510
115. Hara, T., and Mizushima, N. (2009) Role of ULK-FIP200 complex in mammalian autophagy: FIP200, a counterpart of yeast Atg17? *Autophagy* **5**, 85-87
116. Hosokawa, N., Hara, T., Kaizuka, T., Kishi, C., Takamura, A., Miura, Y., Iemura, S., Natsume, T., Takehana, K., Yamada, N., Guan, J. L., Oshiro, N., and Mizushima, N. (2009) Nutrient-dependent mTORC1 association with the ULK1-Atg13-FIP200 complex required for autophagy. *Molecular biology of the cell* **20**, 1981-1991
117. Kang, S. A., Pacold, M. E., Cervantes, C. L., Lim, D., Lou, H. J., Ottina, K., Gray, N. S., Turk, B. E., Yaffe, M. B., and Sabatini, D. M. (2013) mTORC1 phosphorylation sites encode their sensitivity to starvation and rapamycin. *Science* **341**, 1236566
118. Kim, J., Kundu, M., Viollet, B., and Guan, K. L. (2011) AMPK and mTOR regulate autophagy through direct phosphorylation of Ulk1. *Nature cell biology* **13**, 132-141
119. Shang, L., Chen, S., Du, F., Li, S., Zhao, L., and Wang, X. (2011) Nutrient starvation elicits an acute autophagic response mediated by Ulk1 dephosphorylation and its subsequent dissociation from AMPK. *Proceedings of the National Academy of Sciences of the United States of America* **108**, 4788-4793
120. Egan, D. F., Shackelford, D. B., Mihaylova, M. M., Gelino, S., Kohnz, R. A., Mair, W., Vasquez, D. S., Joshi, A., Gwinn, D. M., Taylor, R., Asara, J. M., Fitzpatrick, J., Dillin, A., Viollet, B., Kundu, M., Hansen, M., and Shaw, R. J. (2011) Phosphorylation of ULK1 (hATG1) by AMP-activated protein kinase connects energy sensing to mitophagy. *Science* **331**, 456-461
121. Lee, J. W., Park, S., Takahashi, Y., and Wang, H. G. (2010) The association of AMPK with ULK1 regulates autophagy. *PloS one* **5**, e15394
122. Chan, E. Y., Longatti, A., McKnight, N. C., and Tooze, S. A. (2009) Kinase-inactivated ULK proteins inhibit autophagy via their conserved C-terminal domains using an Atg13-independent mechanism. *Molecular and cellular biology* **29**, 157-171
123. Egan, D. F., Chun, M. G., Vamos, M., Zou, H., Rong, J., Miller, C. J., Lou, H. J., Raveendra-Panickar, D., Yang, C. C., Sheffler, D. J., Teriete, P., Asara, J. M., Turk, B. E., Cosford, N. D., and Shaw, R. J. (2015) Small Molecule Inhibition of the Autophagy Kinase ULK1 and Identification of ULK1 Substrates. *Molecular cell* **59**, 285-297
124. Joo, J. H., Dorsey, F. C., Joshi, A., Hennessy-Walters, K. M., Rose, K. L., McCastlain, K., Zhang, J., Iyengar, R., Jung, C. H., Suen, D. F., Steeves, M. A., Yang, C. Y., Prater, S. M., Kim, D. H., Thompson, C. B., Youle, R. J., Ney, P. A., Cleveland, J. L., and Kundu, M. (2011) Hsp90-Cdc37 chaperone complex regulates Ulk1- and Atg13-mediated mitophagy. *Molecular cell* **43**, 572-585
125. Aita, V. M., Liang, X. H., Murty, V. V., Pincus, D. L., Yu, W., Cayanis, E., Kalachikov, S., Gilliam, T. C., and Levine, B. (1999) Cloning and genomic

organization of beclin 1, a candidate tumor suppressor gene on chromosome 17q21. *Genomics* **59**, 59-65
126. Nakagawa, I., Amano, A., Mizushima, N., Yamamoto, A., Yamaguchi, H., Kamimoto, T., Nara, A., Funao, J., Nakata, M., Tsuda, K., Hamada, S., and Yoshimori, T. (2004) Autophagy defends cells against invading group A Streptococcus. *Science* **306**, 1037-1040
127. Castrejon-Jimenez, N. S., Leyva-Paredes, K., Hernandez-Gonzalez, J. C., Luna-Herrera, J., and Garcia-Perez, B. E. (2015) The role of autophagy in bacterial infections. *Bioscience trends* **9**, 149-159
128. Thurston, T. L., Ryzhakov, G., Bloor, S., von Muhlinen, N., and Randow, F. (2009) The TBK1 adaptor and autophagy receptor NDP52 restricts the proliferation of ubiquitin-coated bacteria. *Nature immunology* **10**, 1215-1221
129. Talloczy, Z., Virgin, H. W. t., and Levine, B. (2006) PKR-dependent autophagic degradation of herpes simplex virus type 1. *Autophagy* **2**, 24-29
130. Orvedahl, A., and Levine, B. (2008) Viral evasion of autophagy. *Autophagy* **4**, 280-285
131. Schmid, D., Pypaert, M., and Munz, C. (2007) Antigen-loading compartments for major histocompatibility complex class II molecules continuously receive input from autophagosomes. *Immunity* **26**, 79-92
132. Rubinsztein, D. C., DiFiglia, M., Heintz, N., Nixon, R. A., Qin, Z. H., Ravikumar, B., Stefanis, L., and Tolkovsky, A. (2005) Autophagy and its possible roles in nervous system diseases, damage and repair. *Autophagy* **1**, 11-22
133. Stefanis, L., Larsen, K. E., Rideout, H. J., Sulzer, D., and Greene, L. A. (2001) Expression of A53T mutant but not wild-type alpha-synuclein in PC12 cells induces alterations of the ubiquitin-dependent degradation system, loss of dopamine release, and autophagic cell death. *The Journal of neuroscience : the official journal of the Society for Neuroscience* **21**, 9549-9560
134. Yu, W. H., Cuervo, A. M., Kumar, A., Peterhoff, C. M., Schmidt, S. D., Lee, J. H., Mohan, P. S., Mercken, M., Farmery, M. R., Tjernberg, L. O., Jiang, Y., Duff, K., Uchiyama, Y., Naslund, J., Mathews, P. M., Cataldo, A. M., and Nixon, R. A. (2005) Macroautophagy--a novel Beta-amyloid peptide-generating pathway activated in Alzheimer's disease. *The Journal of cell biology* **171**, 87-98
135. Nixon, R. A., Wegiel, J., Kumar, A., Yu, W. H., Peterhoff, C., Cataldo, A., and Cuervo, A. M. (2005) Extensive involvement of autophagy in Alzheimer disease: an immuno-electron microscopy study. *Journal of neuropathology and experimental neurology* **64**, 113-122
136. Hara, T., Nakamura, K., Matsui, M., Yamamoto, A., Nakahara, Y., Suzuki-Migishima, R., Yokoyama, M., Mishima, K., Saito, I., Okano, H., and Mizushima, N. (2006) Suppression of basal autophagy in neural cells causes neurodegenerative disease in mice. *Nature* **441**, 885-889
137. Komatsu, M., Waguri, S., Chiba, T., Murata, S., Iwata, J., Tanida, I., Ueno, T., Koike, M., Uchiyama, Y., Kominami, E., and Tanaka, K. (2006) Loss of autophagy in the central nervous system causes neurodegeneration in mice. *Nature* **441**, 880-884
138. Boland, B., Kumar, A., Lee, S., Platt, F. M., Wegiel, J., Yu, W. H., and Nixon, R. A. (2008) Autophagy induction and autophagosome clearance in neurons:

relationship to autophagic pathology in Alzheimer's disease. *The Journal of neuroscience : the official journal of the Society for Neuroscience* **28**, 6926-6937
139. Nixon, R. A., and Yang, D. S. (2011) Autophagy failure in Alzheimer's disease--locating the primary defect. *Neurobiology of disease* **43**, 38-45
140. Nilsson, P., Loganathan, K., Sekiguchi, M., Matsuba, Y., Hui, K., Tsubuki, S., Tanaka, M., Iwata, N., Saito, T., and Saido, T. C. (2013) Abeta secretion and plaque formation depend on autophagy. *Cell reports* **5**, 61-69
141. Spencer, B., Potkar, R., Trejo, M., Rockenstein, E., Patrick, C., Gindi, R., Adame, A., Wyss-Coray, T., and Masliah, E. (2009) Beclin 1 gene transfer activates autophagy and ameliorates the neurodegenerative pathology in alpha-synuclein models of Parkinson's and Lewy body diseases. *The Journal of neuroscience : the official journal of the Society for Neuroscience* **29**, 13578-13588
142. Webb, J. L., Ravikumar, B., Atkins, J., Skepper, J. N., and Rubinsztein, D. C. (2003) Alpha-Synuclein is degraded by both autophagy and the proteasome. *The Journal of biological chemistry* **278**, 25009-25013
143. Karantza-Wadsworth, V., Patel, S., Kravchuk, O., Chen, G., Mathew, R., Jin, S., and White, E. (2007) Autophagy mitigates metabolic stress and genome damage in mammary tumorigenesis. *Genes & development* **21**, 1621-1635
144. Mathew, R., Kongara, S., Beaudoin, B., Karp, C. M., Bray, K., Degenhardt, K., Chen, G., Jin, S., and White, E. (2007) Autophagy suppresses tumor progression by limiting chromosomal instability. *Genes & development* **21**, 1367-1381
145. Degenhardt, K., Mathew, R., Beaudoin, B., Bray, K., Anderson, D., Chen, G., Mukherjee, C., Shi, Y., Gelinas, C., Fan, Y., Nelson, D. A., Jin, S., and White, E. (2006) Autophagy promotes tumor cell survival and restricts necrosis, inflammation, and tumorigenesis. *Cancer cell* **10**, 51-64
146. Guo, J. Y., Karsli-Uzunbas, G., Mathew, R., Aisner, S. C., Kamphorst, J. J., Strohecker, A. M., Chen, G., Price, S., Lu, W., Teng, X., Snyder, E., Santanam, U., Dipaola, R. S., Jacks, T., Rabinowitz, J. D., and White, E. (2013) Autophagy suppresses progression of K-ras-induced lung tumors to oncocytomas and maintains lipid homeostasis. *Genes & development* **27**, 1447-1461
147. Guo, J. Y., Chen, H. Y., Mathew, R., Fan, J., Strohecker, A. M., Karsli-Uzunbas, G., Kamphorst, J. J., Chen, G., Lemons, J. M., Karantza, V., Coller, H. A., Dipaola, R. S., Gelinas, C., Rabinowitz, J. D., and White, E. (2011) Activated Ras requires autophagy to maintain oxidative metabolism and tumorigenesis. *Genes & development* **25**, 460-470
148. Yang, S., Wang, X., Contino, G., Liesa, M., Sahin, E., Ying, H., Bause, A., Li, Y., Stommel, J. M., Dell'antonio, G., Mautner, J., Tonon, G., Haigis, M., Shirihai, O. S., Doglioni, C., Bardeesy, N., and Kimmelman, A. C. (2011) Pancreatic cancers require autophagy for tumor growth. *Genes & development* **25**, 717-729
149. Morgan, M. J., Gamez, G., Menke, C., Hernandez, A., Thorburn, J., Gidan, F., Staskiewicz, L., Morgan, S., Cummings, C., Maycotte, P., and Thorburn, A. (2014) Regulation of autophagy and chloroquine sensitivity by oncogenic RAS in vitro is context-dependent. *Autophagy* **10**, 1814-1826

150. Gammoh, N., Florey, O., Overholtzer, M., and Jiang, X. (2013) Interaction between FIP200 and ATG16L1 distinguishes ULK1 complex-dependent and -independent autophagy. *Nature structural & molecular biology* **20**, 144-149
151. Petherick, K. J., Conway, O. J., Mpamhanga, C., Osborne, S. A., Kamal, A., Saxty, B., and Ganley, I. G. (2015) Pharmacological inhibition of ULK1 kinase blocks mammalian target of rapamycin (mTOR)-dependent autophagy. *The Journal of biological chemistry* **290**, 11376-11383
152. Wong, P. M., Feng, Y., Wang, J., Shi, R., and Jiang, X. (2015) Regulation of autophagy by coordinated action of mTORC1 and protein phosphatase 2A. *Nature communications* **6**, 8048
153. Ha, J., Guan, K. L., and Kim, J. (2015) AMPK and autophagy in glucose/glycogen metabolism. *Molecular aspects of medicine* **46**, 46-62
154. Kim, J., Kim, Y. C., Fang, C., Russell, R. C., Kim, J. H., Fan, W., Liu, R., Zhong, Q., and Guan, K. L. (2013) Differential regulation of distinct Vps34 complexes by AMPK in nutrient stress and autophagy. *Cell* **152**, 290-303
155. Itakura, E., and Mizushima, N. (2010) Characterization of autophagosome formation site by a hierarchical analysis of mammalian Atg proteins. *Autophagy* **6**, 764-776
156. Di Bartolomeo, S., Corazzari, M., Nazio, F., Oliverio, S., Lisi, G., Antonioli, M., Pagliarini, V., Matteoni, S., Fuoco, C., Giunta, L., D'Amelio, M., Nardacci, R., Romagnoli, A., Piacentini, M., Cecconi, F., and Fimia, G. M. (2010) The dynamic interaction of AMBRA1 with the dynein motor complex regulates mammalian autophagy. *The Journal of cell biology* **191**, 155-168
157. Ktistakis, N. T., and Tooze, S. A. (2016) Digesting the Expanding Mechanisms of Autophagy. *Trends in cell biology*
158. Mizushima, N., and Komatsu, M. (2011) Autophagy: renovation of cells and tissues. *Cell* **147**, 728-741
159. Ridley, S. H., Ktistakis, N., Davidson, K., Anderson, K. E., Manifava, M., Ellson, C. D., Lipp, P., Bootman, M., Coadwell, J., Nazarian, A., Erdjument-Bromage, H., Tempst, P., Cooper, M. A., Thuring, J. W., Lim, Z. Y., Holmes, A. B., Stephens, L. R., and Hawkins, P. T. (2001) FENS-1 and DFCP1 are FYVE domain-containing proteins with distinct functions in the endosomal and Golgi compartments. *Journal of cell science* **114**, 3991-4000
160. Polson, H. E., de Lartigue, J., Rigden, D. J., Reedijk, M., Urbe, S., Clague, M. J., and Tooze, S. A. (2010) Mammalian Atg18 (WIPI2) localizes to omegasome-anchored phagophores and positively regulates LC3 lipidation. *Autophagy* **6**, 506-522
161. Kraft, C., Kijanska, M., Kalie, E., Siergiejuk, E., Lee, S. S., Semplicio, G., Stoffel, I., Brezovich, A., Verma, M., Hansmann, I., Ammerer, G., Hofmann, K., Tooze, S., and Peter, M. (2012) Binding of the Atg1/ULK1 kinase to the ubiquitin-like protein Atg8 regulates autophagy. *The EMBO journal* **31**, 3691-3703
162. Park, J. M., Jung, C. H., Seo, M., Otto, N. M., Grunwald, D., Kim, K. H., Moriarity, B., Kim, Y. M., Starker, C., Nho, R. S., Voytas, D., and Kim, D. H. (2016) The ULK1 complex mediates MTORC1 signaling to the autophagy initiation machinery via binding and phosphorylating ATG14. *Autophagy* **12**, 547-564

163. Sebastiaan Winkler, G., Lacomis, L., Philip, J., Erdjument-Bromage, H., Svejstrup, J. Q., and Tempst, P. (2002) Isolation and mass spectrometry of transcription factor complexes. *Methods* **26**, 260-269
164. Erdjument-Bromage, H., Lui, M., Lacomis, L., Grewal, A., Annan, R. S., McNulty, D. E., Carr, S. A., and Tempst, P. (1998) Examination of micro-tip reversed-phase liquid chromatographic extraction of peptide pools for mass spectrometric analysis. *Journal of chromatography. A* **826**, 167-181
165. Mali, P., Yang, L., Esvelt, K. M., Aach, J., Guell, M., DiCarlo, J. E., Norville, J. E., and Church, G. M. (2013) RNA-guided human genome engineering via Cas9. *Science* **339**, 823-826
166. Shah, K., Liu, Y., Deirmengian, C., and Shokat, K. M. (1997) Engineering unnatural nucleotide specificity for Rous sarcoma virus tyrosine kinase to uniquely label its direct substrates. *Proceedings of the National Academy of Sciences of the United States of America* **94**, 3565-3570
167. Liu, Y., Shah, K., Yang, F., Witucki, L., and Shokat, K. M. (1998) Engineering Src family protein kinases with unnatural nucleotide specificity. *Chemistry & biology* **5**, 91-101
168. Bishop, A. C., Shah, K., Liu, Y., Witucki, L., Kung, C., and Shokat, K. M. (1998) Design of allele-specific inhibitors to probe protein kinase signaling. *Current biology : CB* **8**, 257-266
169. Shah, K., and Shokat, K. M. (2003) A chemical genetic approach for the identification of direct substrates of protein kinases. *Methods in molecular biology* **233**, 253-271
170. Bishop, A. C., Ubersax, J. A., Petsch, D. T., Matheos, D. P., Gray, N. S., Blethrow, J., Shimizu, E., Tsien, J. Z., Schultz, P. G., Rose, M. D., Wood, J. L., Morgan, D. O., and Shokat, K. M. (2000) A chemical switch for inhibitor-sensitive alleles of any protein kinase. *Nature* **407**, 395-401
171. Zhang, C., Kenski, D. M., Paulson, J. L., Bonshtien, A., Sessa, G., Cross, J. V., Templeton, D. J., and Shokat, K. M. (2005) A second-site suppressor strategy for chemical genetic analysis of diverse protein kinases. *Nature methods* **2**, 435-441
172. Shoji-Kawata, S., Sumpter, R., Leveno, M., Campbell, G. R., Zou, Z., Kinch, L., Wilkins, A. D., Sun, Q., Pallauf, K., MacDuff, D., Huerta, C., Virgin, H. W., Helms, J. B., Eerland, R., Tooze, S. A., Xavier, R., Lenschow, D. J., Yamamoto, A., King, D., Lichtarge, O., Grishin, N. V., Spector, S. A., Kaloyanova, D. V., and Levine, B. (2013) Identification of a candidate therapeutic autophagy-inducing peptide. *Nature* **494**, 201-206
173. Yang, Y., Fiskus, W., Yong, B., Atadja, P., Takahashi, Y., Pandita, T. K., Wang, H. G., and Bhalla, K. N. (2013) Acetylated hsp70 and KAP1-mediated Vps34 SUMOylation is required for autophagosome creation in autophagy. *Proceedings of the National Academy of Sciences of the United States of America* **110**, 6841-6846
174. Pampliega, O., Orhon, I., Patel, B., Sridhar, S., Diaz-Carretero, A., Beau, I., Codogno, P., Satir, B. H., Satir, P., and Cuervo, A. M. (2013) Functional interaction between autophagy and ciliogenesis. *Nature* **502**, 194-200

175. Tang, Z., Lin, M. G., Stowe, T. R., Chen, S., Zhu, M., Stearns, T., Franco, B., and Zhong, Q. (2013) Autophagy promotes primary ciliogenesis by removing OFD1 from centriolar satellites. *Nature* **502**, 254-257
176. Kim, M., Semple, I., Kim, B., Kiers, A., Nam, S., Park, H. W., Park, H., Ro, S. H., Kim, J. S., Juhasz, G., and Lee, J. H. (2015) Drosophila Gyf/GRB10 interacting GYF protein is an autophagy regulator that controls neuron and muscle homeostasis. *Autophagy* **11**, 1358-1372
177. Nishimura, T., Kaizuka, T., Cadwell, K., Sahani, M. H., Saitoh, T., Akira, S., Virgin, H. W., and Mizushima, N. (2013) FIP200 regulates targeting of Atg16L1 to the isolation membrane. *EMBO reports* **14**, 284-291
178. Gan, B., and Guan, J. L. (2008) FIP200, a key signaling node to coordinately regulate various cellular processes. *Cellular signalling* **20**, 787-794
179. Eberle, H. B., Serrano, R. L., Fullekrug, J., Schlosser, A., Lehmann, W. D., Lottspeich, F., Kaloyanova, D., Wieland, F. T., and Helms, J. B. (2002) Identification and characterization of a novel human plant pathogenesis-related protein that localizes to lipid-enriched microdomains in the Golgi complex. *Journal of cell science* **115**, 827-838
180. Ren, Y., Li, R., Zheng, Y., and Busch, H. (1998) Cloning and characterization of GEF-H1, a microtubule-associated guanine nucleotide exchange factor for Rac and Rho GTPases. *The Journal of biological chemistry* **273**, 34954-34960
181. Pathak, R., Delorme-Walker, V. D., Howell, M. C., Anselmo, A. N., White, M. A., Bokoch, G. M., and Dermardirossian, C. (2012) The microtubule-associated Rho activating factor GEF-H1 interacts with exocyst complex to regulate vesicle traffic. *Developmental cell* **23**, 397-411
182. Chiang, H. S., Zhao, Y., Song, J. H., Liu, S., Wang, N., Terhorst, C., Sharpe, A. H., Basavappa, M., Jeffrey, K. L., and Reinecker, H. C. (2014) GEF-H1 controls microtubule-dependent sensing of nucleic acids for antiviral host defenses. *Nature immunology* **15**, 63-71
183. Chien, Y., Kim, S., Bumeister, R., Loo, Y. M., Kwon, S. W., Johnson, C. L., Balakireva, M. G., Romeo, Y., Kopelovich, L., Gale, M., Jr., Yeaman, C., Camonis, J. H., Zhao, Y., and White, M. A. (2006) RalB GTPase-mediated activation of the IkappaB family kinase TBK1 couples innate immune signaling to tumor cell survival. *Cell* **127**, 157-170
184. Farre, J. C., and Subramani, S. (2011) Rallying the exocyst as an autophagy scaffold. *Cell* **144**, 172-174
185. Bodemann, B. O., Orvedahl, A., Cheng, T., Ram, R. R., Ou, Y. H., Formstecher, E., Maiti, M., Hazelett, C. C., Wauson, E. M., Balakireva, M., Camonis, J. H., Yeaman, C., Levine, B., and White, M. A. (2011) RalB and the exocyst mediate the cellular starvation response by direct activation of autophagosome assembly. *Cell* **144**, 253-267
186. Yuan, H. X., Russell, R. C., and Guan, K. L. (2013) Regulation of PIK3C3/VPS34 complexes by MTOR in nutrient stress-induced autophagy. *Autophagy* **9**, 1983-1995
187. Rapoport, S. I., Primiani, C. T., Chen, C. T., Ahn, K., and Ryan, V. H. (2015) Coordinated Expression of Phosphoinositide Metabolic Genes during

Development and Aging of Human Dorsolateral Prefrontal Cortex. *PloS one* **10**, e0132675
188. Dall'Armi, C., Devereaux, K. A., and Di Paolo, G. (2013) The role of lipids in the control of autophagy. *Current biology : CB* **23**, R33-45
189. Henne, W. M., Zhu, L., Balogi, Z., Stefan, C., Pleiss, J. A., and Emr, S. D. (2015) Mdm1/Snx13 is a novel ER-endolysosomal interorganelle tethering protein. *The Journal of cell biology* **210**, 541-551
190. Mas, C., Norwood, S. J., Bugarcic, A., Kinna, G., Leneva, N., Kovtun, O., Ghai, R., Ona Yanez, L. E., Davis, J. L., Teasdale, R. D., and Collins, B. M. (2014) Structural basis for different phosphoinositide specificities of the PX domains of sorting nexins regulating G-protein signaling. *The Journal of biological chemistry* **289**, 28554-28568
191. Zheng, B., Tang, T., Tang, N., Kudlicka, K., Ohtsubo, K., Ma, P., Marth, J. D., Farquhar, M. G., and Lehtonen, E. (2006) Essential role of RGS-PX1/sorting nexin 13 in mouse development and regulation of endocytosis dynamics. *Proceedings of the National Academy of Sciences of the United States of America* **103**, 16776-16781
192. Kowalewski, B., Lubke, T., Kollmann, K., Braulke, T., Reinheckel, T., Dierks, T., and Damme, M. (2014) Molecular characterization of arylsulfatase G: expression, processing, glycosylation, transport, and activity. *The Journal of biological chemistry* **289**, 27992-28005
193. Kowalewski, B., Lamanna, W. C., Lawrence, R., Damme, M., Stroobants, S., Padva, M., Kalus, I., Frese, M. A., Lubke, T., Lullmann-Rauch, R., D'Hooge, R., Esko, J. D., and Dierks, T. (2012) Arylsulfatase G inactivation causes loss of heparan sulfate 3-O-sulfatase activity and mucopolysaccharidosis in mice. *Proceedings of the National Academy of Sciences of the United States of America* **109**, 10310-10315
194. Martina, J. A., Chen, Y., Gucek, M., and Puertollano, R. (2012) MTORC1 functions as a transcriptional regulator of autophagy by preventing nuclear transport of TFEB. *Autophagy* **8**, 903-914
195. Settembre, C., Zoncu, R., Medina, D. L., Vetrini, F., Erdin, S., Erdin, S., Huynh, T., Ferron, M., Karsenty, G., Vellard, M. C., Facchinetti, V., Sabatini, D. M., and Ballabio, A. (2012) A lysosome-to-nucleus signalling mechanism senses and regulates the lysosome via mTOR and TFEB. *The EMBO journal* **31**, 1095-1108
196. Scheper, G. C., van der Klok, T., van Andel, R. J., van Berkel, C. G., Sissler, M., Smet, J., Muravina, T. I., Serkov, S. V., Uziel, G., Bugiani, M., Schiffmann, R., Krageloh-Mann, I., Smeitink, J. A., Florentz, C., Van Coster, R., Pronk, J. C., and van der Knaap, M. S. (2007) Mitochondrial aspartyl-tRNA synthetase deficiency causes leukoencephalopathy with brain stem and spinal cord involvement and lactate elevation. *Nature genetics* **39**, 534-539
197. Messmer, M., Florentz, C., Schwenzer, H., Scheper, G. C., van der Knaap, M. S., Marechal-Drouard, L., and Sissler, M. (2011) A human pathology-related mutation prevents import of an aminoacyl-tRNA synthetase into mitochondria. *The Biochemical journal* **433**, 441-446

198. Jao, C. C., Ragusa, M. J., Stanley, R. E., and Hurley, J. H. (2013) What the N-terminal domain of Atg13 looks like and what it does: a HORMA fold required for PtdIns 3-kinase recruitment. *Autophagy* **9**, 1112-1114
199. Alers, S., Loffler, A. S., Paasch, F., Dieterle, A. M., Keppeler, H., Lauber, K., Campbell, D. G., Fehrenbacher, B., Schaller, M., Wesselborg, S., and Stork, B. (2011) Atg13 and FIP200 act independently of Ulk1 and Ulk2 in autophagy induction. *Autophagy* **7**, 1423-1433
200. Dorsey, F. C., Rose, K. L., Coenen, S., Prater, S. M., Cavett, V., Cleveland, J. L., and Caldwell-Busby, J. (2009) Mapping the phosphorylation sites of Ulk1. *Journal of proteome research* **8**, 5253-5263
201. Hieke, N., Loffler, A. S., Kaizuka, T., Berleth, N., Bohler, P., Driessen, S., Stuhldreier, F., Friesen, O., Assani, K., Schmitz, K., Peter, C., Diedrich, B., Dengjel, J., Holland, P., Simonsen, A., Wesselborg, S., Mizushima, N., and Stork, B. (2015) Expression of a ULK1/2 binding-deficient ATG13 variant can partially restore autophagic activity in ATG13-deficient cells. *Autophagy* **11**, 1471-1483
202. Kaizuka, T., and Mizushima, N. (2015) Atg13 Is Essential for Autophagy and Cardiac Development in Mice. *Molecular and cellular biology* **36**, 585-595
203. Zhou, X., Babu, J. R., da Silva, S., Shu, Q., Graef, I. A., Oliver, T., Tomoda, T., Tani, T., Wooten, M. W., and Wang, F. (2007) Unc-51-like kinase 1/2-mediated endocytic processes regulate filopodia extension and branching of sensory axons. *Proceedings of the National Academy of Sciences of the United States of America* **104**, 5842-5847
204. Lee, E. J., and Tournier, C. (2011) The requirement of uncoordinated 51-like kinase 1 (ULK1) and ULK2 in the regulation of autophagy. *Autophagy* **7**, 689-695
205. Lazarus, M. B., and Shokat, K. M. (2015) Discovery and structure of a new inhibitor scaffold of the autophagy initiating kinase ULK1. *Bioorganic & medicinal chemistry* **23**, 5483-5488
206. Puente, C., Hendrickson, R. C., and Jiang, X. (2016) Nutrient-Regulated Phosphorylation of ATG13 Inhibits Starvation-Induced Autophagy. *The Journal of biological chemistry*
207. Ozpolat, B., and Benbrook, D. M. (2015) Targeting autophagy in cancer management - strategies and developments. *Cancer management and research* **7**, 291-299
208. Mizushima, N., Levine, B., Cuervo, A. M., and Klionsky, D. J. (2008) Autophagy fights disease through cellular self-digestion. *Nature* **451**, 1069-1075
209. Madeo, F., Tavernarakis, N., and Kroemer, G. (2010) Can autophagy promote longevity? *Nature cell biology* **12**, 842-846
210. Bjedov, I., Toivonen, J. M., Kerr, F., Slack, C., Jacobson, J., Foley, A., and Partridge, L. (2010) Mechanisms of life span extension by rapamycin in the fruit fly Drosophila melanogaster. *Cell metabolism* **11**, 35-46
211. Morselli, E., Maiuri, M. C., Markaki, M., Megalou, E., Pasparaki, A., Palikaras, K., Criollo, A., Galluzzi, L., Malik, S. A., Vitale, I., Michaud, M., Madeo, F., Tavernarakis, N., and Kroemer, G. (2010) Caloric restriction and resveratrol

promote longevity through the Sirtuin-1-dependent induction of autophagy. *Cell death & disease* **1**, e10
212. Simonsen, A., Cumming, R. C., Brech, A., Isakson, P., Schubert, D. R., and Finley, K. D. (2008) Promoting basal levels of autophagy in the nervous system enhances longevity and oxidant resistance in adult Drosophila. *Autophagy* **4**, 176-184
213. Rubinsztein, D. C. (2006) The roles of intracellular protein-degradation pathways in neurodegeneration. *Nature* **443**, 780-786
214. Martinez-Vicente, M., and Cuervo, A. M. (2007) Autophagy and neurodegeneration: when the cleaning crew goes on strike. *The Lancet. Neurology* **6**, 352-361
215. Garcia-Arencibia, M., Hochfeld, W. E., Toh, P. P., and Rubinsztein, D. C. (2010) Autophagy, a guardian against neurodegeneration. *Seminars in cell & developmental biology* **21**, 691-698
216. Ravikumar, B., Berger, Z., Vacher, C., O'Kane, C. J., and Rubinsztein, D. C. (2006) Rapamycin pre-treatment protects against apoptosis. *Human molecular genetics* **15**, 1209-1216
217. Williams, A., Sarkar, S., Cuddon, P., Ttofi, E. K., Saiki, S., Siddiqi, F. H., Jahreiss, L., Fleming, A., Pask, D., Goldsmith, P., O'Kane, C. J., Floto, R. A., and Rubinsztein, D. C. (2008) Novel targets for Huntington's disease in an mTOR-independent autophagy pathway. *Nature chemical biology* **4**, 295-305
218. Maiuri, M. C., Zalckvar, E., Kimchi, A., and Kroemer, G. (2007) Self-eating and self-killing: crosstalk between autophagy and apoptosis. *Nature reviews. Molecular cell biology* **8**, 741-752